

Advanced methodology for optimization of mixture design of asphalt concrete containing reclaimed asphalt pavement material

THÈSE N° 6913 (2016)

PRÉSENTÉE LE 24 MARS 2016

À LA FACULTÉ DE L'ENVIRONNEMENT NATUREL, ARCHITECTURAL ET CONSTRUIT
LABORATOIRE DES VOIES DE CIRCULATION
PROGRAMME DOCTORAL EN GÉNIE CIVIL ET ENVIRONNEMENT

ÉCOLE POLYTECHNIQUE FÉDÉRALE DE LAUSANNE

POUR L'OBTENTION DU GRADE DE DOCTEUR ÈS SCIENCES

PAR

Sara BRESSI

acceptée sur proposition du jury:

Prof. K. Beyer, présidente du jury
Prof. A.-G. Dumont, Dr M. Partl, directeurs de thèse
Prof. A. Carter, rapporteur
Prof. M. Losa, rapporteur
Dr J.-M. Fürbringer, rapporteur



ÉCOLE POLYTECHNIQUE
FÉDÉRALE DE LAUSANNE

Suisse
2016

Abstract

Nonostante l'uso massiccio di materiale riciclato (RAP) nella produzione di conglomerati bituminosi caldi (HMA), alcuni fenomeni chimico-fisici che caratterizzano la fabbricazione di questi conglomerati non sono ancora stati completamente studiati. L'individuazione e la comprensione di questi meccanismi, così come lo studio dell'eterogeneità che caratterizza le produzioni con alto contenuto di RAP, sono fondamentali per migliorare l'approccio al riciclaggio, perché rappresentano l'origine delle caratteristiche e delle performance del conglomerato bituminoso.

Questa tesi ha l'obiettivo di fornire un quadro per la caratterizzazione di diversi fenomeni e meccanismi che avvengono durante una nuova fase di fabbricazione di conglomerati bituminosi con RAP. La variabilità della reologia dei leganti soggetti a diversi stati di invecchiamento è stata analizzata per valutare l'eterogeneità del legante invecchiato e la sua evoluzione nel tempo. Questo passaggio ha fornito informazioni importanti per lo sviluppo di nuove binder blending charts volte a capire come il bitume nuovo e quello invecchiato interagiscono e se la miscela così ottenuta è omogenea. Il comportamento simulato artificialmente, assumendo una miscelazione del bitume vecchio con il nuovo pari al 100% avrebbe fornito informazioni importanti riguardo alle caratteristiche della miscela qualora tale comportamento fosse stato confermato passando dall'analisi del singolo legante a quella del conglomerato bituminoso. Nei successivi passaggi, tuttavia, altri fenomeni più significativi sono emersi, come ad esempio la formazione di agglomerati di particelle di RAP e la presenza di bitume invecchiato riattivato e non riattivato. Pertanto, è stata sviluppata una nuova metodologia attraverso l'utilizzo dell'Indice di Clustering (IC_G^*) per individuare e quantificare gli agglomerati di RAP. La stessa metodologia ha permesso di analizzare i potenziali movimenti del bitume vecchio durante la fase di mix ed evidenziare la presenza di diversi strati nel film di bitume attorno al RAP, come ad esempio una crosta maggiormente invecchiata all'esterno e uno strato di bitume meno invecchiato, sotto la crosta, che agisce come collante facilitando l'agglomerazione di particelle.

Alla luce del quadro emerso dopo queste indagini si è deciso di ripensare all'approccio di progetto delle miscele di conglomerati bituminosi in particolare nel caso in cui siano utilizzate elevate quantità di RAP. Una nuova metodologia è stata quindi sviluppata per stimare il dosaggio di bitume ottimale richiesto per conglomerati bituminosi con o senza RAP, valutandone i contributi specifici di tutti i componenti (aggregati vergini, filler e RAP) e prendendo in considerazione il fenomeno dell'agglomerazione di particelle di RAP e le sue conseguenze. Sono stati quindi calcolati nuovi surface area factors rispetto a quelli presenti in letteratura che superano l'approssimazione del considerare gli inerti come sfere o cubi. Sono state catturate immagini 3D di numerosi aggregati per procedere con un nuovo calcolo della

superficie specifica degli inerti. Inoltre, la *concentrazione critica del filler* ha permesso di ottenere il volume di bitume richiesto per il ricoprimento del filler stesso. Infine, è stato sviluppato un modello per predire la formazione di agglomerati di particelle di RAP che è stato utilizzato per correggere la curva granulometrica modificata dal clustering dopo la fase di mix.

La nuova formula teorica, grazie alla separazione dei diversi contributi, risulta valida per conglomerati con o senza RAP (i termini relativi al RAP diventano zero se la percentuale di RAP introdotta nell'equazione è zero). Le verifiche condotte in laboratorio hanno dato riscontri positivi e i risultati sono promettenti. La metodologia risulta pertanto soddisfacente nello stimare la quantità di bitume vergine ottimale da aggiungere ai conglomerati bituminosi con o senza RAP.

Parole chiave: binder blending, invecchiamento, reologia, mix design, analisi di sensibilità, progettazione della miscela, RAP, filler, aggregati minerali, bitume vergine.

Abstract

Despite the massive use of Reclaimed Asphalt Pavement (RAP) in Hot Mix Asphalt (HMA) production, the chemo-physical phenomena that characterise the fabrication of these mixtures have not yet been completely explored. The detection and understanding of these mechanisms as well as the study of the heterogeneity that characterizes high RAP mix production are fundamental to improving the approach to recycling, because they represent the source of the mixture characteristics and performance.

This thesis aims to provide a framework for the characterisation of several phenomena and mechanisms occurring during a new mix when RAP material is involved. The variability of binder rheology with different ageing levels was analysed to evaluate the RAP binder heterogeneity and its evolution with time. This stage provided important information for the development of new binder blending charts to understand how the aged and the virgin binder interact and to ascertain whether the blend is homogeneous. The artificially simulated behaviour, assuming the hypothesis of 100% blending, would have provided important information regarding the blend characteristics if the behaviour of the binder had been confirmed in the mixture evaluation. However, in the next stages other phenomena occurred such as RAP particle clustering and the presence of re-activated and non-reactivated binder. Thus, a new methodology was developed using a Clustering Index (IC_{G^*}) to detect and quantify the RAP clusters. The same methodology allowed the investigation of the mobilisation of RAP binder and highlighted the presence of different layers in the RAP binder film thickness such as an over-aged crust and softer bitumen under the crust that acts as glue facilitating the clustering.

The framework that emerged after these investigations led to the rethinking of the mix design approach, especially when high RAP quantities are used. Therefore, a new methodology was developed for estimating the dosage of virgin bitumen required in asphalt mixtures with or without RAP, investigating the specific contributions of all the components of the mixtures (virgin aggregates, filler and RAP) and taking into account the RAP cluster phenomenon and its consequences during the mixture. Indeed, new revised surface area factors were computed thanks to the 3D images of several stones for the calculation of the specific surface area of the aggregates and the *critical filler concentration* allowed the volume of bitumen required for coating the filler to be obtained. Finally a RAP clustering prediction model was developed to readjust the grading curve after the RAP particle agglomerations occurring during the mix.

The new theoretical formula, thanks to the separation of all the contributions, provides results valid for mixtures with and without RAP (the terms related to the RAP become zero if the RAP percentage introduced in the formula is zero). The verifications carried out in the laboratory gave positive and

promising results and the methodology is considered successful in estimating the value of the optimal bitumen quantity for mixtures with and without RAP.

Keywords: binder blending, ageing, rheology, mix design, sensitivity analysis, RAP, filler, mineral aggregates, virgin bitumen.

Ringraziamenti

In queste poche righe a disposizione vorrei ringraziare le persone che mi hanno sostenuta in questo percorso e hanno partecipato alla realizzazione di questo importante obiettivo. Sicuramente questa lista non sarà esaustiva e mi scuso fin da ora per la possibile dimenticanza, seppur involontaria, di alcune persone.

Vorrei ringraziare prima di tutto la mia famiglia (Barbara, Morri e Pitri), che come in ogni percorso della mia vita, è stata sempre presente e al mio fianco, un punto di riferimento essenziale durante i miei viaggi e i cambiamenti che mi hanno interessato negli ultimi anni. Un viaggio in cui la crescita personale e professionale hanno permesso oggi di riconoscermi in una persona più forte e più consapevole. Vorrei ringraziare Riccardo, che con pazienza mi ha supportato nei momenti di sconforto e ha gioito dei miei successi con entusiasmo.

Veniamo agli amici. Importantissimi. Grazie a Sofia ed Anastasia, la mia famiglia a Losanna, le mie due sorelle acquisite, amiche straordinarie a cui sarò sempre legata. Grazie anche agli amici di vecchia data: Enrico, Silvia, Davide e Pietro per esserci sempre stati al mio ritorno, per aver ascoltato e partecipato alle mie avventure.

Un grazie particolare ai membri della commissione di dottorato Prof. Alan Carter, Prof. Manfred Partl (codirettore di tesi), Prof. Massimo Losa e Dr. Jean-Marie Fuerbringer che è stato anche un collaboratore prezioso. Grazie a Nicolas Bueche per la collaborazione e l'interesse dimostrato verso il mio lavoro.

Grazie a tutti i membri del LAVOC che hanno seguito e partecipato alla realizzazione di questa tesi, in particolare Michel Pittet per le discussioni scientifiche e per il supporto in laboratorio. Ringrazio anche Jean-Claude, David, Dominique, Marc-Antoine, Bastien e Charles. Un pensiero particolare va al mio compagno d'ufficio e caro amico José per tutte le chiacchiere, le discussioni, gli scambi e l'aiuto reciproco in fase di ultimazione della tesi.

Grazie anche alla VSS che ha reso possibile il periodo scientifico all'Ecole Technologique Supérieure a Montreal fondamentale per il proseguimento del mio studio e la nascita di collaborazioni internazionali.

Vorrei infine esprimere la mia riconoscenza profonda verso il mio direttore di tesi, il Professor André-Gilles Dumont che sin dall'inizio ha dimostrato fiducia nelle mie capacità e mi ha dato la possibilità di far crescere le mie competenze professionali in un contesto internazionale quale l'EPFL e soprattutto di realizzare il mio sogno di fare un dottorato e di lavorare nell'ambito della ricerca scientifica.

Vorrei chiudere questa sezione con una dedica e un augurio a me stessa. Dedico questo lavoro alla forza e di volontà con cui ho perseguito i miei obiettivi, che è stata ampiamente ricompensata. Mi auguro di continuare sulla strada della ricerca con lo stesso entusiasmo e la stessa dedizione con cui ho iniziato, quasi quattro anni fa, questo percorso straordinario.

Table of contents

Abstract (in Italian)

Abstract (in English)

1 Introduction	9
1.1 Context	9
1.2 Problem statement and objectives	10
1.3 Research approach.....	10
1.4 Characterization of the materials.....	12
1.4.1 Virgin aggregates and fillers	12
1.4.2 RAP material and virgin bitumen.....	12
2 Impact of different ageing levels on binder rheology	14
2.1 Materials and tests	15
2.1.1 Bending Beam Rheometer (BBR).....	16
2.1.2 Dynamic Shear Rheometer (DSR)	16
2.2 Methodology	16
2.3 Results analysis	18
2.3.1 Stiffness at low temperatures	19
2.3.2 Complex modulus at medium and low temperatures	23
2.4 Evolution of binder rheological properties	27
2.5 Summary of findings	28
3 Binder blending charts	30
3.1 Artificially-aged binder blending charts.....	30
3.1.1 Experimental plan	31
3.1.2 Research approach and methodology.....	33
3.1.2.1 Low temperature domain.....	36
3.1.2.2 Medium and high temperature domain.....	45
3.2 RAP binder blending charts.....	54
3.3 Conclusions	56
4 Cluster phenomenon in RAP mixtures	58
4.1 Methodology and experimental plan	59
4.2 The Clustering Index (IC_G^*)	61

4.2.1 G^*_{design}	61
4.3 Selected model parameters	63
4.3.1 Response Surface Model (RSM) and Doehlert Design	64
4.1 Results and Modelling	66
4.4.1 G^*_{fine} , G^*_{design} and IC_{G^*} results	67
4.4.2 Modelling results	71
4.4.3 Mobilisation of RAP binder: the coarse part analysis	77
4.5 Conclusions	79
5 New analytical method for optimising the mix design of asphalt mixtures	81
5.1 Background	81
5.1.1 Mix design of asphalt mixtures containing RAP	82
5.2 Objectives and research approach	83
5.3 Methodology	84
5.3.1 Revision of the surface area factors	84
5.3.2 Scale factors	85
5.3.3 Filler	86
5.3.3.1 Particle size distribution (PSD) based on laser diffraction	89
5.3.3.2 Brunauer, Emmett and Teller (BET) method and agglomeration factor	90
5.3.3.3 Environmental Scanning Electron Microscope (ESEM)	90
5.3.3.4 Critical filler concentration	91
5.3.4 Modelling of RAP clustering	92
5.4 Verification in the laboratory	93
5.5 Results and specific applications	95
5.5.1 Aggregates	95
5.5.2 Filler	99
5.5.3 RAP clustering prediction model	101
5.6 Final theoretical formulation and laboratory verification	104
5.7 Summary of findings and conclusions	115
6 General conclusions and future work	118
References	123
Annexes	128

Chapter 1

Introduction

1.1.Context

When Hot Mix Asphalt (HMA) reaches the end of its service life, the milled materials, Reclaimed Asphalt Pavement (RAP), still retain considerable value and can be reused in virgin HMA to reduce the amount of new material necessary. The growing increase in the accumulation of stocks of RAP had led to a search for practical solutions for the reuse of this material via the development of new production technologies. However, it is necessary to take this reuse of old materials into account in the HMA design process. During service, the blend of aggregates and binders undergoes various physical and rheological changes that must be considered in the design process to ensure that HMA mixtures comprising RAP perform as well as HMA produced from virgin materials.

To facilitate the incorporation of RAP into the design of HMA, in the US several guidelines have been followed since the launching of the Federal Highway Administration project (FHWA 1978). The National Cooperative Highway Research Program published guidelines (NCHRP 1978) followed by the Guidelines for Recycling Pavement Materials two years later (Epps et al. 1980). Most states have also established limits on the maximum percentage of RAP that can be used, typically ranging between 10 to 50%, although high percentages of RAP are not commonly used in practice.

After the implementation of Superior Performing Asphalt Pavements (Superpave) in the 1990s many state transportation departments stopped allowing the use of high amounts of RAP in favour of implementing the Superpave system with virgin materials to reduce the variability of the final mix (FHWA 2011). Despite the fact that the original Superpave HMA design procedure did not incorporate the use of RAP, many states have continued its use. This is one of the reasons why the use of RAP is diversified in different countries, even among the European ones as reported by recent studies (Kalman et al. 2013). The addition of 10% of RAP appears to be the norm and most suppliers do not exceed 30% of recycled asphalt content due to manufacturing restraints within the plant. However, more modern mixing plants are now capable of handling 70% of RAP (De la Roche et al. 2013).

1.2.Problem statement and objectives

The problem, when RAP, is used lies in ensuring the same performance level as that of traditional asphalt

using a certain amount of RAP and controlling its heterogeneity and other chemical and physical phenomena occurring during a new mix. Despite the massive use of RAP in asphalt mixture production, the physical and chemical phenomena occurring during a new mix when a high RAP content is involved have not yet been completely explored. The detection and comprehension of these mechanisms as well as the study of the heterogeneity that characterize high RAP mix production are fundamental to improving the approach to recycling. Indeed, they may have important effects on the mechanical behaviour and performance expectations. The present work aims to detect and quantify the physical phenomena occurring during a mix containing RAP: the binder blends, the cluster phenomenon, the presence of re-activated and non-reactivated aged binder. The effects on the optimal dosage of virgin bitumen and on the expected grading curve were analysed in order to establish a new methodology for the mix design optimization of RAP mixtures that takes into account all the above-mentioned phenomena.

The methodology has been developed using only one type of RAP, virgin aggregates and filler, thus it is valid only for the specific case treated in this work. Nevertheless, the methodology could be extended to other cases once the characteristics of the materials involved are defined.

1.3. Research approach

The research work presented in this study is composed of several stages of investigation, starting with the bitumen through to the asphalt mixtures. Those stages are:

- *Impact of different ageing levels on binder rheology.* It analyses the variability of the rheology of virgin and artificially aged bitumen.
- *Binder blending.* The blending of artificially aged or RAP extracted binder and virgin bitumen will be widely discussed in this section. Nonlinear binder blending charts were developed at low, medium and high temperatures in order to predict the behaviour of the blend depending on several variables. The behaviour of artificial blends was studied in order to obtain important information regarding the potential behaviour of the simulated blend in the mixture.
- *Cluster phenomenon in RAP mixtures.* This represents the transition from the bitumen scale to the mixture scale. The initial objective was to confirm the behaviours artificially recreated in the section above, nevertheless other phenomena appeared. A specific methodology was applied to detect the cluster phenomenon involving small size RAP particles, activated and non-activated binder and the migration of aged binder. These phenomena and the possible effects on the recycling approach will be discussed.
- *New theoretical mix design for RAP mixtures.* The phenomena detected in the previous section raised problems regarding the correct dosage of virgin bitumen to add to the mixtures and the design grading

curve. Therefore, the need for a new mix design approach when a high RAP content is used becomes inevitable for the production of durable RAP mixtures. For this purpose, a new methodology is proposed considering individually all the components (virgin aggregates, RAP and filler) that play a role in the mix design process. Their behaviour was separately investigated and included in the calculation.

- *Laboratory verification and specific applications.* The verification of the methodology proposed was carried out in the laboratory considering a typical Swiss binder course AC B 16 (i.e. maximum nominal diameter 16 mm). Several tests were conducted to verify that the calculated optimal bitumen quantity to be added to the asphalt mixtures, with and without RAP, represents a good estimation of the measured one.

The research plan is schematically shown in Figure 1.1.

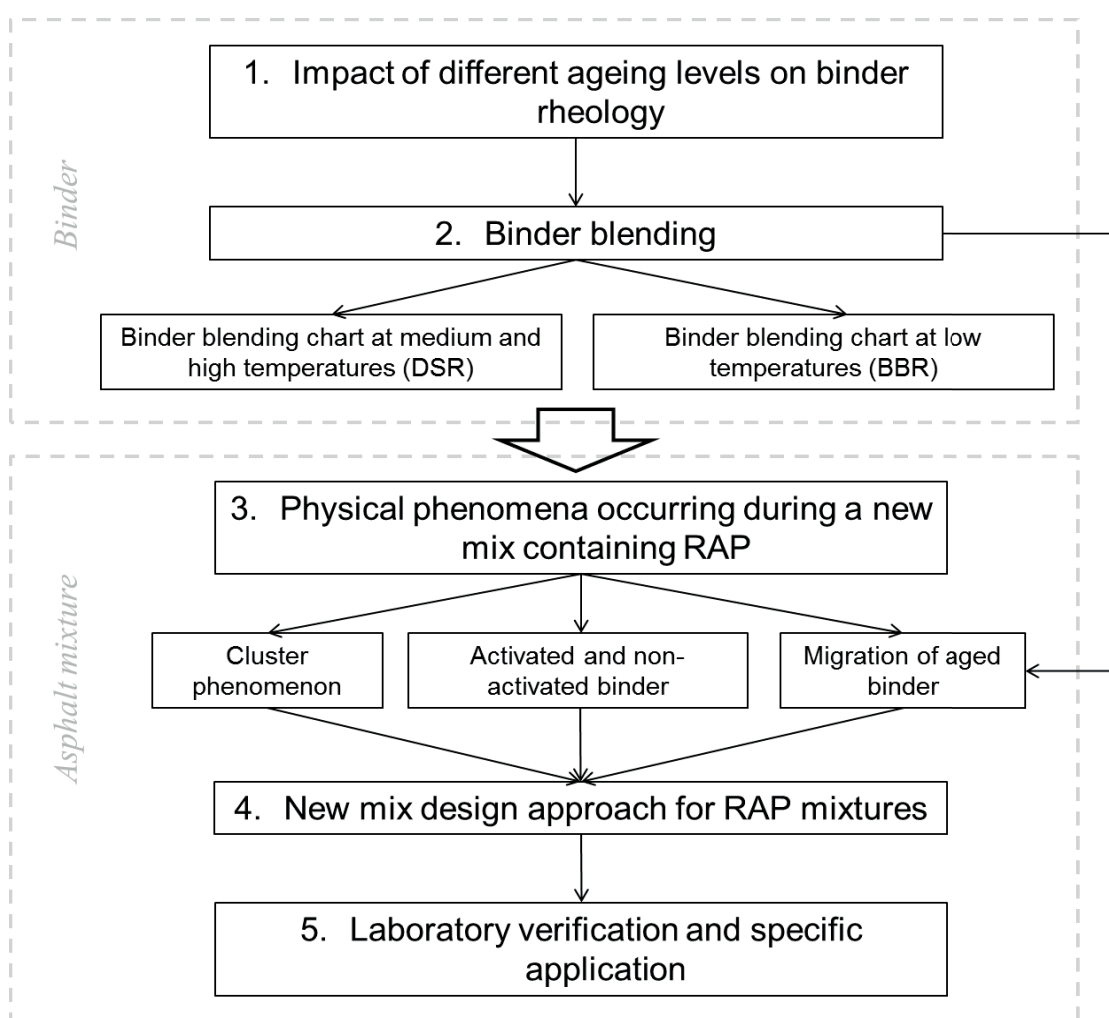


Figure 1.1 Research plan overview.

1.4.Characterization of the materials

The material characterization is conducted to verify the compliance with the requirements and provide the basic data necessary for the study. The traditional analyses of aggregates, filler and bitumen were conducted. Throughout the research, the same aggregates, filler and bitumen were used.

1.4.1. Virgin aggregates and fillers

Quarry aggregates from Choex-Massongex (Switzerland) were used as virgin aggregates in the mixture. The average characteristics of all the fractions used for the study are summarised in Table 1.1.

Table 1.1 Summary of aggregate characteristics.

Property description	Test method	Value
Polished Stone Value	DIN EN 1097-8	60-62
Los Angeles	SN EN 1097-2	11-15
Affinity with bituminous binders [%]	SN 670 460	U=85.1 (Adequate adherence of the bitumen on the aggregates is ensured for the majority of uses)
Phyllosilicates content [%]	SN 670 115	From 1.9 to 4.9 in mass (admissible)

The filler characteristics are summarised in Table 1.2.

Table 1.2 Summary of filler characteristics.

Property description	Test method	Limestone	Hydrated Lime
Density [kg/m ³]	EN 1097-4	2705	2249
Rigden Voids [%]	EN 1097-4	32	58
Methylene Blue (clay content)	EN 933-9 (C837-09)	4.00	-

1.4.2. RAP material and virgin bitumen

RAP 0/16 from Granges-de-Vesin (Switzerland) was selected from a singular stock. The bitumen content extracted and recovered (EN 12697-1 and 3) was 5.60% of the mixture. The RAP grading curve is reported in Table 1.3.

Table 1.3 RAP grading curve.

Sieve [mm]	Percentage of passing material [%]
22.4	100.0
16.0	100.0
8.0	72.8
4.0	37.6
2.0	16.6
1.0	6.7
0.500	2.4
0.250	0.9
0.125	0.3
0.063	0.1

Three types of unmodified virgin bitumen were used. The penetration grades (EN 1426), the softening points R&B (EN 1427), the penetration index (PI) (EN 12591) and the SARA fractions of the RAP and virgin binder are reported in Table 1.4.

Table 1.4 Summary of binder characteristics.

Type of bitumen	Penetration @25°C [10-1 mm]	R&B Temp [°C]	PI [-]	Saturates [%]	Aromatics [%]	Resins [%]	Asphaltenes [%]
Virgin bitumen 50/70	58	54.3	0.2	4.97	17.89	48.14	29.00
Virgin bitumen 70/100	82	47.8	-0.6	6.69	24.64	41.23	27.54
Virgin bitumen 100/150	107	46.7	-0.1	4.62	28.02	42.74	24.63
RAP binder	26	64.6	0.4	5.18	10.51	57.69	26.63

Chapter 2

Impact of different ageing levels on binder rheology

The aim of this chapter is to provide a complete study of the inherent variability of the rheological properties of binders, analysing different ageing levels that represent different stages of pavement service life. This preliminary part represents a first step towards a probabilistic approach to apply to mix design methods and it allows some conclusions to be drawn regarding the reliability of the results obtained later in the study.

It is well known that during the construction of any road pavement, variations in layer material quality, homogeneity, environmental influences, and variations of the construction techniques all lead to non-uniform spatial variations in layer material properties and layer thicknesses comprising the pavement structure. As vehicle loads are applied to the pavement, these spatial variations result in the development of non-uniform distributions of stress, strain, and deformation within the pavement, in turn causing non-uniform distributions of defects in the pavement. Additionally, external influences arising after construction such as the infiltration of water, drying out and freeze-thaw cycles also affect the uniformity of defects (Kenis and Wang 2004). Evaluating uncertainties regarding the input parameters and understanding how they will be transferred to the results are fundamental to acquiring a more realistic assessment of the durability of roads. With regard to material properties the most heterogeneous are bituminous mixtures containing RAP.

The heterogeneity of the milled RAP depends on the variation of the quantity of the components at the start of the service life of the new asphalt pavement, the quantity of additional materials used for the repair of damage in pavement exploitation as well as RAP loading, transporting and stockpiling technologies. Ensuring confidence in the design procedure and the successful use of RAP would require addressing many durability concerns related to its variability (Al Qadi 2007).

The variability regarding material properties affecting pavement performance can be divided into the following two categories:

1. *Spatial variability* that includes an actual difference in the basic properties of materials from one point to another in what are assumed to be homogeneous layers and a fluctuation in the material and cross-sectional properties due to construction quality (Kim and Buch 2003).
2. *Input parameter variability* that stems from the inherent variability of the mechanical properties of the materials and the variability of the tests used to measure those properties.

Inherent variability takes into account the measurement uncertainties and dispersion of the results around the average value, providing information about the evolution of the binder characteristics during ageing and the random error for the values considered as representative. The spatial variability is not studied here.

2.1. Materials and tests

This statistical analysis was carried out using the 70/100 non-polymer modified asphalt binder (Table 3 Chapter 1). The ageing of the binder was performed using two different methods. First, the rolling thin film oven test (RTFOT, ASTM D 2872) was used. This technique simulates the changes in binder properties occurring during hot mixing at the plant and the lay-down process. The second method used was the pressure ageing vessel (PAV), that simulates in-situ field ageing (ASTM D 6521).

For each ageing levels - virgin (no ageing), short-term (RTFOT) and long-term (RTFOT+PAV) - several samples were made to test stiffness at low temperatures using a Bending Beam Rheometer (BBR) and the complex modulus at high temperatures using a Dynamic Shear Rheometer (DSR) as explained in Table 2.1 for a total of 252 experiments.

Table 2.1 Summary of the experiments.

Ageing level	Type of test	Testing temperature [°C]	N. of experiments
Virgin	BBR	-30	12
Virgin	BBR	-20	12
Virgin	BBR	-10	12
Virgin	DSR	20	8
Virgin	DSR	40	16
Virgin	DSR	50	16
RTFOT	BBR	-30	12
RTFOT	BBR	-20	12
RTFOT	BBR	-10	12
RTFOT	DSR	20	8
RTFOT	DSR	40	16
RTFOT	DSR	50	16
RTFOT+PAV	BBR	-30	12
RTFOT+PAV	BBR	-20	12
RTFOT+PAV	BBR	-10	12
RTFOT+PAV	DSR	20	14
RTFOT+PAV	DSR	40	16
RTFOT+PAV	DSR	50	16

A DSR complex modulus test at medium temperatures was also performed but because the results at high and medium temperatures exhibited the same trend, it was decided not to show the results at medium temperature in order to simplify the content of the thesis.

In the case of medium and high temperatures the aim was not to test at extreme temperatures but investigate useful domains for pavement design methods and temperatures also suitable for bitumen with a narrow PG grade.

2.1.1. Bending Beam Rheometer (BBR)

The Bending Beam Rheometer (BBR) test provides a measure of the low temperature stiffness and relaxation properties of asphalt binders. These parameters give an indication of an asphalt binder's ability to resist low temperature cracking. The stiffness is calculated with the following equation:

$$S(t) = \frac{pL^3}{4bh^3\delta(t)} \quad (2.1)$$

$S(t)$ = time-dependent flexural creep stiffness [MPa]

P = constant load [N]

L = span length [mm]

b = width of beam [mm]

h = depth of beam [mm]

$\delta(t)$ = deflection of beam [mm]

The maximum stiffness registered during the test was considered in this study and 12 samples for each ageing level were tested at three temperatures: -10; -20; -30°C.

2.1.2. Dynamic Shear Rheometer (DSR)

The DSR was used to characterise the viscous and elastic behaviours of asphalt binders at medium and high temperatures. Several frequency sweeps (21 frequencies tested) were conducted at 20, 40 and 50°C measuring the complex modulus. Among these frequencies, three were selected to be compared and be representative of low, medium and high frequencies respectively 0.4; 1.0 and 10.3 Hz.

2.2. Methodology

Before undertaking a more complex statistical study, certain criteria need to be met in order to assess the repeatability of the measurements (i.e. statement on a single-operator precision). According to Equation 2.1, the *acceptable range r* (acceptable difference between highest and lowest value for each point) was

defined. The real range was not expected to exceed the acceptance range with a probability of 5% in the normal and correct operation of the test method (ASTM C670).

$$r = \sigma \cdot f \quad (2.2)$$

r=acceptable range

σ =single-operator standard deviation for single test determination

f= coefficient depending on number of repetitions for each determination (ASTM C670)

In this study the reproducibility, the statement on multilaboratory precision, was not evaluated since all the measurements were provided by a single operator and in a single laboratory (ASTM C802). Nevertheless, it was really important to go a step further in the statistical analysis to determine the probability distribution of the results, and the evolution of differences with the ageing of the materials. Indeed, the second important step of this analysis was to determine the probability distribution of the DSR and BBR results in order to evaluate which theoretical models best represent real data. In the literature, there is limited information on this subject. The goodness of fit was also determined by computing a probability plot.

An *F*-test (Fisher test) is used to ascertain whether the variances of two populations are equal (Snedecor and Cochran, 1983). For the third step, the *F*-test was computed based on results for different ageing levels and temperatures. A 95% confidence interval was used. In this case, the temperature was first kept constant and the ageing level was varied and subsequently, the ageing level was kept constant and the temperature varied. Moreover based on the DSR results, a comparison was made among different frequencies in order to evaluate whether ageing has any effect on the variance of the response at different frequencies. Where the *F*-test demonstrated that the hypothesis of the same variance was acceptable, the ANOVA was performed. Where the *F*-test demonstrated that this hypothesis was not verified, a Welch test was performed instead of the ANOVA. The Welch test is a more robust method that accepts samples exhibiting possibly unequal variances (Welch 1938).

The fourth step consists of the comparison of the means. Once it has been verified that all the results follows a normal distribution (Step 2) and the variance is equal among the groups (Step 3), it is possible to compute an ANOVA to determine significant differences between the means of rheological properties for different ageing levels. In the ANOVA the variation in the response measurements is partitioned into components that correspond to different sources of variation. The goal in this procedure is to split the total variation of the data into a portion due to random error and a portion due to changes in the values of the independent variable. Assessing that the results were normally distributed was essential in

order to satisfy one of the main hypotheses of the ANOVA test. Indeed, the hypotheses underlying the use of the ANOVA are (Box et al. 1978) as follows:

- Data normally distributed
- Independent values
- Homoscedasticity (i.e. the variance of the groups is the same for the population). The group variances for each treatment are equal to each other and, together, are equal to the variance of the population.

Where the last hypothesis was not verified a more robust model was used: the Welch test that compares the means allowing unequal variance among the groups (Welch 1938).

If the means vary, the aim is to define which means change. For this purpose a *Least Significant Difference (LSD) test* is performed (Ott and Longnecker 2000) using the following Equation:

$$LSD = t_{\frac{\alpha}{2},df} \cdot \sqrt{\frac{2S_e^2}{n}} \quad (2.3)$$

where:

$t_{\frac{\alpha}{2},df}$ = value of t-student related to the level of confidence ($\alpha= 0.05$), and the degrees of freedom of the residual variance.

S_e = residual variance

n = number of experiments for each group

At this point, the differences between the means of all groups are calculated. If the difference (in absolute value) is greater than LSD then the means are significantly different. If it is less, then the means are equal.

2.3.Results analysis

For all the measurements an acceptable repeatability was found. An example of the calculation is reported in Table 2.2 that provides the precision (acceptance range) of the measurement of the virgin binder with BBR at -30°C. The difference between the largest and smallest of the twelve determinations is less than the acceptance range, thus the repeatability is verified (ASTM C670).

Table 2.2 Example of acceptance and real range for BBR results at -30°C for virgin binder.

Stiffness measurement [MPa]	1050	1010	988	964	930	922	922	910	884	881	787	750
Stiffness mean [MPa]	916.50											
STD	85.83											
Real range [MPa]	300											
Acceptance range [MPa]	386.2											

2.3.1. Stiffness at low temperatures

The main results of the BBR are shown in Table 2.3, which gives the mean, the standard variation (STD) and coefficient of variation (COV) for each group. All the stiffness results are reported in the Annexes (Table A-1).

Table 2.3 Mean, STD and COV of stiffness values obtained with BBR at different temperatures and for different ageing levels.

Level of ageing	Testing temperature [°C]	Stiffness mean [MPa]	STD	COV [%]
Virgin	-30	916.50	85.83	9.4
Virgin	-20	414.33	21.46	5.2
Virgin	-10	109.22	15.76	14.4
RTFOT	-30	1 029.82	91.18	8.9
RTFOT	-20	486.25	38.06	7.8
RTFOT	-10	152.83	12.67	8.3
RTFOT+PAV	-30	1 039.33	71.61	6.9
RTFOT+PAV	-20	522.25	56.81	10.9
RTFOT+PAV	-10	205.67	20.34	9.9

At all the testing temperatures, and for all the ageing levels, it can be said that the normal distribution fits the results accurately. In Figures 2.1 and 2.2, the example of virgin binder at -10°C is shown. The cumulative probability function is compared to the theoretical model in Figure 2.1, as well as the Gaussian distribution of the experimental data. In Figure 2.2, the normal probability plot is used to evaluate the goodness of fit, which verifies that the points are distributed along a straight line.

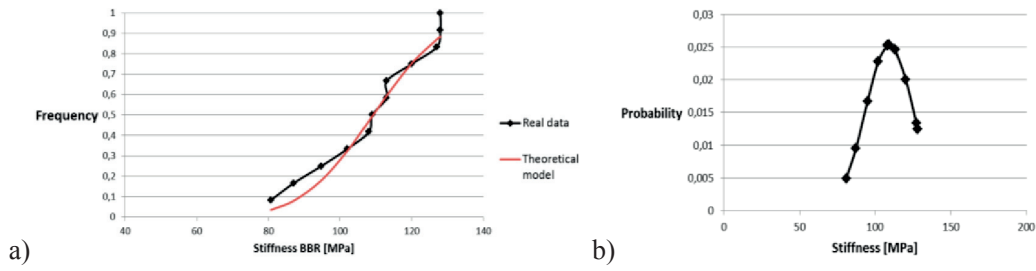


Figure 2.1 a) Cumulative probability function and b) probability mass function for virgin binder at -10°C.

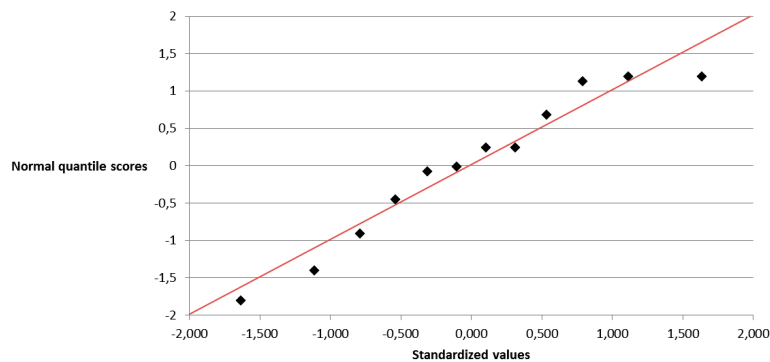


Figure 2.2 Goodness of fit using normal probability plot for virgin binder at -10°C.

Even with this limited set of experimental points, the results shown in Figures 2.1 and 2.2 clearly demonstrate that the results of the stiffness measured with the BBR at -10°C for this binder follow a normal distribution. The same distribution was observed for the results at the other test temperatures (-20 and -30°C). The data follow a normal distribution and, as mentioned earlier, this is one of the hypotheses required to conduct an ANOVA. The next step was to verify the other hypothesis that concerns the equality of variance among the groups. Table 2.4 shows the results of the F-test and it can be seen that only in one case (-20°C RTFOT+PAV – virgin) the null hypothesis (Hypothesis 1) is rejected because the p-value is <0.05 (α). In all other cases, Hypothesis 1 is verified.

$$H_0: \sigma_1^2 = \sigma_2^2 \quad (\text{Hypothesis 1})$$

$$H_a: \sigma_1^2 \neq \sigma_2^2 \quad (\text{Hypothesis 2})$$

In the majority of cases, the variance does not change with ageing. The variance of the binder stiffness at low temperatures, independent of the temperature chosen, does not change with short- and long-term ageing.

Table 2.4 F-Test that compares variance of different ageing levels with temperature kept constant.

-30°C	RTFOT	Virgin	RTFOT	RTFOT+PAV	Virgin	RTFOT+PAV
Mean	1029.818	916.500	1029.818	1039.333	916.500	1039.333
Variance	8313.164	7633.09	8313.164	5127.515	5127.51	5127.515
Observations	11	12	11	12	12	12
df	10	11	10	11	11	11
F	1.129		1.621		1.437	
Alpha	0.05		0.05		0.05	
p-value	0.841		0.440		0.558	
F-critic	3.526		3.526		3.474	
Significance	no		no		no	
-20°C	RTFOT	Virgin	RTFOT	RTFOT+PAV	Virgin	RTFOT+PAV
Mean	486.25	414.333	522.250	486.250	522.250	414.333
Variance	1448.386	460.424	3227.477	1448.386	3227.47	460.424
Observations	12	12	12	12	12	12
df	11	11	11	11	11	11
F	3.146		2.228		7.010	
Alpha	0.05		0.05		0.05	
p-value	0.070		0.200		0.003	
F-critic	3.474		3.474		3.474	
Significance	no		no		yes	
-10°C	RTFOT	Virgin	RTFOT	RTFOT+PAV	Virgin	RTFOT+PAV
Mean	109.217	152.833	205.667	152.833	205.667	109.217
Variance	248.234	160.515	413.697	160.515	413.697	248.234
Observations	12	12	12	12	12	12
df	11	11	11	11	11	11
F	1.546		2.577		1.667	
Alpha	0.05		0.05		0.05	
p-value	0.481		0.132		0.410	
F-critic	3.474		3.474		3.474	
Significance	no		no		no	

Even if, as seen in Table 2.4, the ageing has no effect on the variance of the BBR results at constant temperature, the artificial ageing used in this study makes stiffness variance more sensitive to temperature change, as shown in Table 2.5. Indeed, if the same test is computed for comparing the variance for different temperatures at the same ageing level, different results are obtained.

Table 2.5 F-Test that compares variance of different temperatures with ageing level kept constant.

Virgin binder	-30°C	-20°C	-20°C	-10°C	-30°C	-10°C
Mean	916.5	414.333	414.333	109.217	916.500	109.217
Variance	7366.091	460.424	460.424	248.234	5127.51	248.234
Observations	12	12	12	12	12	12
df	11	11	11	11	11	11
F	0.063		1.855		29.674	
Alpha	0.05		0.05		0.05	
p-value	2.000		0.320		0.000	
F-critic	3.474		3.474		3.474	
Significance	no		no		yes	
RTFOT	-30°C	-20°C	-20°C	-10°C	-30°C	-10°C
Mean	1029.818	486.25	486.25	152.833	1029.81	152.833
Variance	8313.164	1448.38	1448.386	160.515	8313.16	160.515
Observations	11	12	12	12	11	12
df	10	11	11	11	10	11
F	0.174		9.023		51.791	
Alpha	0.05		0.05		0.05	
p-value	1.992		0.001		1.71E-	
F-critic	3.665		3.474		3.526	
Significance	no		yes		yes	
RTFOT+PAV	-30°C	-20°C	-20°C	-10°C	-30°C	-10°C
Mean	1039.333	522.25	522.25	205.667	1039.33	205.667
Variance	5127.515	3227.47	3227.477	413.697	5127.51	413.697
Observations	12	12	12	12	12	12
df	11	11	11	11	11	11
F	0.629		27.802		12.394	
Alpha	0.05		0.05		0.05	
p-value	1.545		0.002		2.28E-4	
F-critic	3.474		3.474		3.474	
Significance	no		yes		yes	

As can be seen, both short- and long-term ageing have an effect on the variance. Table 2.5 shows that, for most cases, the null hypothesis is not verified, which means that the variance differs according to temperature. For the rest of this study, the data were analysed at constant temperature, for which the null hypothesis is respected. Since the F-test has shown that the variance does not change with ageing, it is now possible to carry out an ANOVA. In all cases (Table 2.6), the null hypotheses in the ANOVA were rejected (p-value <0.05) and it is thus possible to conclude that there is a highly significant difference between the means of groups, which is not only due to random errors.

Table 2.6 ANOVA for comparison of mean of stiffness for different ageing levels.

-30°C	SS ¹	df ¹	MS ¹	F ¹	p-value
Within group	110846.9	3	55423.43	8.04	0.0004
Between groups	220561.3	32	6892.541		
Total	331408.2	35			
-20°C	SS	df	MS	F	p-value
Within group	72456.06	3	36228.03	21.16	7.9167E-08
Between groups	56499.17	33	1712.096		
Total	128955.2	36			
-10°C	SS	df	MS	F	p-value
Within group	55985.51	3	27992.75	102.11	8.9193E-17
Between groups	9046.91	33	274.149		
Total	65032.42	36			

¹SS: Sum of the square; df: degree of freedom; MS: Mean square; F-statistic=MS within/MS between

Once it was clear that the mean varies, the aim is to define which means change. An LSD test was performed and the results are shown in Table 2.7. As can be seen, the only case in which the means between two groups do not change is at -30°C between the RTFOT and RTFOT+PAV results.

Table 2.7 Summary of LSD test performed at each temperature with different ageing levels.

T [°C]	$t_{\frac{\alpha}{2},df}$	LSD	Difference mean Virgin-RTFOT	Difference mean RTFOT-RTFOT+PAV	Difference mean Virgin-RTFOT+PAV
-30	2.036933	69.04	113.32	9.52	122.83
-20	2.034515	34.37	71.92	36	107.92
-10	2.034515	13.75	43.62	52.83	96.45

2.3.2. Complex modulus at medium and high temperatures

Before undertaking the complex modulus test, it is necessary to do a stress sweep at the test temperature in order to establish the limit of the linear viscoelastic region of the behaviour of the binder. The Linear Viscoelastic (LVE) limit was defined as the point where the storage modulus (G') decreased to 95% of its initial value as prescribed by the SHRP specification (Anderson et al. 1994). An example of the graphical representation of the LVE limit obtained at 50°C is provided in Figure 2.3.

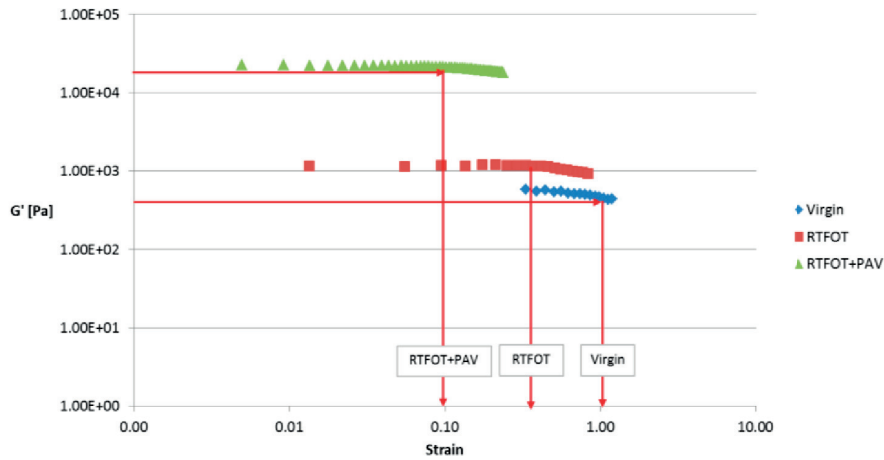


Figure 2.3 Stress sweep at 50°C with different ageing levels.

Subsequently, a complex modulus test can be performed. A frequency sweep conducted at 40 and 50°C registered 21 points corresponding to different frequencies. From those points, three representatives of low, medium and high frequencies were selected, 0.4, 1.01 and 10.3 Hz, to represent different traffic speeds. In Tables 2.8 and 2.9, a summary of the mean, variance and COV obtained at 20 and 50°C is given. All the complex modulus values at 20 and 50°C are reported in the Annexes (Tables A-2 and A-3).

Table 2.8 Mean, variance and COV of complex modulus obtained at different frequencies and for different ageing levels at 20°C.

Level of ageing	Frequency [Hz]	Complex Modulus Mean [Pa]	STD	COV [%]
Virgin	0.4	549 380	5 946.42	1.1
Virgin	1.01	1 012 811	140 460.7	13.9
Virgin	10.3	3 076 900	572 850.1	18.6
RTFOT	0.4	1 322 500	36 747.99	2.8
RTFOT	1.01	2 067 729	39 633.39	1.9
RTFOT	10.3	3 813 011	505 864.9	13.3
RTFOT+PAV	0.4	3198757	307130.4	9.6
RTFOT+PAV	1.01	3674042	370083.7	10.1
RTFOT+PAV	10.3	4773753	350038.6	7.3

Table 2.9 Mean, variance and COV of complex modulus obtained at different frequencies and for different ageing levels at 50°C.

Level of ageing	Frequency [Hz]	Complex Modulus Mean [Pa]	STD	COV [%]
Virgin	0.4	1 213	127.67	10.5
Virgin	1.01	2 800	379.01	13.5
Virgin	10.3	20 940	3 501.38	16.7
RTFOT	0.4	3 743	467.36	12.5
RTFOT	1.01	8 030	1 343.36	16.7
RTFOT	10.3	60 022	9 942.06	16.6
RTFOT+PAV	0.4	33 539	4 450.78	13.3
RTFOT+PAV	1.01	63 940	9 985.58	15.6
RTFOT+PAV	10.3	332 202	46 768.84	14.1

The probability distribution at 50°C is also represented in this case by a normal distribution as shown in Figures 2.4 and 2.5. The same tendency was observed at 20 and 40°C.

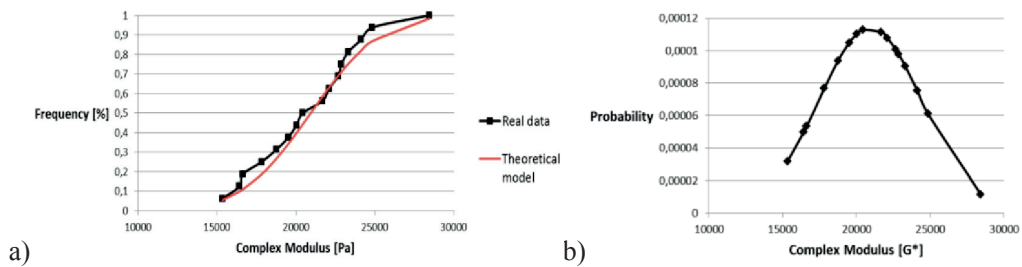


Figure 2.4 a) Cumulative probability function and b) probability mass function for virgin binder at 50°C at high frequency (10.3 Hz).

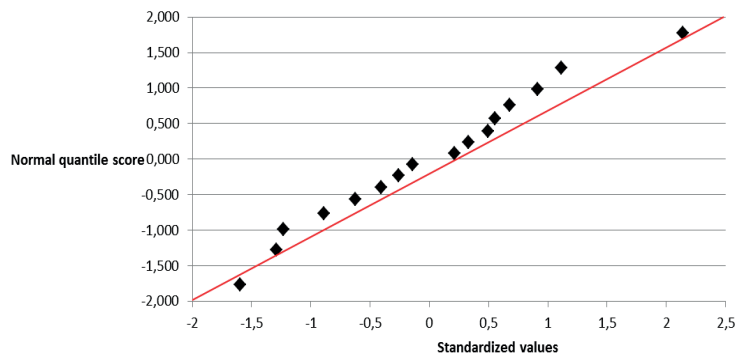


Figure 2.5 Goodness of fit using normal probability plot.

Similarly to the case for low temperatures, an F-test was performed. The F-test in this framework provided completely different results. In all cases (Table 2.10), the null hypothesis is rejected. The variance of the complex modulus at high temperatures, independently of the frequency chosen, changes with short- and long-term ageing, and thus probably changes during pavement service life.

Table 2.10 F-Test comparing variances of different ageing levels with frequency kept constant at 50°C.

0.4 Hz	RTFOT	Virgin	RTFOT+PAV	RTFOT	RTFOT+PAV	Virgin
Mean	3744	1213	33539	3744	33539	1213
Variance	2.184E+0	1.630E+0	1.981E+07	2.184E+0	1.981E+07	1.630E+0
Observations	16	16	16	16	16	16
df	15	15	15	15	15	15
F	13.40		90.69		1215.32	
Alpha	0.05		0.05		0.05	
p-value	9.041E-06		1.195E-11		4.811E-20	
F-critic	2.862		2.862		2.862	
Significance	yes		yes		yes	
1.01 Hz	RTFOT	Virgin	RTFOT+PAV	RTFOT	RTFOT+PAV	Virgin
Mean	8.030E+0	2.801E+0	6.394E+04	8.030E+0	6.394E+04	2.801E+0
Variance	1.805E+0	1.436E+0	9.971E+07	1.805E+0	9.971E+07	1.436E+0
Observations	16	16	16	16	16	16
df	15	15	15	15	15	15
F	12.563		55.254		694.152	
Alpha	0.05		0.05		0.05	
p-value	1.381E-05		4.481E-10		3.184E-18	
F-critic	2.862		2.862		2.862	
Significance	yes		yes		yes	
10.3 Hz	RTFOT	Virgin	RTFOT+PAV	RTFOT	RTFOT+PAV	Virgin
Mean	6.002E+0	2.094E+0	3.322E+05	6.002E+0	3.322E+05	2.094E+0
Variance	9.884E+0	1.266E+0	2.187E+09	9.884E+0	2.187E+09	1.226E+0
Observations	16	16	16	16	16	16
df	15	15	15	15	15	15
F	8.063		22.129		178.416	
Alpha	0.05		0.05		0.05	
p-value	2.264E-04		3.029E-07		8.021E-14	
F-critic	2.862		2.862		2.862	
Significance	yes		yes		yes	

Because the variances did change with ageing, it was not possible to use the ANOVA and the comparison between the averages was thus done using a more robust method, the Welch test. This test admits inequality between the variances. The results in Table 2.11 show (all p-values <0.05) that there is a significant difference between the means of complex modulus, considering any frequency.

Table 2.11 Results of Welch test for comparison of means.

Frequency	Compared groups	p-value
0.4 Hz	Virgin-RTFOT	1.12E-13
	RTFOT-RTFOT+PAV	4.15E-03
	Virgin-RTFOT+PAV	2.73E-03
1.01 Hz	Virgin-RTFOT	1.41E-07
	RTFOT-RTFOT+PAV	2.80E-10
	Virgin-RTFOT+PAV	1.12E-10
10.3 Hz	Virgin-RTFOT	3.71E-09
	RTFOT-RTFOT+PAV	6.07E-02
	Virgin-RTFOT+PAV	4.88E-02

2.4. Evolution of binder rheological properties

The results obtained earlier can be projected on the pavement service life. It is possible, for instance, to see graphically (Figures 2.6 and 2.7) how the mean and variance change over the pavement service life. First, it is assumed that the RTFOT results correspond to time 0, just after the mixing process in the plant, and RTFOT + PAV results correspond to a certain point in the pavement service life. Moreover, it will be assumed that the evolution model is linear. It can be seen that the stiffness and complex modulus results show that means are significantly different for different ageing levels. Concerning the variance, while in the case of stiffness at low temperatures measured with the BBR, it is not significantly different, in the case of the complex modulus at medium and high temperatures measured with the DSR, the variance is different.

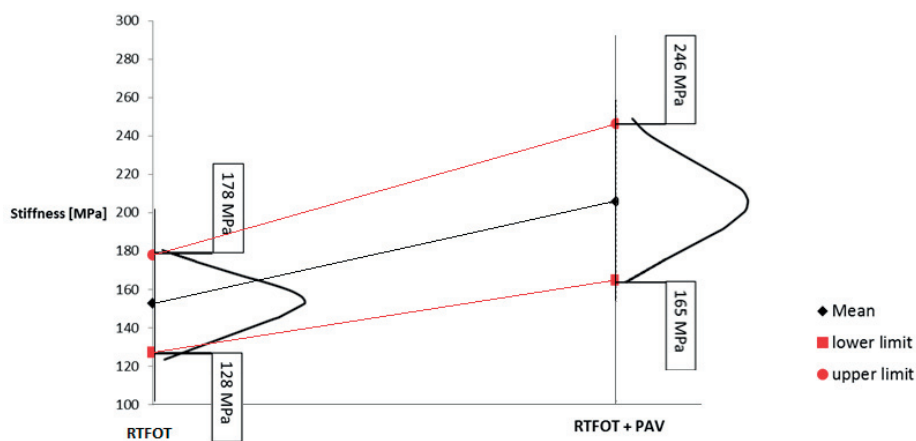


Figure 2.6 Evolution of stiffness mean and variance over pavement service life using BBR results at -10°C.

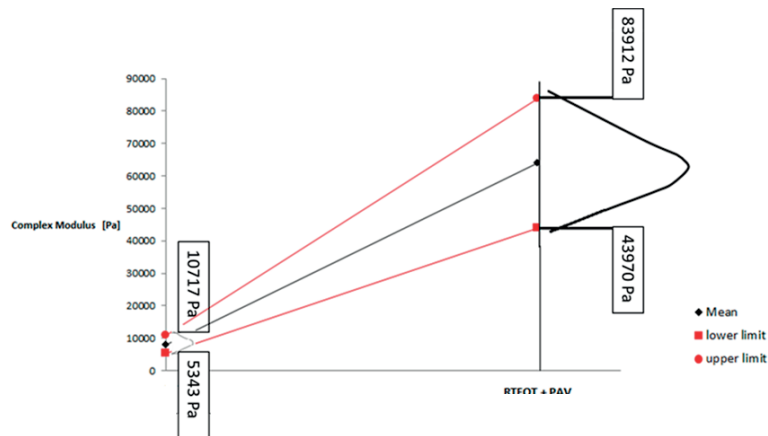


Figure 2.7 Evolution of complex modulus mean and variance over pavement service life using DSR results at 50°C at 1.01 Hz.

In Figures 2.6 and 2.7, it is important to note that the slopes of the evolution of the variances are different from the slope of the evolution of the mean.

For the purpose of the study it is important to notice that the higher variability for the aged binder could also have an impact on the mix design for mixtures containing RAP. Indeed, if RAP material is used for the fabrication of new mixtures the RAP binder may blend with the virgin bitumen and increase the variability of the rheological properties of the blend. Consequently the performance of the RAP mixtures may be characterised by higher uncertainties.

2.5. Summary of findings

This chapter aimed at analysing the variability that affects the rheological properties of binders when different ageing levels are considered. It represents a first step towards a probabilistic approach for mix design methods because the variability of the parameters involved is an essential part of the probabilistic process. Moreover, it will allow a comparison between the variability of the bitumen and mixtures properties once the methodology developed for the mix design optimization of asphalt mixtures containing RAP will be completed.

This chapter provided a statistical study, based on more than 250 tests, of the variability of binder rheology for different ageing levels, determining the probability distribution that represents the results, validated with a goodness of fit. Afterwards, a rigorous statistical analysis for the evaluation of the effects of different ageing levels on the variance of stiffness at low temperatures and complex modulus at medium and high temperatures of binder (F -test) was carried out. The ANOVA and the Welch test were used to determine whether the differences between means were significant or due to random error. From the results obtained, it is possible to conclude that:

- The normal probability distribution fits the trend of stiffness results at low temperatures. Also in the case of the complex modulus at medium and high temperatures, the results for the virgin binder and the binder artificially aged at each level are well represented by a normal probability distribution. The goodness of fit in every case verified this assumption.
- At low temperatures, the stiffness changes significantly for different ageing levels and thus the differences are not due only to random error. Material properties change with time and also after the fabrication process, while the variability remains constant. This means that the ageing does not produce an increase in the inherent variability of the binder at low temperatures, but the increase in variability results from external factors such as humidity and exposure, which are termed spatial variability.
- In the low-temperature domain, by analysing every single ageing level separately, it is possible to assess that the stiffness variance becomes more sensitive to temperature change (Table 2.5).
- At medium and high temperatures, the complex modulus results are significantly different, considering different ageing levels for all the frequencies chosen. The response of the binder under different traffic speeds changes significantly during pavement service life and is also subject to increasing variability, not only due to external factors but also to an inherent variability of the material itself. The variability is increased by not only spatial variability but also variability intrinsic to the material that changes with ageing.

The consequences of these conclusions lead to other considerations regarding pavement design or the mix design process. When the variability of one or more of the input parameters changes, this must be reflected in a change of the predicted reliability of a certain pavement structure. All methods currently base the calculation of reliability on the variability and values of the parameters set at the beginning of road construction and these are held constant throughout the life cycle. For the purpose of the study an important conclusion can be drawn regarding the mix design of mixtures containing RAP. The inclusion of RAP material and consequently RAP binder in the mixture may result in an increase of the uncertainties regarding the process. Therefore, it is necessary to consider that the results of a mix design calculation for RAP mixtures could be affected by higher variability.

Chapter 3

Binder blending charts

Knowing that the variability of the aged binder is higher than that of the virgin binder may have important consequences if the binders blend during a new mix phase. Thus, it becomes essential to understand how the aged and the virgin binder interact and to know whether the blend is homogeneous. This represents one of the main current challenges in the domain as demonstrated by the many efforts made in recent studies in this direction (Shirodkar et al. 2010, Nahar et al. 2012, Booshehrian 2013). In recent years the viscoelastic characteristics of the old and virgin bitumen have been computed (Al Qadi et al. 2007, Swiertz et al. 2011), and a new calibration of the parameters for the 2S2PID model has been defined for certain types of blends (Mangiafico et al. 2014). Also in this specific research domain there are many different methods available to determine the characteristics of a blend. In Europe for example the method is based on the penetration and softening point of the RAP and virgin binder (EN 13108-8:2005), while in the US the blending models take into consideration the initial rheological characteristics of the binders as described by the NCHRP Report 452 (2001). Both blending charts are represented by a straight line that expresses linearity with the variation of RAP binder in the blend. This chapter aims to investigate the rheology of binder blends composed of artificially aged binder or binder extracted and recovered from RAP and virgin bitumen. The objective is to provide a simulation of what happens in a new mix containing RAP assuming the hypothesis of 100% blending. Non-linear binder blending charts to predict the stiffness and complex modulus of binder blends at low, medium and high temperatures have been developed. The models comprise several variables at the same time: the stiffness or complex modulus of the virgin binder, the stiffness or complex modulus of the aged binder, the percentage of the aged binder and the loading frequency. A sensitivity analysis was carried out to understand which factors have the strongest influence on the results. The models, in a specific range of validity, provide a stiffness prediction for different binder blends in the low temperature (thermal cracking) and complex modulus in the medium and high temperature (rutting) domains. A comparison between blends with artificially-aged binder and binder extracted from RAP was made in order to highlight similarities or differences in the blending charts. This is because if the blending phenomenon between virgin and aged binder is detected by the methodology proposed in the next chapter, the behaviours artificially recreated in this chapter may lead to important information for the characterization of the rheology and behaviour of the blends.

3.1. Artificially-aged binder blending charts

Two unmodified virgin binders are used with different penetration grades (50/70 and 70/100). The main

characteristics of the binder are summarised in Table 1.3 in Chapter 1. Artificial ageing was performed using the Rolling Thin Film Oven Test, (RTFOT) (ASTM D 2872) and the Pressurized Aging Vessel, (PAV) (ASTM D6521). The resulting aged binder is subsequently mixed with a virgin binder to create blends with different percentages of artificially-aged binder.

Four blend combinations were prepared using several blending ratios:

- Combination 1: virgin bitumen 50/70 and artificially-aged bitumen 50/70
- Combination 2: virgin bitumen 70/100 and artificially-aged bitumen 70/100
- Combination 3: virgin bitumen 50/70 and artificially-aged bitumen 70/100
- Combination 4: virgin bitumen 70/100 and artificially-aged bitumen 50/70

For each combination the following procedure was undertaken to create the samples:

- The virgin binders 50/70 and 70/100 were heated at 136°C and 133°C respectively for one hour;
- The aged binder (RTFOT+PAV) was heated at 135°C for one hour (Poulikakos et al. 2013);
- The virgin and the aged binders were mixed together for two minutes. The time span of two minutes was chosen as a reasonable compromise to obtain a homogeneous mixture and simulate the mixing time in the plant.

The blend thus composed represents a mix of artificially-aged binder, simulating the RAP binder originating from the milled material, and virgin bitumen. All the blends were then subjected to short-term RTFOT ageing in order to simulate a new asphalt production. The steps are summarised in Figure 3.1.

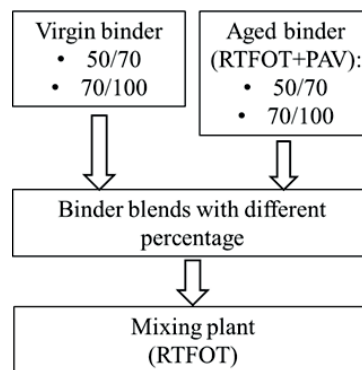


Figure 3.1 Sequence that reproduces creation of samples.

Several percentages of aged binder in the blend between 0 and 100% were tested for all the combinations in order to gain a better understanding of the stiffness and complex modulus evolution and take into account the possible behaviours between the black rock effect (Shirodkar et al. 2010) and full blending. The characteristics of the binders obtained after artificial ageing are summarised in Table 3.1.

Table 3.1 Characteristics of two artificially-aged binders.

	70/100 (RTFOT+PAV)	50/70 (RTFOT+PAV)
Penetration @ 25°C	26	19
R&B (Temp. °C)	62	58
IP [EN 12591]	-0.05	-1.34

3.1.1. Experimental plan

For each combination that corresponds to a different blend, several samples were prepared varying the content of aged binder and tested with the BBR in the low temperature domain and DSR in the medium and high temperature domains. The combinations and the experiments conducted are summarised in Table 3.2. The location of the measurement points in the experimental domain (Figure 3.2) was planned with the idea of obtaining the maximum information for three different ranges: low, medium and high percentage of aged binder.

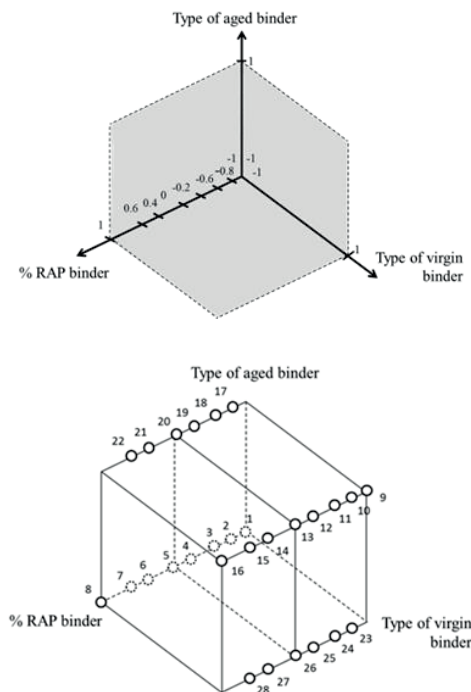


Figure 3.2 Distribution of measurement points in experimental domain.

Table 3.2 Summary of combinations and experiments conducted.

Combinations	Number of experiments	Type of virgin binder	Type of aged binder	Content of aged binder	BBR	DSR
virgin bitumen 50/70 and artificially-aged bitumen 50/70	1	50/70	50/70	0%	x	x
	2	50/70	50/70	10%	x	x
	3	50/70	50/70	20%	x	x
	4	50/70	50/70	40%	x	x
	5	50/70	50/70	50%	x	x
	6	50/70	50/70	70%	x	x
	7	50/70	50/70	80%	x	x
	8	50/70	50/70	100%	x	
virgin bitumen 70/100 and artificially-aged bitumen 70/100	9	70/100	70/100	0%	x	x
	10	70/100	70/100	10%	x	x
	11	70/100	70/100	20%	x	x
	12	70/100	70/100	40%	x	x
	13	70/100	70/100	50%	x	x
	14	70/100	70/100	70%	x	x
	15	70/100	70/100	80%	x	x
	16	70/100	70/100	100%	x	
virgin bitumen 50/70 and artificially aged bitumen 70/100	17	50/70	70/100	10%	x	x
	18	50/70	70/100	20%	x	
	19	50/70	70/100	40%	x	
	20	50/70	70/100	50%	x	x
	21	50/70	70/100	70%	x	x
	22	50/70	70/100	80%	x	x
virgin bitumen 70/100 and artificially-aged bitumen 50/70	23	70/100	50/70	10%	x	x
	24	70/100	50/70	20%	x	
	25	70/100	50/70	40%	x	
	26	70/100	50/70	50%	x	x
	27	70/100	50/70	70%	x	x
	28	70/100	50/70	80%	x	x

3.1.2. Research approach and methodology

The *accuracy* is a measure of how close the result of an experiment is to the true value; the *precision* (or variability) is a measure of how well the result has been determined (Bevington and Robinson 1969). The isolation of the measurement *accuracy* of the stiffness, as a component of the precision of the result

determination, is an important preliminary step. Indeed, the comparison between the accuracy and variability of the phenomenon will allow important information to be obtained concerning the experimental methodology and the sources of uncertainties in the results (heterogeneity of the blend). The measurement *accuracy* and the overall precision of the results were defined at low temperatures for the BBR measurements.

A *multiple regression analysis* is a technique for modelling and analysing several variables, when the behaviour of one dependent variable (in this case the BBR stiffness or the complex modulus) is a function of several independent variables (Mickey et al. 2009). It is a generalisation of the simple linear regression model. Its result is then a mathematical model expressing the relationship between a response variable y and k explanatory variables (Equation 3.1):

$$y = f(x_1, \dots, x_k) \quad (3.1)$$

A variable or factor is any parameter that has, in reality or all likelihood, an influence on the studied phenomenon. The factors are considered as the possible causes of the response. Usually when several variables are treated at the same time, they are expressed in different units, and it is thus convenient to convert them to a common scale to proceed with the model implementation. For this reason, the variables are standardised so that the coefficients are not dependent on the measurement unit (Bilal & Mc Cuen 2011).

The case of a first-degree multiple regression is expressed by Equation 3.2:

$$y_i = \beta_0 + \beta_1 x_{i1} + \beta_2 x_{i2} + \dots + \beta_k x_{ik} + \varepsilon_i \quad (3.2)$$

Then in a matrix form:

$$y = X\beta + \varepsilon \quad (3.3)$$

where:

y = vector ($n \times 1$) of the observation of the dependent variable (measurements of stiffness or complex modulus)

X = model matrix ($n \times (k+1)$)

β = vector ($(k+1) \times 1$) of unknown coefficients of the model

ε = vector ($n \times 1$) of stochastic errors

The *matrix of the model* is the matrix X , corresponding to a linear system of equations, which has one line per experiment and one column per coefficient of the model. Thus to calculate the coefficients it is possible to use the least square fit algorithm (Equation 3.4):

$$\beta = (X'X)^{-1} \cdot X'y \quad (3.4)$$

The matrix and vectors of the system are defined as (Equation 3.5):

$$y = \begin{bmatrix} y_1 \\ y_2 \\ \cdot \\ \cdot \\ y_n \end{bmatrix} X = \begin{bmatrix} 1 & x_{11} & x_{12} & \cdot & \cdot & x_{1k} \\ 1 & x_{21} & x_{22} & \cdot & \cdot & x_{2k} \\ \cdot & \cdot & \cdot & \cdot & \cdot & \cdot \\ \cdot & \cdot & \cdot & \cdot & \cdot & \cdot \\ 1 & x_{n1} & x_{n2} & \cdot & \cdot & x_{nk} \end{bmatrix} \beta = \begin{bmatrix} \beta_0 \\ \beta_1 \\ \beta_2 \\ \cdot \\ \beta_k \end{bmatrix} \quad (3.5)$$

The ratio between the effects (or coefficients) and the constant term allows the relative effects to be obtained (Equation 3.6).

$$\beta_i^* = \frac{\beta_i}{\beta_0} \quad (3.6)$$

The computation of the coefficients of the models is essential for carrying out a sensitivity analysis evaluating the effect that each parameter has on the final result. The coefficients of the model show the sensitivity of the related parameters as an average value over the entire domain of validity - the higher the coefficient, the greater the importance of the related parameter.

The first-degree model is the simplest linear model, therefore following the parsimony principle. The complexity of the model can be increased if necessary to ensure higher accuracy by adding interactions between the variables, as well as higher order terms (Bilal & Mc Cuen 2011).

The models are developed for different testing temperatures and the validity range is defined by the extremes of the experimental domain (Figure 3.2). In order to understand which type of model (linear, quadratic, cubic) best fits the data, the *goodness of fit* is evaluated by the use of R^2 , Analysis of Variance (ANOVA) and Lack of Fit.

The coefficient of determination (R^2) represents the proportion of total variability explained by the model, i.e. a measure of the adaptability of the model to the observed data. The formula to calculate R^2 (Equation 3.7) is similar to that of the simple regression, but it takes into account the variability given by all the regressors (Mickey et al. 2009).

$$R^2 = \frac{SQR}{SQT} \quad (3.7)$$

where:

SQR=Sum of the Square of Regression

SQT=Total Sum of the Square

It is possible to determine R^2 directly from the ANOVA table that gives other important indications about the goodness of fit of the chosen models. Moreover, in order to go a step further in the goodness of fit, a *Lack of Fit (LoF)* has also been conducted. LoF is one of the components of a partition of the sum of squares (SS) in the ANOVA and is used when replicate runs are available (i.e. more than one observation

on y at the same x design point). This test suggests that the error should be decomposed into two components (Equations 3.8-3.9): one part due to the LoF (SS_{LoF}) of the model and the second part due to the random error ("pure error") (SS_{pe}) (Bilal & Mc Cuen 2011).

$$SS(e) = SS_{pe} + SS_{LoF} \quad (3.8)$$

$$\sum_{i,j} (Y_{i,j} - \hat{Y}_l)^2 = \sum_{i,j} (Y_{i,j} - \bar{Y}_l)^2 + \sum_{i,j} (\bar{Y}_l - \hat{Y}_l)^2 \quad (3.9)$$

where:

$Y_{i,j}$ = real observations

\hat{Y}_l = estimated values

\bar{Y}_l = average of observations

If most of the error is attributed to LoF and not to the variability in the response (pure or random error) then the proposed model is not adequate. The LoF has been conducted only on the BBR results where more replicates were available.

3.1.2.1. Low temperature domain

For each experiment of the four combinations summarised in Table 3.2, three or more samples were tested at three different temperatures (-30, -20 and -10°C) with the BBR. The maximum stiffness registered during the test is considered. The measurement accuracy is calculated with the following equations:

$$\Delta S^2 = \sum \left(\frac{\partial S}{\partial x_i} \Delta x_i \right)^2 \quad (3.10)$$

$$\Delta^2 S = S^2 \left(\frac{\Delta^2 p}{p^2} + \frac{9\Delta^2 L}{L^2} + \frac{\Delta^2 b}{b^2} + \frac{9\Delta^2 h}{h^2} + \frac{\Delta^2 \delta(t)}{\delta(t)^2} \right) \quad (3.11)$$

$$\frac{\Delta S}{S} = \sqrt{\left(\frac{\Delta^2 p}{p^2} + \frac{9\Delta^2 L}{L^2} + \frac{\Delta^2 b}{b^2} + \frac{9\Delta^2 h}{h^2} + \frac{\Delta^2 \delta(t)}{\delta(t)^2} \right)} \quad (3.12)$$

Based on the accuracy of the different components (Superpave 1994) it is possible to determine the measurement accuracy with Equation 3.12.

Since the deformation is not constant and depends on the testing temperature, the measurement accuracy is calculated at -10, -20 and -30°C in a range determined by the maximum and minimum stiffness obtained, as shown in Table 3.3. Thus, it is possible to see that the stiffness accuracy remains almost constant (2.8 %) as the temperature changes.

Table 3.3 Stiffness accuracy calculated for each testing temperature.

	-10°C		-20°C		-30°C	
	Values for Smin.	Values for Smax.	Values for Smin.	Values for Smax.	Values for Smin.	Values for Smax.
S [MPa]	118	248	384	547	750	1230
δ [mm]	0.6776	0.3224	0.2082	0.1462	0.1066	0.0650
Δδ [μm]	0.155	0.155	0.155	0.155	0.155	0.155
(Δδ/ δ)²	5.23E-08	2.31E-07	5.54E-07	1.12E-06	2.11E-06	5.69E-06
ΔS/S	0.0281	0.0281	0.0281	0.0281	0.0281	0.0282

For the low temperature domain three variables were considered as input parameters of the multiple regression analysis:

- x_1 = the stiffness of the virgin binder
- x_2 = the stiffness of the aged binder
- x_3 = the percentage of aged binder in the blend

The main stiffness results are shown in Table 3.4, where the mean of three or more repetitions for each experiment is reported.

Table 3.4 Summary of stiffness results at different testing temperatures considering an average of three or more repetitions for each experiment.

Number of experiments	Stiffness of virgin binder (x_1)	Stiffness of aged binder (x_2)	Percentage of aged binder (x_3)	Results at -30°C [MPa]	Results at -20°C [MPa]	Results at -10°C [MPa]
1	50/70	50/70	0	934.00	419.75	119.50
2	70/100	70/100	0	1029.82	470.50	152.83
3	50/70	50/70	10	939.00	417.00	124.00
4	70/100	50/70	10	964.00	481.50	147.00
5	50/70	70/100	10	952.50	432.00	129.50
6	70/100	70/100	10	1006.70	479.67	160.00
7	50/70	50/70	20	970.00	435.00	140.33
8	70/100	70/100	20	959.67	482.33	173.00
9	70/100	50/70	20	971.33	487.50	151.33
10	50/70	70/100	20	1001.67	474.33	133.00
11	50/70	50/70	40	1010.00	436.00	142.33
12	70/100	70/100	40	1023.33	485.00	170.00
13	70/100	50/70	40	947.50	475.00	157.50
14	50/70	70/100	40	1001.50	497.00	167.00
15	50/70	50/70	50	900.75	440.67	148.25
16	70/100	70/100	50	1076.67	420.00	170.00
17	50/70	70/100	50	1020.33	493.00	168.00
18	70/100	50/70	50	982.67	504.33	171.33
19	50/70	50/70	70	975.50	454.50	158.00
20	70/100	70/100	70	905.33	494.67	164.00
21	70/100	50/70	70	834.00	512.00	177.40
22	50/70	70/100	70	1170.00	502.00	178.17
23	70/100	70/100	80	1046.67	492.00	197.33
24	50/70	50/70	80	960.50	468.67	167.33
25	50/70	70/100	80	1053.33	519.00	203.33
26	70/100	50/70	80	1003.33	515.00	181.00
27	50/70	50/70	100	942.40	468.40	167.00
28	70/100	70/100	100	1039.33	522.25	205.67

An evaluation of the variability of each combination led to the determination of the maximum and average Coefficient of Variation (COV) calculated at each temperature (Table 3.5). The COV is defined as the standard deviation of a random variable divided by its mean.

Table 3.5 Maximum and average variability at each testing temperature.

Temperature [°C]	COV_{max}	\overline{COV}
-10	12.9 %	5.3 %
-20	12.6 %	5.5 %
-30	12.0 %	6.6 %

Before going further with the analysis, it is important to evaluate the precision of the results compared with the accuracy of the measurements. As calculated with Equation 3.12 the systematic error is 2.8%. Observing the results in Table 3.5 it is possible to assert that the variability is higher than the accuracy of the device, even if the latter is not negligible. This is the first result that leads to the hypothesis of non-homogeneous materials, even with small percentages of aged binder in the blend.

From a first comparison between the results at -10°C for the stiffness of two different blends in Figure 3.3 (virgin and artificially-aged bitumen 50/70 and virgin and artificially-aged bitumen 70/100) it is possible to detect approximately the same behaviour: a rapid increase of the stiffness with up to 20% of aged binder, a central plateau of different amplitude for the two blends in which the stiffness remains almost constant, and then a rapid increase for high percentages of aged binder content. This result is in accordance with other cases treated in recent studies (Hussain & Yanjun 2013).

For the blend composed of the whole bitumen 70/100 (combination 2) the stiffness remains almost constant between 20% and 70% of aged bitumen in the blend. The “plateau region” for the blend composed of the whole bitumen 50/70 (combination 1) is smaller: it appears between 20 and 40%.

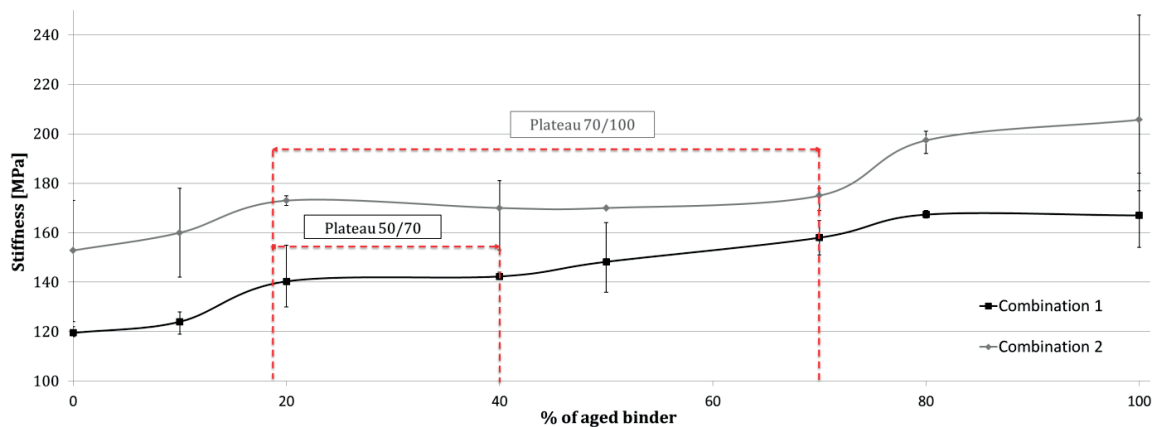


Figure 3.3 Stiffness evolutions for blend combinations at -10°C.

The existence of the plateau region leads to the hypothesis of a *latent stiffness*, i.e. the components of the aged bitumen float in the blend, but their effect is absorbed and cushioned by the new bitumen. When the percentage of aged binder becomes predominant, a network formed among aged binder particles makes the stiffness increase rapidly. This observed phenomenon finds its explanation in the microscopic study of

the blend, where the investigation of the compound of new and aged bitumen reveals that the blend is non-homogeneous (El Beze 2008 and Nguyen 2009).

From the statistical study discussed in Chapter 2 it emerges that the difference between ageing levels (virgin, RTFOT and RTFOT+PAV) is statistically significant at -10 and -20°C and this is a necessary condition to develop the stiffness prediction models. The LSD results show that the only case in which the means between two groups do not change is at -30°C between the RTFOT and RTFOT+PAV results. Since the stiffness does not change, the difference in its value is due only to the random error. For very low temperatures the mean value of the stiffness after RTFOT does not change as the aging level of the binder increases. Therefore the prediction models are developed only for two temperatures (-10 and -20°C).

Figure 3.3 provides information regarding the degree of the model required for the multiple regression analysis. Indeed, even if a second-degree model was tested and it fits the data, in order to include the plateau region and highlight the presence of a *latent stiffness* a third degree model with interactions is preferred.

After the standardisation of the variables, a model matrix is determined with all the coefficients of the model. In this three-factored experiment the stiffness model can be partitioned into 10 coefficients as shown in Table 3.6.

Table 3.6 Summary of coefficients used in model.

Coefficient notation	Type of coefficient	Coefficient meaning
β_0	Constant factor term	Constant
β_1	Main effects	Stiffness of virgin binder
β_2		Stiffness of aged binder
β_3		Percentage of aged binder
β_{12}	Two-way interaction effects	Stiffness virgin/aged binder
β_{13}		Stiffness virgin binder/ percentage of aged binder
β_{23}		Stiffness aged binder/percentage of aged binder
β_{123}	Three-way interaction effect	Stiffness virgin binder/ Stiffness aged binder/ percentage of aged binder
β_{33}	Second-degree factor term	Second-degree coefficient related to percentage of aged binder
β_{333}	Third-degree factor term	Third-degree coefficient related to percentage of aged binder

The coefficients of the model are reported in Table 3.7 and the measure of importance of the different parameters given by the sum of the contribution of the relative effects is shown in Figure 3.4.

Table 3.7 Coefficients of models at different testing temperatures.

	Coefficients of model -10°C	Coefficients of model -20°C
β_0	163.96	480.16
β_1	7.94	9.65
β_2	7.06	12.15
β_3	23.61	17.89
β_{12}	-2.34	-10.13
β_{13}	-5.01	-15.65
β_{23}	4.66	9.45
β_{123}	-7.66	-0.76
β_{33}	1.22	-6.30
β_{333}	10.17	3.47

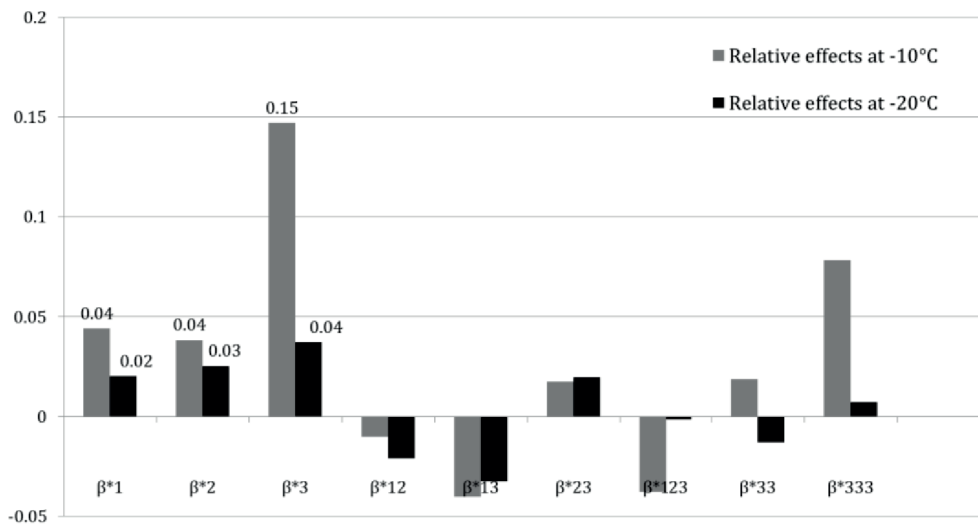


Figure 3.4 Relative effects (β_i^*) at -10°C and -20°C.

As can be seen, the relative effects of the factors vary with the temperature. At -10°C the most important factor is the percentage of aged binder in the blend (β_3). Consequently there are impacts on the interaction terms (β_{13} , β_{123}), which means that the shape of the model curve changes as the values of the variables change, and on the third-degree term (β_{333}). It is important to notice that the effects of the stiffness of the virgin binder and the aged binder are almost equivalent and they are significantly lower than the effect of the percentage of aged binder in the blend. Thus, the stiffness of the blend is more influenced by the amount of aged binder than by the rheological characteristics of the aged binder. This is a positive result

since it is easier to control the amount of RAP in the mixture than the rheological characteristics of its binder. If the temperature decreases (-20°C) the results change. Although the most important parameter is still the percentage of aged binder in the blend, the effect decreases significantly. This is in accordance with the results obtained in Chapter 2. If the temperature decreases the ageing level of the binder becomes more and more negligible in the stiffness results, until there is an absence of significant difference at -30°C where the mean values for different ageing levels RTFOT and RTOFT+PAV can be considered the same.

An ANOVA was computed to estimate the goodness of fit of the models and the results are shown in Table 3.8. For both temperatures the chosen models give a very low p value ($p \ll 0.05$) indicating that there is no evidence of discrepancy between the data and the models. In both cases *the coefficients of determination* (R^2) reveal a very good fit of the models to the distribution of the real data.

Table 3.8 ANOVA tables for models developed at -10 and -20°C.

ANOVA sources -10°C	SS*	df*	MS*	F*	p-value	R ²
Regression (3 rd degree)	1.940E+07	10	1.940E+06	2 409.33	9.2E-90	0.994
Residual	6.039E+04	75	805.19			
Total	1.946E+07	85				
ANOVA sources -20°C	SS*	df*	MS*	F*	p-value	R ²
Regression (3 rd degree)	2.940E+06	10	2.940E+05	1840.8	4.4E-113	0.997
Residual	1.677E+04	105	159.7			
Total	2.957E+06	115				

*SS=Sum of the Squares, df=degree of freedom, MS=Mean Squares, F=SS/MS

In order to ascertain which part of the total error is due to the regression and which is due to the random error the *Lack of Fit* (LoF) is computed (Table 3.9).

Table 3.9 LoF results at -10 and -20°C.

-10°C	SS	df	MS	$\frac{MS_{LoF}}{MS_{pure\ error}}$	p
LoF	3.350E+03	29	116	0.654	0.8988
Pure error	1.342E+04	76	177		
Residue	1.677E+04	105	160		
-20°C	SS	df	MS	$\frac{MS_{LoF}}{MS_{pure\ error}}$	p
LoF	4.875E+03	19	257	0.260	0.9990
Pure error	5.551E+04	56	991		
Residue	6.039E+04	75	805		

Since repetitions for each combination are available, the LoF allows the decomposition of the error into the pure error (random) and the error due to the model (LoF). If the ratio $\frac{MS_{LoF}}{MS_{pure\ error}} < 1$ means that the lack of fit is improbable.

The models allow the blending chart (Figures 3.5 and 3.6) for each blend combination to be predicted at every temperature.

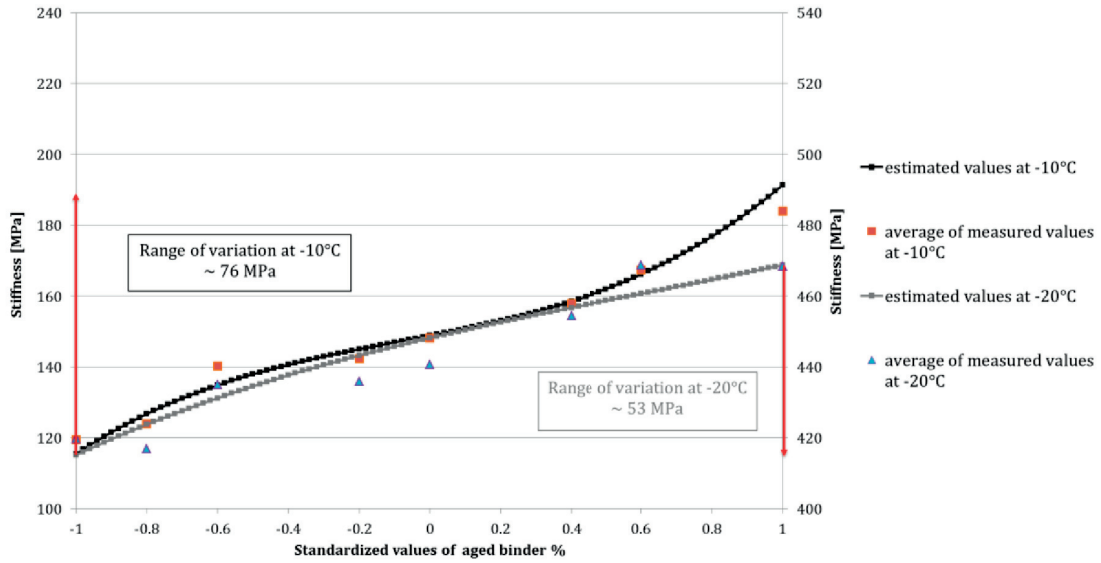


Figure 3.5 Stiffness prediction model for blend combination 1 at -10 and -20°C.

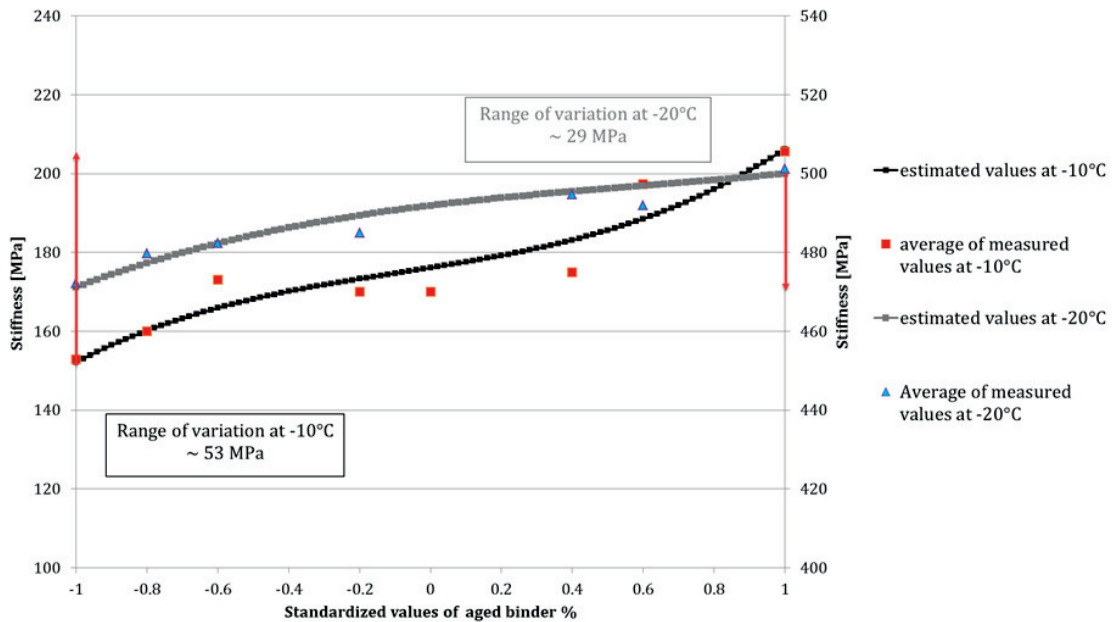


Figure 3.6 Stiffness prediction model for blend combination 2 at -10 and -20°C.

From Figures 3.5 and 3.6 it can be seen that even if the general trend is the same, there are some differences in the behaviour of different blends. For instance the range of variation is not the same. At both temperatures the range of stiffness variation of the 50/70 blend (combination 1) is higher than the 70/100 blend (combination 2) and for the latter the plateau region is more evident. The range of variation at -20°C is smaller than at -10°C because at this temperature the impact of each effect is reduced as demonstrated by the sensitivity analysis (Figure 3.4). In the case of the blending of two different binders the distortions at the extremes points are not negligible. Thus the models are considered valid in the range tested with between 10% and 80% of aged binder. The blending charts in these cases are shown in Figures 3.7 and 3.8.

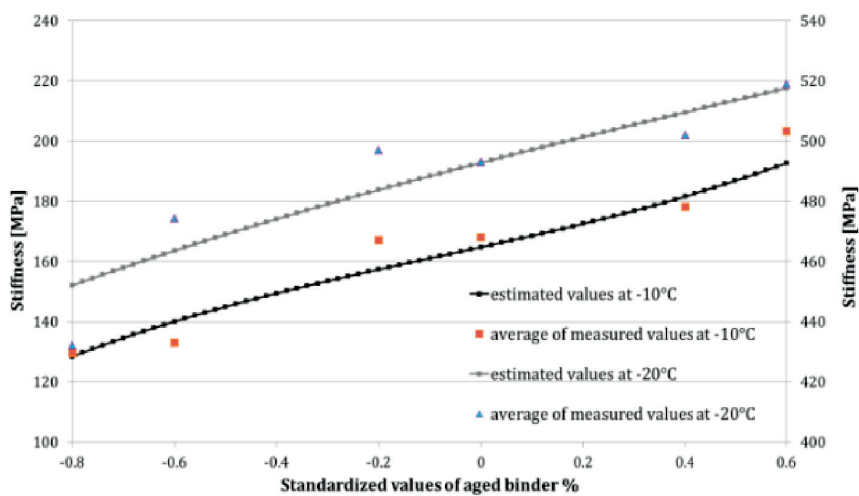


Figure 3.7 Stiffness prediction model for virgin bitumen 50/70 and aged binder 70/100 blend (combination 4).

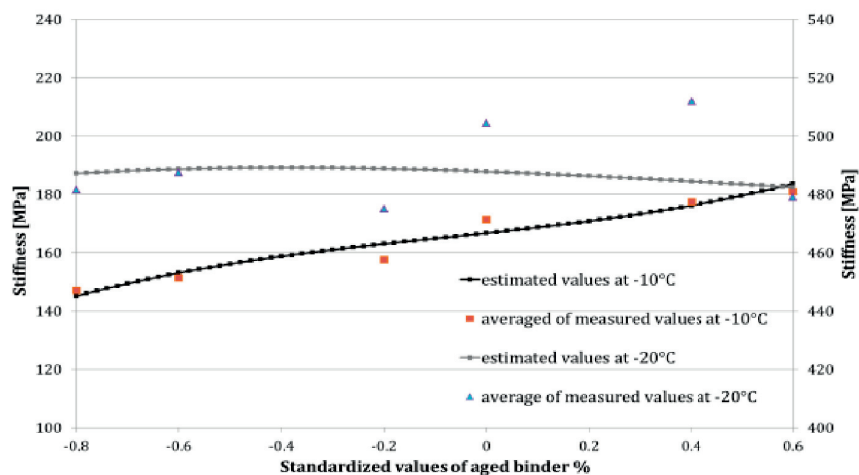


Figure 3.8 Stiffness prediction model for virgin bitumen 70/100 and aged binder 50/70 (combination 3).

When the more flexible bitumen (virgin bitumen 50/70) and the stiffer one (aged binder 70/100) are combined (combination 4 see Figure 3.7), as expected the stiffness increases very rapidly and the plateau region at -10°C is reduced to just an inflection point. The curve becomes almost a straight line parallel with the curve obtained at -20°C .

For the blend composed of virgin bitumen 70/100 and aged binder 50/70 (combination 3 see Figure 3.8) the results are different. The main difference is at -20°C where the stiffness decreases instead of increasing. It is the only case where the stiffness decreases as the percentage of aged binder in the blend increases because the stiffness of the aged binder is a little bit lower than that of the virgin binder. This result constitutes a case that is probably not so common but requires analysis. If the aged binder is less stiff than the virgin binder used for the new mix, it is necessary to study a specific case of blending chart, taking into account the fact that the stiffness could decrease as the amount of aged binder in the blend increases.

The empirical models (Figures 3.5, 3.6, 3.7 and 3.8) should converge two by two at the points corresponding to 0% and 100% of aged binder. For instance, the blend composed of the virgin bitumen 70/100 and the aged binder 50/70 should be characterised by the same results as those for the blend composed of virgin bitumen 50/70 and aged binder 50/70 if 100% of aged binder is considered. Some experimental convergences are observed, but in most cases this does not occur. The experimental inaccuracy is not sufficient to explain the lack of convergence at the extreme points. The results exhibit a large dispersion due to a large variability of the phenomenon and not only due to the instrument measurement uncertainty. Since the microscopic investigation revealed that the blend is chemically non-homogeneous (El Beze 2008 and Nguyen 2009) the uncertainty in the final response is high, especially at -20°C .

3.1.2.2. Medium and high temperature domain

At medium and high temperatures the complex modulus and the phase angle of the blending were investigated using the DSR to test the blend combinations reported in Table 3.2.

A nonlinear multiple regression model was developed for the prediction of the rheological properties at 30, 40, 50 and 60°C , considering several variables at the same time: the complex modulus of the virgin and aged binders, the loading frequency, the testing temperature and the percentage of aged binder in the blend. A sensitivity analysis was carried out to ascertain which factors have the strongest influence on the results.

The master curves of the complex modulus and phase angle (Figure 3.9) were firstly computed on the virgin binders, testing the *frequency sweep* (21 frequencies tested from 0.16 to 16.7 Hz) with the DSR (Anderson 1994) and using the Time-Temperature Superposition (TTS) principle (Ferry 1980) with a reference temperature of 20°C .

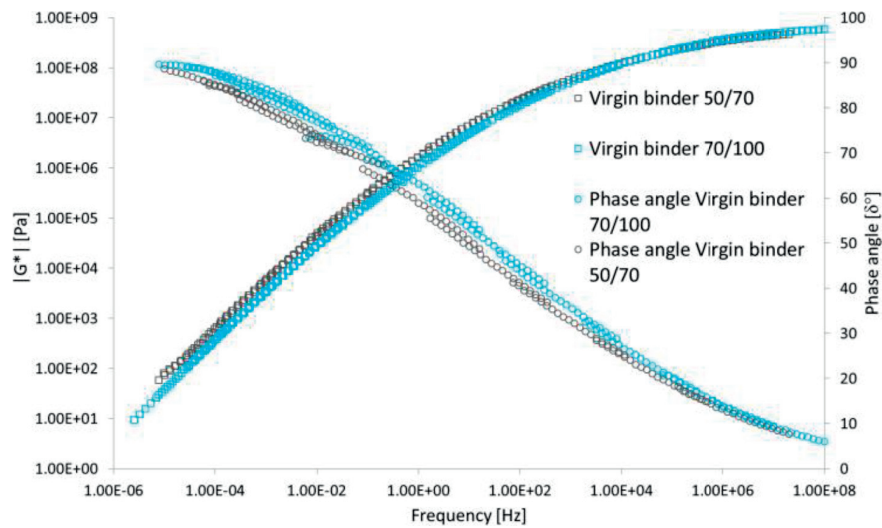


Figure 3.9 Master curves of complex modulus and phase angle of virgin binders 50/70 and 70/100
($T_{ref}= 20^{\circ}\text{C}$).

Shear strains or stresses were applied to test specimens in the DSR by mounting the test specimens between parallel plates. All the tests were conducted in the Linear Viscoelastic Region (LVR), determined in Chapter 2. Subsequently, several frequency sweeps (21 frequencies tested from 0.16 to 16.7 Hz) were conducted at 30, 40, 50 and 60°C measuring the complex modulus and phase angle. A multiple regression model was developed for every testing temperature. These models allowed not only the observation of the evolution of the importance of the parameters involved, as the temperature increases, but also the prediction of the complex modulus and phase angle once the initial parameters were set. The variables considered were:

- x_1 = complex modulus of virgin binder
- x_2 = complex modulus of aged binder
- x_3 = percentage of aged binder in blend
- x_4 = loading frequency

The values of the complex modulus and phase angle at each testing temperature for each blend were extrapolated from the frequency sweep at 1 Hz. The results are summarised in Table 3.10.

Table 3.10 Results of $|G^*|$ for all blends at 50°C and 1 Hz.

Number of combination	Type of virgin binder	Type of aged binder	Content of aged binder	Complex modulus $ G^* $ [Pa]	Phase angle (δ) [°]
1	50/70	50/70	0%	19 104	76,1
2	50/70	50/70	10%	20 520	76,2
3	50/70	50/70	20%	21 706	71
4	50/70	50/70	40%	51 582	69,3
5	50/70	50/70	50%	58 907	65
6	50/70	50/70	70%	102 800	63,6
7	50/70	50/70	80%	115 520	63,3
8	70/100	70/100	0%	7 009	84,6
9	70/100	70/100	10%	8 533	80,2
10	70/100	70/100	20%	10 964	81,5
11	70/100	70/100	40%	20 291	79,3
12	70/100	70/100	50%	23 770	76,4
13	70/100	70/100	70%	32 306	74
14	70/100	70/100	80%	55 398	72,1
15	50/70	70/100	10%	17 267	82,1
16	50/70	70/100	50%	26 933	66,4
17	50/70	70/100	70%	-	-
18	50/70	70/100	80%	61 539	63,2
19	70/100	50/70	10%	14 380	73,3
20	70/100	50/70	50%	32 207	73,5
21	70/100	50/70	70%	98 642	63,7
22	70/100	50/70	80%	-	-

As can be seen from Table 3.10, the addition of small quantities of RAP bitumen does not significantly change the complex modulus of the blend. Indeed, up to 20% of RAP bitumen content (combinations 1-2-3 and 8-9-10) the complex modulus of the blend does not exhibit significant variation. For the phase angle, small oscillations occur up till 10% of RAP binder in the blend, after which the phase angle starts to decrease more rapidly.

After testing all the possible models fitting the data, a second-degree model with interactions was chosen since it showed the highest goodness of fit. All the complex modulus prediction models were developed by applying the least square fit technique with multiple variables. These can be divided into several sections: the constant factor term (a_0), four main factor terms ($a_1=|G^*|$ of the virgin binder, $a_2=|G^*|$ of the aged binder, a_3 =percentage of aged binder, a_4 = frequency), six two-way factor interaction terms (a_{12} , a_{13} , a_{23} , a_{14} , a_{24} , a_{34}), three three-way factors (a_{123} , a_{124} , a_{234}), one four-way factor (a_{1234}) and two second-degree

factor terms (a_{33} , a_{44}). The values of all the coefficients at every testing temperature are summarised in Tables 3.11 and 3.12.

Table 3.11 Coefficients of models for complex modulus prediction.

Coefficients	30°C	40°C	50°C	60°C
a_0	2 426 798	731 198	190 651	29 220
a_1	-217 312	-134 328	-24 684	-10 707
a_2	-31 930	-52 840	-41 047	-16 905
a_3	524 911	303 162	144 309	18 359
a_4	1 155 825	480 596	142 377	7 528
a_{12}	58 044	76 673	-5 465	13 917
a_{13}	10 500	-73 404	-18 626	-11 401
a_{14}	-143 738	-89 364	-14 778	-6 380
a_{23}	-16 432	-982	-11 071	-7 164
a_{24}	30 131	-41 788	-38 839	-19 015
a_{34}	28 507	212 570	128 702	16 243
a_{123}	132 491	98 814	-18 095	20 024
a_{124}	10 327	54 427	-7 694	17 390
a_{134}	-11 968	-50 611	-15 577	-15 416
a_{1234}	125 693	72 505	-27 134	18 009
a_{33}	127 833	67 197	6 756	1 206
a_{44}	-756 757	-204 564	-34 473	-15 894

Table 3.12 Coefficients of models for phase angle prediction.

Coefficients	30°C	40°C	50°C	60°C
a_0	34,75	52,41	65,45	75,12
a_1	3,65	2,10	2,09	1,66
a_2	1,69	1,44	1,90	3,38
a_3	-8,08	-7,61	-7,06	-4,56
a_4	-8,53	-6,34	-4,88	-0,34
a_{12}	-0,43	0,06	0,31	-0,91
a_{13}	-1,00	-0,59	0,21	-3,04
a_{14}	1,59	-1,82	-0,68	-1,45
a_{23}	-1,43	-0,21	-0,13	2,58

a ₂₄	1,92	0,29	-0,82	3,49
a ₃₄	1,69	-2,52	1,10	-2,19
a ₁₂₃	-1,07	-1,33	2,40	-1,25
a ₁₂₄	1,55	-0,97	-1,13	-1,94
a ₁₃₄	-1,03	-2,01	0,09	-1,39
a ₁₂₃₄	1.39	1,32	0,24	0,85
a ₃₃	-0.24	3,59	3,24	1,32
a ₄₄	10.30	2,52	0,33	6,08

The results of the R² and ANOVA for the type of model chosen are shown in Table 3.13 for the complex modulus and in Table 3.14 for the phase angle.

Table 3.13 ANOVA table and R² for second-degree model at every temperature for complex modulus.

30°C	SS ¹	df ¹	MS ¹	F ¹	P ¹	R ²
2° degree	5,1E+14	17	3,0E+13	3,0E+02	2,7E-144	0,96
Residual	2,3E+13	226	1,0E+11			
Total	5,3E+14	243				
40°C	SS ¹	df ¹	MS ¹	F ¹	P ¹	R ²
2° degree	5,5E+13	17	3,2E+12	2,3E+02	2,3E-138	0,94
Residual	3,3E+12	239	1,4E+10			
Total	5,8E+13	256				
50°C	SS ¹	df ¹	MS ¹	F ¹	P ¹	R ²
2° degree	4,6E+12	17	2,7E+11	1,7E+02	6,1E-144	0,91
Residual	4,7E+11	300	1,6E+09			
Total	5,1E+12	317				
60°C	SS ¹	df ¹	MS ¹	F ¹	P ¹	R ²
2° degree	1,9E+11	17	1,1E+10	2,6E+02	1,8E-151	0,95
Residual	1,1E+10	256	4,2E+07			
Total	2,0E+11	273				

¹SS: Sum of the squares; df: degree of freedom; MS: Mean Squares; F-statistic; p-value, R²= coefficient of determination

Table 3.14 ANOVA table and R² for second-degree model at every temperature for phase angle.

30°C	SS ¹	df ¹	MS ¹	F ¹	P ¹	R ²
2° degree	5,9E+05	17	3,5E+04	7,4E+02	1,4E-187	0,98
Residual	1,1E+04	226	4,7E+01			
Total	6,0E+05	243				
40°C	SS ¹	df ¹	MS ¹	F ¹	P ¹	R ²
2° degree	9,5E+05	17	5,6E+04	3,6E+02	1,9E-159	0,96
Residual	3,7E+04	239	1,6E+02			
Total	9,9E+05	256				
50°C	SS ¹	df ¹	MS ¹	F ¹	P ¹	R ²
2° degree	1,7E+06	17	9,7E+04	1,1E+03	3,1E-265	0,98
Residual	2,7E+04	310	8,9E+01			
Total	1,7E+06	327				
60°C	SS ¹	df ¹	MS ¹	F ¹	P ¹	R ²
2° degree	1,8E+06	17	1,0E+05	1,6E+02	8,9E-125	0,91
Residual	1,7E+05	256	6,7E+02			
Total	2,0E+06	273				

¹SS: Sum of the squares; df: degree of freedom; MS: Mean Squares; F-statistic; p-value, R²= coefficient of determination

For all the models at every temperature the ANOVA table shows p-values <0.05 and R² in every case is higher than 0.9; the developed models thus accurately fit the real data set.

After having carried out the calculation of the relative effects with Equation 3.6, it was possible to determine which parameters most influence the result by summing all the contributions (in absolute value) provided by the main effects and the interaction terms related to the corresponding main effect. This was particularly important at high temperatures (50 and 60°C) because the interaction terms were not negligible and it would not be possible to determine the importance of a parameter by only looking at the main effect. The fact that the interactions between the main effects increase as the temperature increases means that the non-linear components in the model, which describes the physical phenomena occurring, increase. Note that, in this case of multiple regression, the nonlinearities are developed in five dimensions (four independent variables and one dependent variable). The results regarding the *measure of importance* for the complex modulus are shown in Figure 3.10 and for the phase angle in Figure 3.11.

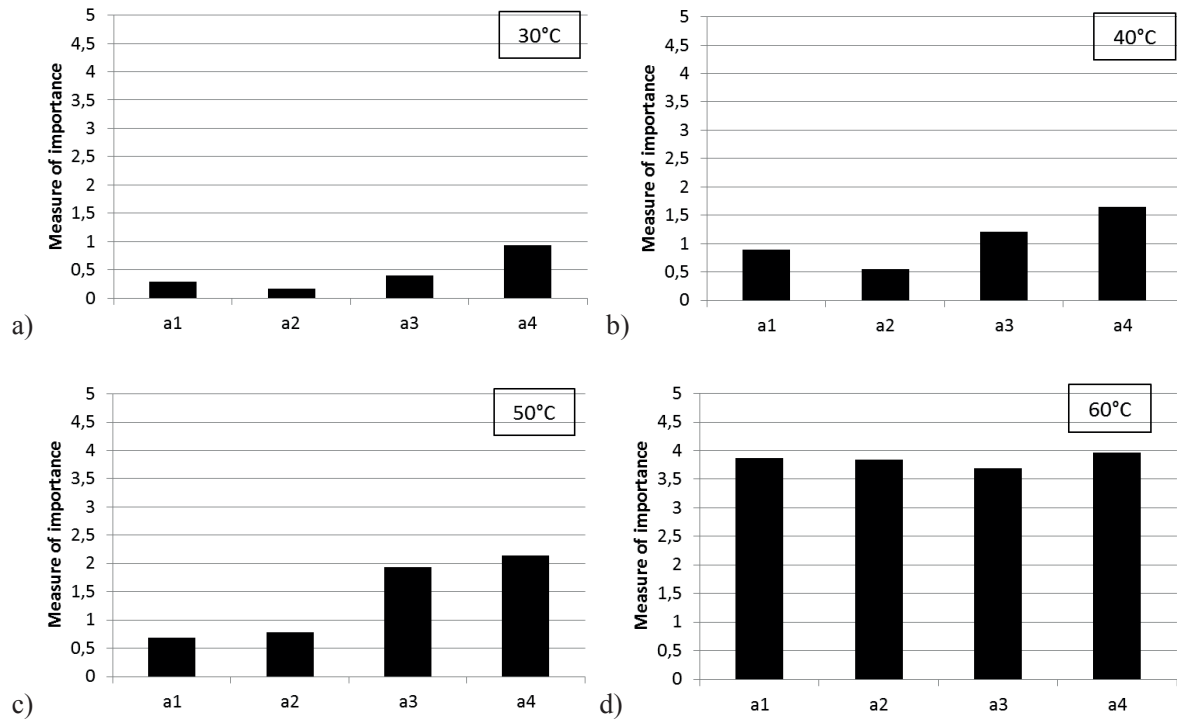


Figure 3.10 Relative effects on $|G^*|$ blend results at a) 30; b) 40; c) 50 and d) 60°C (a1= type of virgin binder, a2 = type of aged binder, a3 = % of aged binder, a4 = load frequency).

From a comparison of Figure 3.10 and Table 3.11 it is possible to draw certain conclusions regarding the complex modulus:

- The general trend showed that the importance of each parameter increases as the temperature rises. This confirms that in the high temperature domain binders are generally more sensitive to blending than in the low temperature domain (Kandhal et al. 1997). When the temperature of 60°C is exceeded all the effects exhibited a similar importance.
- The effect of the complex modulus of the virgin binder (a_1) is, as expected, negative, (Table 3.11) which means that the lower the complex modulus of the virgin binder, the lower the complex modulus of the blend will be.
- The same trend was observed for the complex modulus of the aged binder (a_2); the effect is negative. It is possible to state that the complex modulus of the virgin binder is more relevant than the complex modulus of the aged binder for 30 and 40°C, but for 50°C and 60°C they become similar.
- The percentage of aged binder (a_3) and the loading frequency (a_4) are the most important factors until 50°C. As the temperature rises, both effects increase. This is particularly apparent for the

effect of the percentage of aged binder that increases considerably as the temperature changes until the effect becomes as important as that of the load frequency at 50°C.

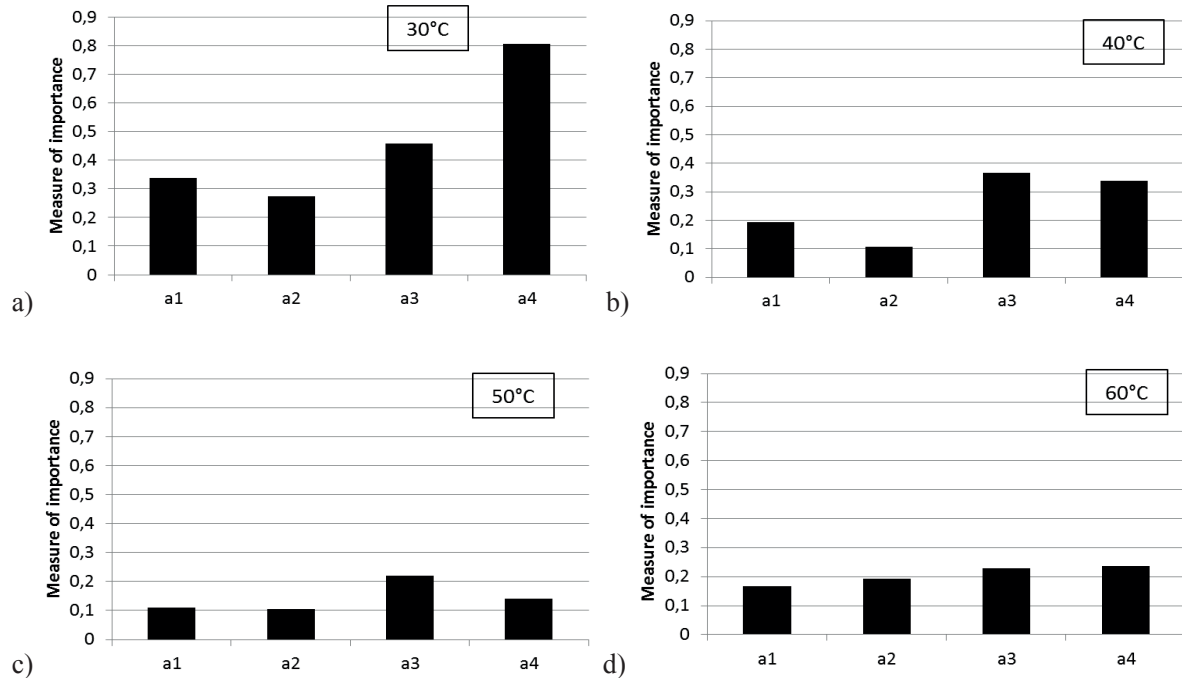


Figure 3.11 Relative effects on phase angle results at a) 30; b) 40; c) 50 and d) 60°C (a1= type of virgin binder, a2 = type of aged binder, a3 = % of aged binder, a4 = load frequency).

From a comparison of Figure 3.11 and Table 3.12, it is possible to draw certain conclusions regarding the phase angle:

- The general trend showed that the importance of each parameter decreases as the temperature rises. When the temperature of 60°C is exceeded all the effects showed similar importance, slightly higher than that at 50°C.
- The effects of the complex modulus of the virgin and aged bitumen are positive (Table 3.12), which means that if the complex modulus of both increases the phase angle also slightly increases.
- The percentage of aged bitumen and the load frequency have the strongest impact on the phase angle, meaning that if the amount of aged binder in the blend or the loading frequency increases, the phase angle decreases significantly. The loss modulus (G') will become predominant in relation to the storage modulus (G''), indicating a greater hardening of the blend as the quantity of aged binder or the load frequency increases. Moreover at 40, 50 and 60°C the percentage of aged binder has an effect comparable to or higher than that of the frequency, which indicates the comparative significance of this parameter.

Summarising, after the results have been obtained for the sensitivity analysis, it is possible to assert that the complex modulus and phase angle of the blend are influenced more by the amount of aged bitumen than by its rheology at medium and high temperatures (with the only exception being for the complex modulus at 60°C where all the parameters show similar significance). This represents a remarkable conclusion since it is more difficult to control the characteristics of the RAP binder during the mix production than to control the amount of RAP. The same assertion is valid if a comparison is made between the effects of virgin and aged binder properties. The rheological characteristics of the virgin binder have greater significance than those of the aged binder at 30 and 40°C. The scenario changes when the temperature of 50°C is exceeded, as then the effect of the aged binder becomes comparable to or higher than that of the complex modulus of the virgin binder. By calibrating the second-degree model at every testing temperature with the coefficients in Tables 3.11 and 3.12 it is possible to predict the final complex modulus and phase angle. A 2D graphical representation, where only the percentage of aged binder is varied and the other parameters are kept constant (70/100 virgin binder, 70/100 RAP binder and load frequency equal to 1 Hz), is provided in Figure 3.12 for the complex modulus and in Figure 3.13 for the phase angle.

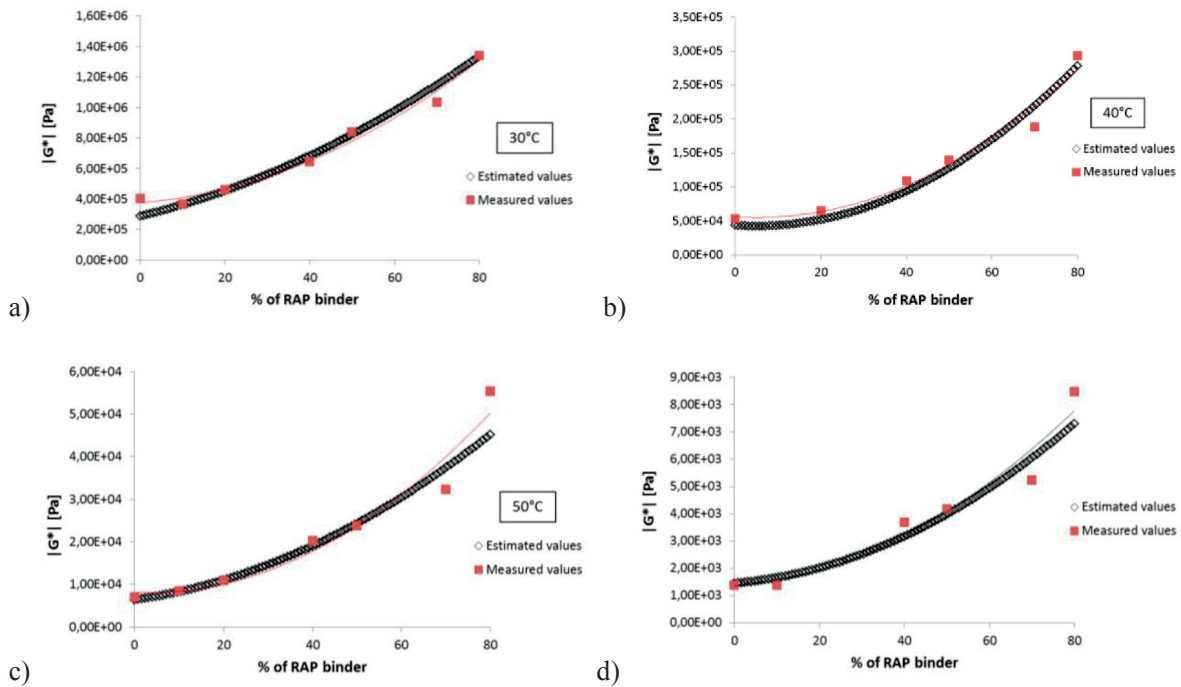


Figure 3.12 Example of $|G^*|$ prediction model for combination 2 at a) 30; b) 40; c) 50 and d) 60°C at 1 Hz.

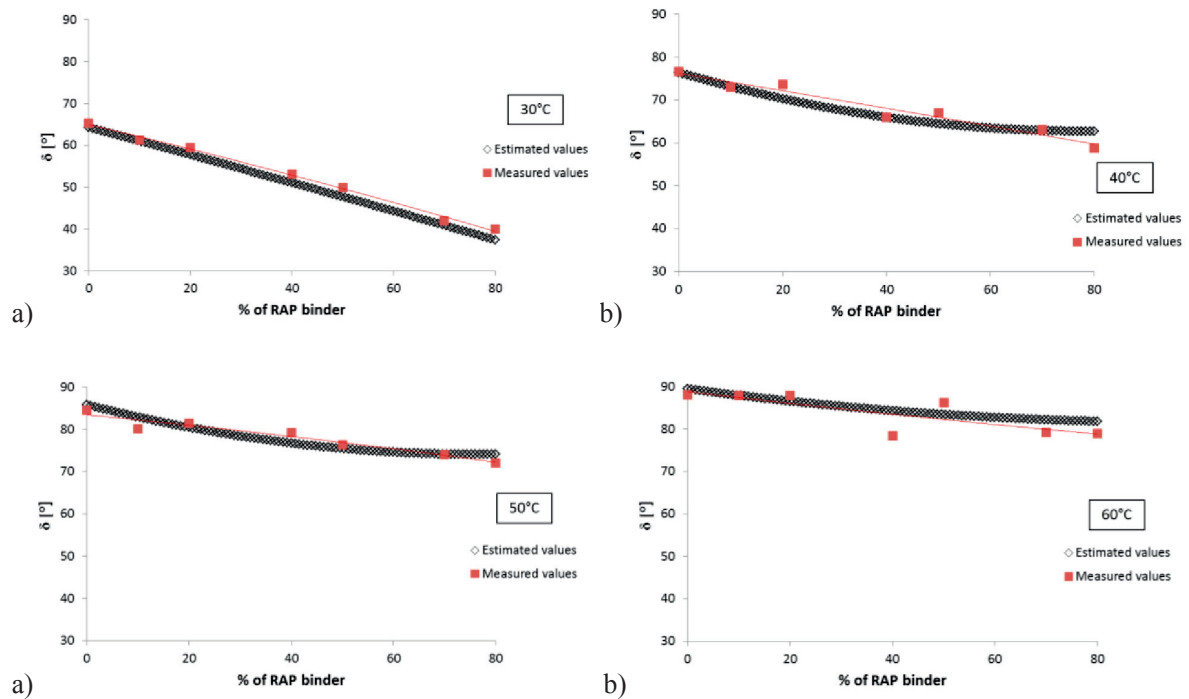


Figure 3.13 Example of δ prediction model for combination 2 at a) 30; b) 40; c) 50 and d) 60°C at 1 Hz.

Regarding the complex modulus prediction (Figure 3.12), with the exception of the case at 30°C where the curve is represented by an almost straight line, for higher temperatures (40, 50, 60°C) the relationship shows higher nonlinearities. The curves show an upward facing concavity and in those cases with a small quantity of aged binder in the blend the complex modulus does not vary significantly. The same trend was observed for all the blend combinations tested. In the case of the phase angle, an almost linear behaviour was observed at 30°C. As expected based on the sensitivity analysis results, the impact of the percentage of aged binder is stronger at 30 and 40°C; indeed the decrease of the phase angle is more evident at these temperatures, while it becomes negligible at 60°C.

3.2.RAP binder blending charts

One step further was made by testing the blend composed of the binder extracted and recovered from RAP 0/16 mm and the unmodified virgin binder 70/100. The RAP binder characteristics are summarised in Table 1.3 in Chapter 1 and the same procedure for the sample creation as described in Section 3.1 was adopted. Several combinations with different RAP binder percentages were tested. Figures 3.14 and 3.15 compare the blending charts obtained with artificially-aged binder and the binder extracted and recovered from RAP. The combination with the artificially aged binder 70/100 and the virgin bitumen 70/100 was

chosen for the comparison because the binder 70/100 aged (RTFOT+PAV) has the same penetration of the bitumen extracted and recovered from RAP (26 10⁻¹ mm).

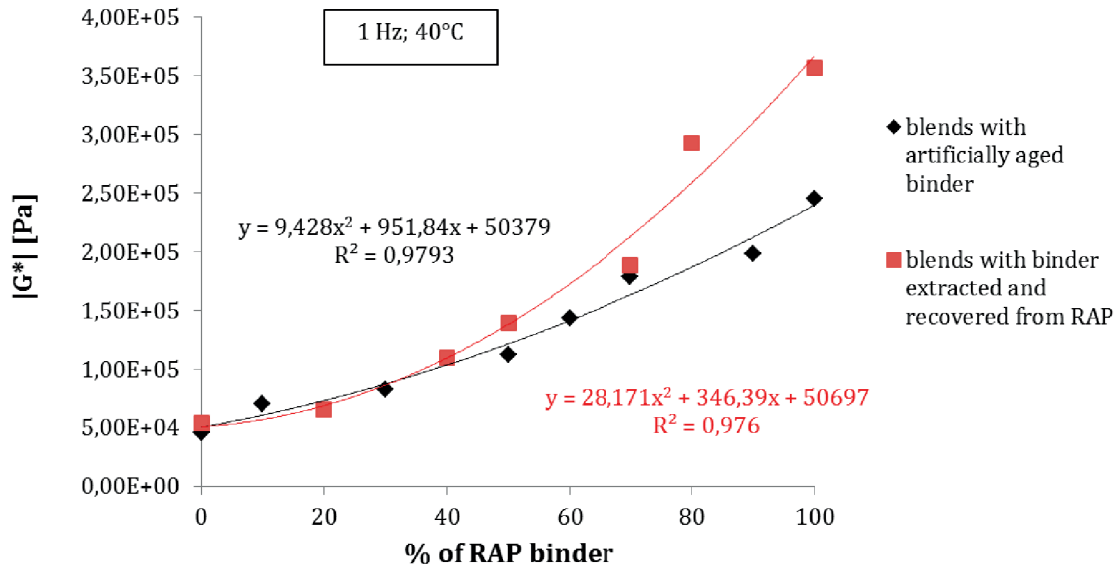


Figure 3.14 Binder blending charts at 40°C obtained with artificially-aged binder and binder extracted and recovered from RAP.

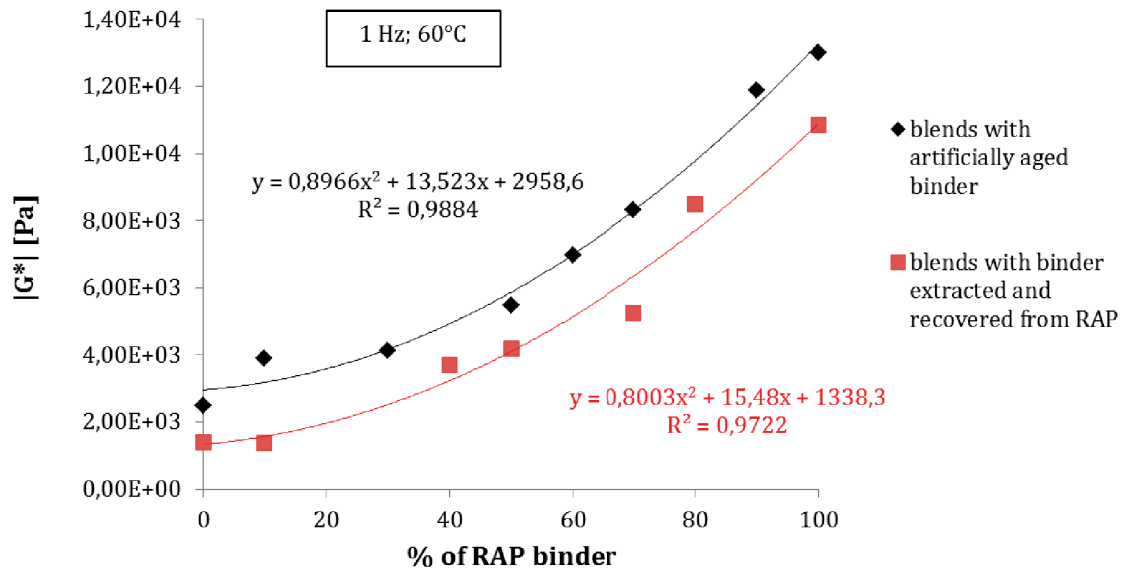


Figure 3.15 Binder blending charts at 60°C obtained with artificially-aged binder and binder extracted and recovered from RAP.

From Figures 3.14 and 3.15 it is possible to see that also for the blends with the binder extracted and recovered from RAP the second-degree models chosen to predict the binder blending charts fit the data. However, depending on the rheological characteristics of the RAP binder it is possible to obtain different final results and different blending charts. This highlights another important point: the traditional artificial ageing (RTFOT+PAV) cannot be considered reliable for predicting bitumen ageing in a general sense. Moreover, the RAP binder was subjected to extraction and recovery, which can have an effect on its rheological properties.

3.3. Conclusions

The rheology of the binder blend was investigated in different temperature domains with BBR (low temperature domain) and DSR (medium-high temperature domain) using different virgin bitumens and several percentages of artificially-aged binder. Different models (i.e. one for every testing temperature) were developed in order to predict the stiffness (or complex modulus) of the final binder blend, considering different input parameters at the same time. This constitutes a new blending chart developed on the basis of the rheology characteristics, and not only the penetration grade and softening point as the current European method proposes.

From the results obtained the following conclusions regarding blend behaviour at low temperatures can be drawn:

- Decomposing the variability of the results into the measurement accuracy and the variability due to the physical phenomenon allows the assertion that most of the variability detected is due to the phenomenon. This leads to the hypothesis of non-homogenous material.
- The blend is non-homogenous and the presence of a plateau region in the stiffness behaviour suggests the existence of a *latent stiffness*, i.e. the heavier molecules of the aged bitumen float in the blend, but their effect is absorbed and cushioned by a predominant matrix of new bitumen. When the aged binder starts to create a dense network in the blend the stiffness increases rapidly. Further work is needed to confirm this behaviour.
- All the effects on stiffness decrease as the temperature decreases. At -10°C the percentage of aged binder has the strongest impact on the results, while the effects of the stiffness of virgin and aged binder are minor and similar. The stiffness of the blend is more influenced by the amount of aged binder than by the rheological characteristics of the aged binder. This is a positive result as far as production is concerned, since once the degree of blending is determined; it is easier to control the amount of RAP in the mix than the rheological characteristics of its binder. At -20°C the results show that the influence of the percentage of aged binder in the blend on the stiffness decreases.

Similar conclusions can be drawn at medium and high temperatures (30, 40, 50 and 60°C):

- As the temperature increases, all the effects become more significant for the complex modulus (i.e. higher absolute values). This confirms that in the high temperature domain binders are generally more sensitive to blending than in the low temperature domain.
- The complex modulus of the virgin binder will have a stronger influence on the final modulus of the blend than the complex modulus of the aged binder at medium temperatures (30 and 40°C). This represents an advantage because the rheology of the new binder is less variable than the rheology of the aged binder. Nevertheless since this does not apply at 50°C and 60°C, the rheological characteristics of the aged binder cannot be neglected at high temperatures.
- As in the low temperature domain, the amount of aged binder in the blend and the loading frequency have the greatest effect. The complex modulus of the blend is more influenced by the amount of aged binder than by the rheological characteristics of the aged binder.

The comparison between the blends composed of artificially-aged binder and the blends composed of the old binder extracted and recovered from RAP highlighted the different evolution of the complex modulus of the blend when the amount of aged binder increases, even if the polynomial is the same for both blending charts. The differences are probably due to the fact that the traditional artificial ageing procedure (RTFOT+PAV) does not always represent a reliable method to simulate the long-term bitumen ageing and/or the recovery and extraction may have an effect on the binder rheological properties.

Chapter 4

Cluster phenomenon in RAP mixtures

After having simulated the binder blending (with artificially-aged binder and binder extracted and recovered from RAP), assuming the hypothesis of 100% blending, the present chapter aims at verifying the real percentage of blending, passing from the bitumen scale to the mixture scale. The initial objective was to confirm the behaviours artificially recreated in the previous chapter; other physical phenomena occurred however. These phenomena and the possible effects on the recycling approach and mix design will be discussed. Indeed, it is essential to investigate and understand the chemo-physical phenomena and mechanisms occurring during the mixing process that represent the source of the mixture characteristics in order to define a new methodology for optimising the mix design of RAP mixtures.

Despite considerable efforts devoted to characterising the interaction between virgin and RAP binders (Navaro et al. 2012, El Beze 2008, Nguyen 2009, Kriz et al. 2014, Booshehrian et al. 2012, Nahar et al. 2013) and consequently the degree of blending of the two binders (Drut et al. 2009, Shirodkar et al. 2010, Yousefi 2013, Rinaldini et al. 2014, NCHRP Report 452 2001, Bressi et al. 2015a, Mangiafico et al. 2014, Bowers et al. 2014), little fundamental information on the chemo-physical phenomena and mechanisms occurring during the mixing phase of a new mixture with RAP is available in literature.

For the purpose of the study it was necessary to introduce two definitions: mobilisation of RAP binder and RAP clustering (old and new RAP clusters).

The mobilisation of RAP binder concerns the RAP binder that moves from RAP aggregates to virgin stones or other RAP aggregates or that blends with the virgin binder. The RAP clustering refers to two types of particle agglomeration that could be present in a mixture containing RAP: “old clusters” refer to RAP particle agglomeration already present before the mixing phase of the new mixture; “new clusters” refer to the clusters of RAP particles and/or “old clusters” that are created during the new mixing phase.

Whatever the origin of the cluster formation (milling, transport, stockpiling or mixing of RAP), this cluster formation may have important consequences concerning the RAP mixture behaviour. They could prevent the uniform distribution of the virgin binder, increasing the heterogeneity of the mixture. In addition, the agglomeration of RAP particles may lead to a reduction of the amount of small-size grains in the mixture, resulting in changes in the design grading curve. This may have consequences regarding the voids and quantity of virgin bitumen required for an adequate coating of the grains. Moreover, the quality and quantity of virgin aggregates could play a fundamental role in the cluster

formation. Indeed, it was observed (Bressi et al. 2015b) that an abrasion effect due to their sharp shape could partially remove the outer over-aged crust of RAP bitumen, and expose points of less aged, still active binder that then becomes available as glue for cluster formation at potential contact points.

The objective is to provide a verification and quantification of the above-mentioned phenomena using different unmodified virgin bitumen (penetration grades 50/70, 70/100 and 100/150) as well as several RAP percentages in the mixture (from 10% to 90% by weight). The effects of these parameters were evaluated at different testing temperatures (40, 60 and 80°C). The cluster detection in this work is based on rheological tests that provide an indication of the amount of aged binder present in the blend by measuring its complex modulus. Consequently it becomes important to conduct the tests in a range of temperatures where the difference between the two complex moduli is high in order to make the gap between them more discernable.

Moreover binders are generally more sensitive to blending at these temperatures than at low ones (Kandhal et al. 1996).

In order to predict the clustering over the entire experimental domain a multiple variable model was developed using the Response Surface Methodology (RSM), varying simultaneously the factors mentioned above that define also the validity range of the model.

4.1. Methodology and Experimental Plan

Different mixtures with RAP for Swiss standard binder course with 16-mm nominal maximum aggregate size AC B 16 (SN 640 431-1b) were prepared in the laboratory.

All the three types of unmodified virgin bitumen were used and their characteristics are summarised in Table 1.3, Chapter 1. Quarry aggregates from Choëx-Massongex (Switzerland) were used as virgin aggregates in the mixture and the average characteristics of all the fractions used for the study are summarised in Table 1.1 in Chapter 1. RAP 0/16 from Granges-de-Vesin (Switzerland) described in Chapter 1 was selected.

The following steps were undertaken for the sample production:

- A target grading curve of AC B 16 was chosen and a *threshold sieve* was selected to separate the RAP and the virgin aggregates in the grading curve. Thus, before the mixing phase, all the material below the sieve was composed of RAP and all the material above was composed of virgin aggregates (Figure 4.1).

The *threshold sieve* depends on the percentage of RAP in the mixture. Indeed the threshold sieve size increases as the RAP quantity in the mixture increases in order to keep the target grading curve constant. For instance, with 30% of RAP the *threshold sieve* was 2 mm (Figure 4.1a) in order to remain in the grading envelope, following the target grading curve. Consequently, in the case of 50% of RAP the *threshold sieve* was placed at 4 mm (Figure

4.1b). The same considerations were applied for all the RAP percentages used. This separation of RAP and virgin aggregates has two advantages. On one hand, it allows an easier detection of RAP clustering, because cluster formation occurs mainly among small-size particles (Navaro et al. 2012) which, for all mixtures in this study, by definition, were composed of RAP (“old clusters” and/or individual particles). On the other hand it enables the possible presence of RAP binder to be detected and its mobilisation to be estimated by analysing the binder coating of the coarse virgin aggregates.

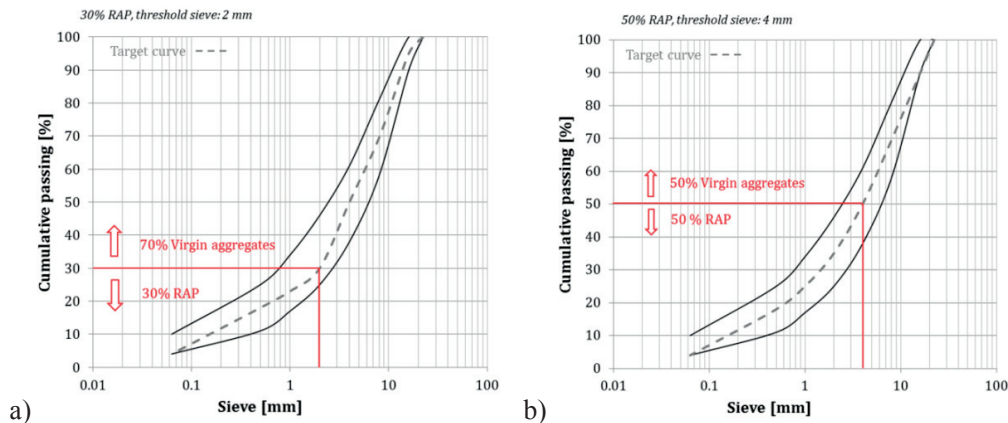


Figure 4.1 AC-16 grading curve and threshold sieve for 30% (a) and 50% of RAP (b)

- The virgin aggregates were washed, dried and heated at 180°C for 3 hours. The RAP was laid in pans with a thickness of 1 cm (AASHTO) and heated at 135°C for one hour. RAP heating in Switzerland envisages three hours (Poulikakos et al. 2013). However, since the RAP would later remain in the oven for two more hours to complete the procedure, only one hour of preheating was required.
- The RAP fractions and virgin aggregates were subsequently mixed for one minute by hand and left in the oven for 30 minutes at 160°C to bring the mixture to the selected fabrication temperature. The fabrication temperature was kept constant for every mixture preparation despite the use of different virgin bitumens. In this way, the probable effect of different types of heating on the thickness and state of the RAP bitumen was avoided.
- The preheated virgin bitumen was added to the mixture, which was mixed for two minutes by hand.
- The final mixture was subsequently left in the oven for 90 minutes at 160°C.
- Once the mixture had cooled down, it was sieved with the *threshold sieve*. After this procedure, the *fine part* (below the *threshold sieve*) could be considered to be composed of RAP particles (individual particles, old and new clusters) covered by virgin bitumen and the *coarse part* (above the *threshold sieve*) was composed of virgin aggregates, RAP particles

adhering to virgin stones and RAP particles sticking together retained by the *threshold sieve*, all covered by the virgin bitumen.

4.2. The Clustering Index (IC_{G^*})

The bitumen extracted and recovered from the fine part is a blend composed of certain proportions of RAP and virgin binder. Therefore, the resulting complex modulus (G_{fine}^*) of this blend reflects the quantity of RAP and virgin binder in the extracted blend. G_{fine}^* is the first term used to calculate the clustering index (IC_{G^*}) according to Equation 4.1.

$$IC_{G^*} = \frac{G_{fine}^*}{G_{design}^*} \quad (4.1)$$

The second term, represented by the denominator in Equation 4.1, is a design reference complex modulus (G_{design}^*) for a fine fraction without any clusters. It is obtained from an artificial blend between the extracted RAP binder and the virgin bitumen. The quantities of both binders are dosed, simulating the proportions in the blend extracted and recovered from the fine part in case no clustering and RAP binder re-activation occur. This represents an ideal situation used as a reference, only considering the presence of individual RAP particles covered by virgin bitumen. Since both blends (design and fine) are subjected to an extraction the possible effect of the solvent is ignored because it is assumed that its influence increases (or decreases) linearly with the complex modulus of the blend. With this assumption the effect of the solvent disappears in Equation 4.1. Both complex moduli are determined with DSR from a frequency sweep at 1Hz conducted in the LinearViscoElastic region (LVE) previously determined by stress sweeps, at three testing temperatures (40, 60 and 80°C).

If IC_{G^*} as defined above is higher than 1 the blend extracted from the fine part is stiffer than from the design reference blend. This would reveal a higher presence of RAP binder and less virgin bitumen than expected in the ideal reference situation. The lower amount of virgin bitumen is an indicator of the reduction of the specific surface. This leads to the hypothesis of the formation of clusters of RAP particles. If $IC_{G^*}=1$ this indicates no presence of clusters.

4.2.1. G_{design}^*

At this point of the study it is necessary to define how the ideal proportions in the artificial blend are calculated for mixing RAP and virgin binder, which gives the design reference value of the complex modulus (G_{design}^*). The proportions of the two binders were calculated considering both bitumen weights in the fine part, simulating a case in which every individual RAP particle would be covered by RAP and virgin binder of a certain thickness. The following procedure was undertaken:

1. The bitumen was extracted and recovered from the fine part of the mixtures. G_{fine}^* was measured on the bitumen and the grading curve was determined on the residual aggregates.
2. Every RAP fraction (0.063/0.5 mm, 0.5/1 mm, 1/2 mm, 2/4 mm, 4/8 mm, 8/16 mm) was previously characterised by knowing the amount of RAP binder trapped in them.
3. Multiplying the weight of every fraction in the fine part (as a result of step 1) by the percentage (weight) of bitumen trapped in every fraction (step 2) and summing up all the weight contributions it is possible to ascertain the total amount of RAP bitumen present in the fine part.
4. The average thickness of virgin bitumen around the aggregates in the target grading curve (virgin and RAP) is estimated by (NCAT 1996):

$$t = \frac{V_{asp}}{SSA \cdot W} \quad (4.2)$$

where

t = average thickness of virgin bitumen around all aggregates [m]

V_{asp} = effective volume of virgin bitumen added to mixture [m³].

SSA = total specific surface area of all aggregates [m²/kg]

W = mass of aggregates [kg]

The amount of bitumen absorbed from the aggregates is considered negligible, thus the effective volume is considered as being equal to the total volume of virgin bitumen added to the mix. The total specific surface area of all aggregates is calculated with the Asphalt Institute procedure (Asphalt Institute 1993) using the surface area factors adapted to the European sieves.

5. Subsequently, the surface area of the RAP aggregates was computed, multiplying the surface area factors by the percentage of the passing material in the fine part of the grading curve, i.e. the material passing through the threshold sieve (and below this sieve) after bitumen extraction (step 1).
6. With the average film thickness calculated with Equation 4.2 and the surface of RAP aggregates of the fine part it is possible to estimate the volume of virgin bitumen coating the RAP particles as follows:

$$V_{fine-virgin\ bit.} = SSA_{RAP\ fine} \cdot W_{RAP} \cdot t \quad (4.3)$$

where:

$V_{fine-virgin\ bit.}$ = volume of virgin bitumen that should coat RAP aggregates in fine part if no clusters and no re-activation of RAP binder occur [m³].

$SSA_{RAP\ fine}$ = surface area per mass of RAP aggregates in fine part [m^2/kg]

W_{RAP} = mass of RAP aggregates [kg]

- The virgin bitumen weight covering each individual RAP particle is calculated assuming the bitumen density as 1020 kg/m^3 . The RAP binder and virgin bitumen weights allow the determination of the design proportions.

A schematic representation of the material components and the procedure considered in the study is presented in Figure 4.2.

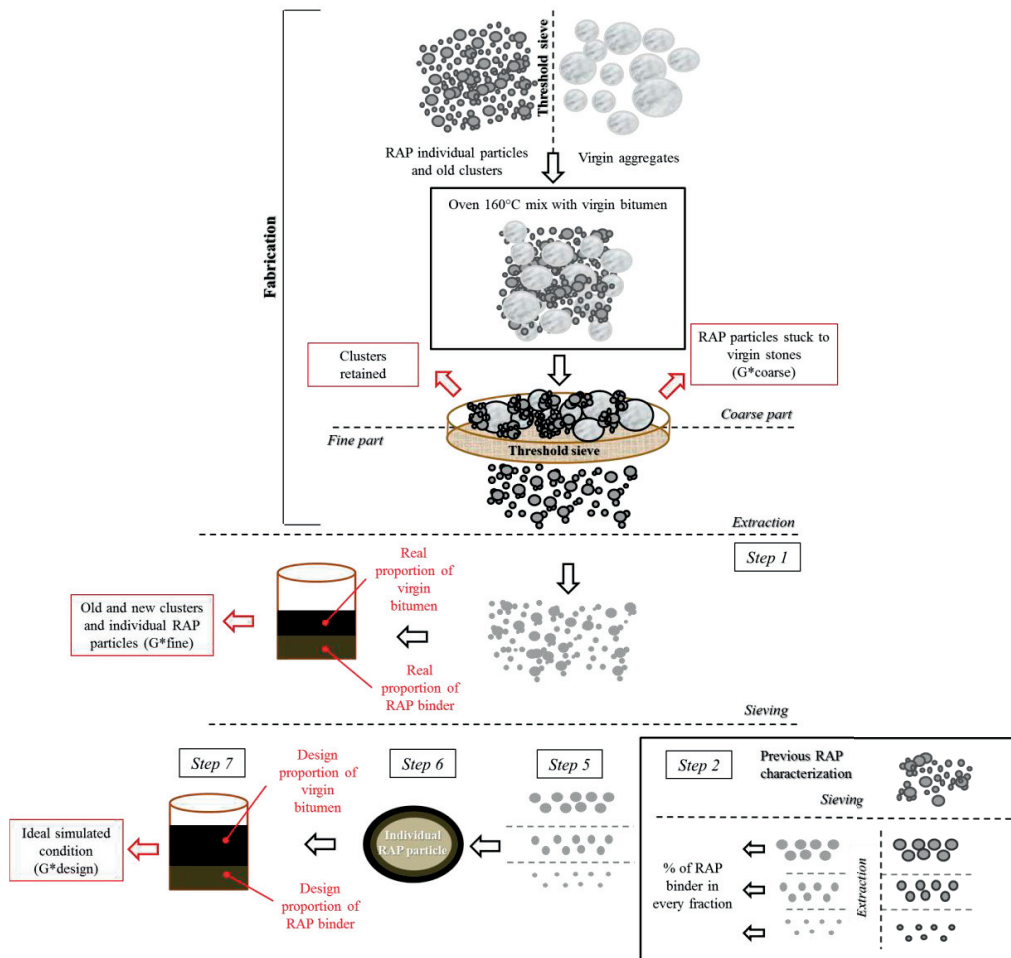


Figure 4.2 Schematic representation of different components used in study and procedure undertaken.

4.3. Selected model parameters

The cluster phenomenon could be affected by the fabrication temperature, the mixing energy and time, the type of bitumen added to the mixture and the percentage of RAP, etc. In the present paper, a first approach was proposed by evaluating the effect of certain selected parameters (with different levels) at different testing temperatures (40, 60 and $80^{\circ}C$):

x_1 = percentage of RAP in mixture (from 0 to 100% by weight),

x_2 = penetration grade of virgin binder (50/70, 70/100 and 100/150);

Usually when several variables are treated at the same time, they are expressed in different units and thus the variables were standardised, making the coefficients independent of the unit of measurement (Bilal and Cuen 2011). For the modelling and problem analysis with multiple parameters one possible technique is the application of the Response Surface Model (RSM) (Doehlert 1970).

4.3.1. Response Surface Model (RSM) and Doehlert Design

In order to develop an empirical model for a system in a defined domain of experiments, it is possible to perform a polynomial fit with a limited set of points that models the behaviour of the system in the validity range defined by the experimental domain. This is known as response surface methodology.

A second-degree model with interaction terms was applied (Equation 4.4) (Montgomery 2000):

$$y = \beta_0 + \sum_{i=1}^k \beta_i x_i + \sum_{i=1}^k \beta_{ii} x_i^2 + \sum_{i<j} \sum \beta_{ij} x_i x_j + \varepsilon \quad (4.4)$$

where:

k = number of variables

β_0 = constant term

β_i = coefficients of first-degree terms

x_i = first-degree terms

β_{ii} = coefficients of second-degree terms

x_i^2 = second-degree terms

β_{ij} =coefficients of interaction terms

$x_i x_j$ =interaction terms

ε = unknown error

For the second-degree model, the location of the measurement points can be optimised in order to minimise the variance of the fitted model over the experimental space. Indeed, the model parameters can be estimated most effectively if adequate experimental designs are used to collect the data. This can be done using the Doehlert design (Doehlert 1970).

The Doehlert design optimisation strategy was chosen since it has a uniform distribution across the experimental space with a rhomboidal net pattern (two factors give a hexagonal shape) and because it provides the same variance of the predicted response (Equation 4.5), i.e. equal precision of estimation, in all directions (rotatable design). Indeed, it is important for the second-order model to provide good predictions throughout the whole experimental domain.

$$V[\hat{y}(x)] = \sigma^2 x' (X' X)^{-1} x \quad (4.5)$$

where:

$\hat{y}(x)$ = vector of predicted response

$V[\hat{y}(x)]$ = variance of predicted response

σ^2 = standard deviation

x = generical point in domain

$(X'X)^{-1}$ = dispersion matrix, where every element in the i,j position represents the covariance between the element i and the element j .

The same design was applied for each testing temperature. The Doehlert design allows the description of a phenomenon in a region, optimising the number of experiments. It contains $k^2 + k + 1$ points for k variables. One of the properties of the Doehlert design is the uniform distribution of the experiments in a k -dimensional space. For two factors, (the percentage of RAP in the mixture and the type of virgin bitumen) a set of seven experiments is required and six experiments are equidistant from the central experiment (Figure 4.3). Hence, according to the coordinates of the Doehlert's network in Figure 4.3 the combinations in Table 4.1 were tested. One advantage of the Doehlert design is the possibility to extend the domain by adding another factor later without changing the coordinates of the experiments previously conducted. Thus, the RSM could be implemented by adding another parameter without running the entire set of experiments from the beginning, but only the experiments that are missing to complete the design network for three factors.

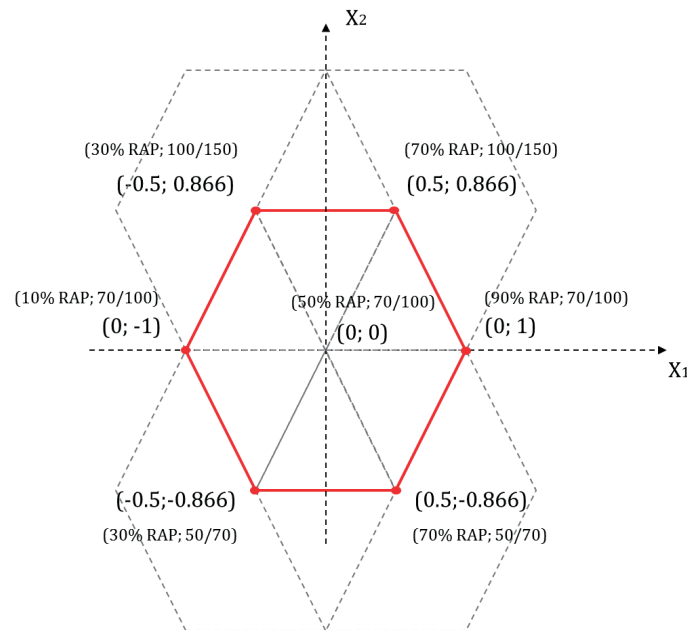


Figure 4.3 Doehlert's network for two factors (percentage of RAP and penetration grade of virgin binder).

Table 4.1 Combinations tested resulting from application of Doehlert's network for two factors.

No. of experiment	Testing temperature [°C]	x_1 = Percentage of RAP in mixture [%]	x_2 = Type of virgin bitumen (Pen. grade)	Threshold sieve [mm]
1	40-60-80	10	70/100	0.5
2	40-60-80	30	50/70	2
3	40-60-80	30	100/150	2
4	40-60-80	50	70/100	4
5	40-60-80	70	50/70	8
6	40-60-80	70	100/150	8
7	40-60-80	90	70/100	16

The goodness of fit of the models proposed was verified with an Analysis of Variance (ANOVA) and with the coefficient of determination (R^2) that expresses the variability of all regressions (Bilal and Cuen 2011).

4.4. Results and Modelling

The first step was to analyse the rheological characteristics of all the bitumens involved in the study (virgin bitumen 50/70, 70/100, 100/150 and the RAP binder) since IC_G^* is based on rheological measurements of their blends. For this purpose, the master curves of complex modulus and phase angle were calculated using the Time-Temperature Superposition (TTS) principle with the WLF equation (Ferry 1980). Frequency sweeps (22 points from 0.1 to 20 Hz) were conducted in increments of 10°C from -20°C to 80°C using as reference temperature $T_{ref}=20^\circ\text{C}$. The results are shown in Figure 4.4. The measurements were performed in the LVE region, previously determined by stress sweep tests.

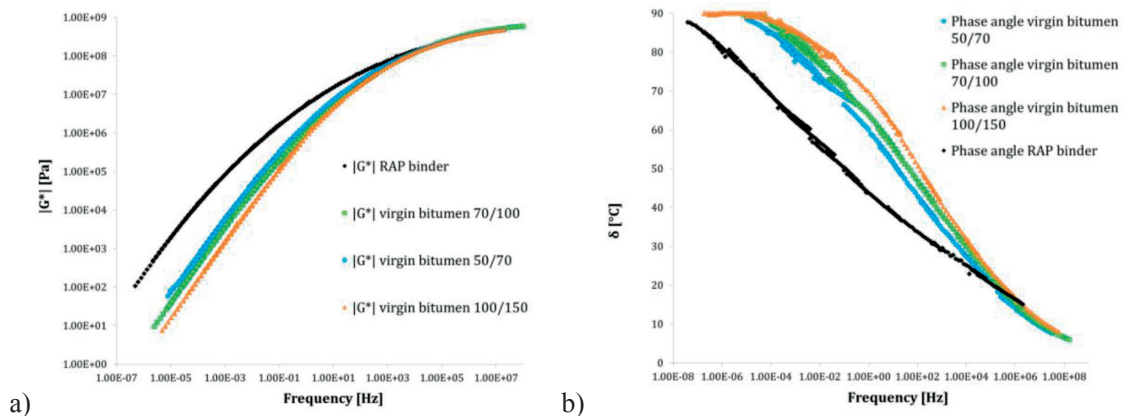


Figure 4.4 a) $|G^*|$ and b) phase angle master curves ($T_{ref}=20^\circ\text{C}$) of all bitumens involved in study (virgin bitumen 50/70, 70/100, 100/150 and RAP binder).

The master curves show that at high temperatures and low frequencies the virgin bitumen 50/70 is the stiffest among all the virgin binders, followed by the virgin bitumens 70/100 and 100/150. The RAP binder has a considerably higher complex modulus and lower phase angle than the virgin binders at low frequencies and high temperatures. This is why for IC_{G^*} the measurements of G_{fine}^* were taken in this temperature range (40-80°C). Indeed, in this range, the differences between the complex modulus of RAP and that of the virgin binders are higher and the effect on IC_{G^*} is more evident.

4.4.1. G_{fine}^* , G_{design}^* and IC_{G^*} Results

The determination of G_{design}^* was performed by first calculating the RAP bitumen weight in the fine part, as explained above. An example is shown in Table 4.2 for 50% of RAP.

Table 4.2 Calculated value of RAP bitumen weight in fine part for 50% of RAP.

Fraction [mm]	Percentage of passing material [%]	Weight of passing material [g]	Percentage of bitumen for each fraction [%]	Weight of RAP bitumen for each fraction [g]
4	100.0	217.2	4.26	1.67
2	82.0	178.1	6.47	3.30
1	58.5	127.1	8.45	1.71
0.5	49.2	106.9	8.89	3.24
0.25	32.4	70.4	7.89	2.02
0.125	20.6	44.7	7.89	1.08
0.063	14.3	31.1	7.89	2.45
Total RAP bitumen ideal weight in fine part [g]				15.47

To determine the ideal amount of virgin bitumen the total specific surface area (SSA_{tot}) was calculated based on the Asphalt Institute procedure (Asphalt Institute 1993) as mentioned earlier (Table 4.3).

Table 4.3 Calculated surface area per mass of aggregates composing whole target grading curve and surface area per mass of RAP aggregates after extraction for case with 50% of RAP.

	Sieve size [mm]	Percentage of passing material target grading curve [%]	Surface area factors	Total surface area per mass of aggregate [m^2/kg]	Percentage of passing material fine part after extraction [%]	RAP surface area per mass of aggregate [m^2/kg]
Virgin aggregates	22.4	100	0.41	0.410	-	-
	16	95	0.41	0.390	-	-
	8	70	0.41	0.287	-	-
RAP	4	50	0.80	0.398	100.0	0.795
	2	35	1.39	0.487	82.0	1.142
	1	25	2.44	0.609	58.5	1.426
	0.5	20	27	0.854	49.2	2.100

	0.25	14	7.47	1.046	32.4	2.421
	0.125	8	13.08	1.047	20.6	2.695
	0.063	0	22.76	0.000	14.3	3.254
			(SSA_{tot})	5.527	SSA_{RAP fine}	13.833

The average thickness was then computed with Equation 4.2. The same surface area factors were used for the calculation of the RAP surface ($SSA_{RAP\ fine}$) that was finally used in Equation 4.3 to calculate the volume of virgin bitumen in the fine part (Table 4.3). The design proportions of RAP and virgin bitumen around the RAP particles are summarised in Table 4.4.

Table 4.4 Results of design proportions of RAP and virgin binders covering RAP aggregates in fine part of aggregates.

No. of experiment	x_1 =Percentage of RAP in mixture [%]	x_2 =Type of virgin bitumen (Pen. grade)	RAP bitumen weight [g]	Virgin bitumen weight [g]	Percentage of RAP binder around individual RAP particles [%]	Percentage of virgin binder around RAP particles [%]
1	10	70/100	8.72	52.97	14.1	85.9
2	30	50/70	5.49	8.74	38.6	61.4
3	30	100/150	10.61	15.55	40.5	59.5
4	50	70/100	15.47	18.53	45.5	54.5
5	70	50/70	38.65	52.66	42.3	57.7
6	70	100/150	68.88	104.74	39.7	60.3
7	90	70/100	93.38	63.97	59.3	40.7

Several artificial blends (0, 10, 30, 50, 70, 90 and 100% of RAP binder) were tested in order to define a curve representing the modulus evolution with increasing RAP binder percentages. A very good coefficient of determination ($R^2 > 0.9$ in all cases) was found between the percentage of RAP binder (weight) in the blend and the complex modulus of the blend. Using the equation related to the curve (examples at 80°C are shown in Figures 4.5, 4.6, 4.7 the other are shown in Annexes in Figures A-1; A-2 and A-3) allowed the extrapolation of the G^*_{design} . Indeed, replacing the values of the RAP binder percentages (Table 4.4) in the polynomial equation fit for the experimental data allowed the obtaining of the design complex modulus corresponding to the design proportion of RAP and virgin binder in the blend when no clustering or re-activation of RAP binder occurs. This procedure was undertaken at every testing temperature (40, 60 and 80°C). Examples of extrapolation of the design complex modulus for each virgin bitumen at 80°C are shown in Figures 4.5, 4.6 and 4.7.

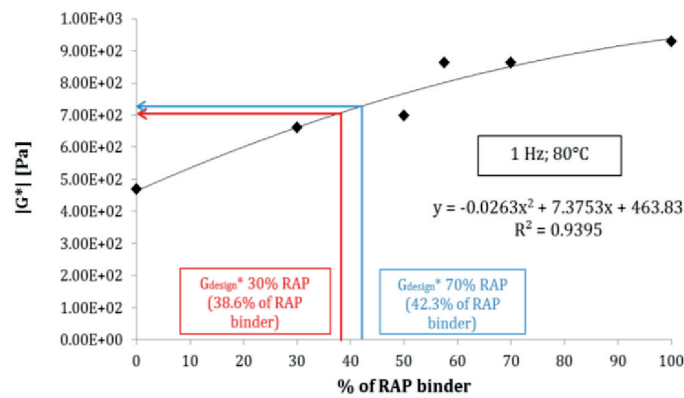


Figure 4.5 Extrapolation of G^*_{design} for 30 and 70% of RAP with virgin binder 50/70 at 80°C.

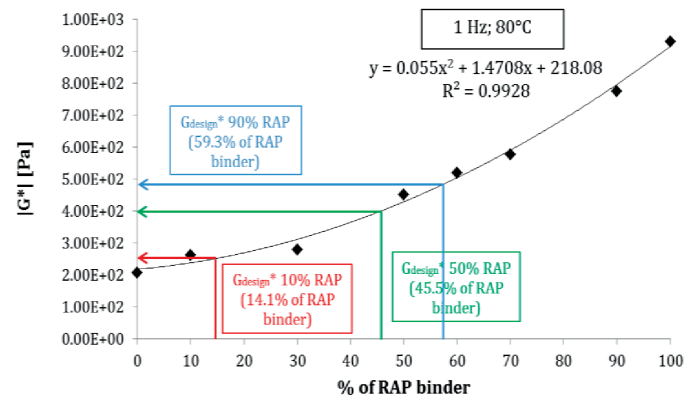


Figure 4.6 Extrapolation of G^*_{design} for 10, 50 and 90% of RAP with virgin binder 70/100 at 80°C.

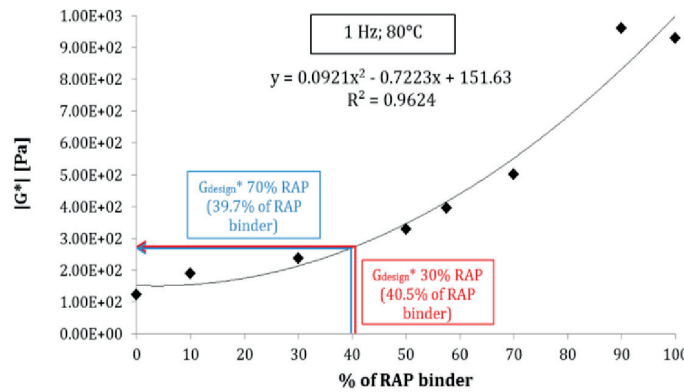


Figure 4.7 Extrapolation of G^*_{design} for 30 and 70% of RAP with virgin binder 100/150 at 80°C.

The evolutions of the blend complex modulus in Figures 4.5-4.6 clearly show different rheological behaviours of the artificial blends that depend on the virgin binder used. Indeed, the 50/70 blending chart presents a curve that denotes a rapid increase of complex modulus up to 30% RAP binder in the blend. After 60% RAP binder in the blend the complex modulus tends to stabilise at values representing 100% RAP binder.

On the other hand, for soft virgin binders (in particular for 100/150) small quantities of RAP binder (up to 30%) do not change the complex modulus of the blend significantly. Hence, using soft virgin binders in RAP mixtures is recommended; it allows the rheological properties to be kept constant until 30% of RAP. Nevertheless, with high percentages of RAP binder the complex modulus of the blends with soft virgin binder appears to increase more rapidly as compared to a blend with stiff virgin bitumen.

After having identified the G_{design}^* and measured the G_{fine}^* Equation 4.1 can be used to calculate IC_{G^*} . The results are summarised in Table 4.5. The values of G_{fine}^* are calculated as an average of three measurements, obtained from three different mixtures and the Coefficient Of Variance (COV) was reported to indicate the dispersion of the results for every experiment.

Table 4.5 Summary of results of G_{design}^* and G_{fine}^* and IC_{G^*} .

No. of experiment	Testing temperature [°C]	x_1 =Percentage of RAP in mixture [%]	x_2 =Type of virgin bitumen (Pen. grade)	$ G_{\text{design}}^* $ [Pa]	$ G_{\text{fine}}^* $ [Pa]	COV on $ G_{\text{R}}^* $ [%]	IC_{G^*} [-]
1	40	10	70/100	65674	83453	4.4	1.27
2	40	30	50/70	186943	229940	11.1	1.23
3	40	30	100/150	76402	108490	24.8	1.42
4	40	50	70/100	113206	172483	25.1	1.52
5	40	70	50/70	192775	201897	15.6	1.05
6	40	70	100/150	74963	117780	3.4	1.57
7	40	90	70/100	139977	156750	12.6	1.12
8	60	10	70/100	3328	4461	11.2	1.34
9	60	30	50/70	10050	13768	10.2	1.37
10	60	30	100/150	3914	5676	11	1.45
11	60	50	70/100	5430	10462	14.7	1.93
12	60	70	50/70	10344	11658	15	1.13
13	60	70	100/150	3826	6275	7.3	1.64
14	60	90	70/100	6913	6738	8.4	0.97
15	80	10	70/100	249.8	324.0	1.3	1.30
16	80	30	50/70	709.3	450.9	3.3	0.64
17	80	30	100/150	273.4	262.7	7.1	0.96
18	80	50	70/100	398.9	743.0	13.6	1.86
19	80	70	50/70	728.7	1106.6	4.3	1.56
20	80	70	100/150	268.1	451.2	11.1	1.65
21	80	90	70/100	498.7	573.0	5.2	1.15

The clustering index provides important information on the physical phenomena when preparing a new mixture. IC_{G^*} is higher than 1 in all the cases analysed (with the exception of experiments No. 14-

16-17). This means that clustering occurs with all the virgin binders considered and with all the RAP percentages. The analysis of cases with the same percentage of RAP shows that IC_{G^*} varies with different virgin bitumens (experiments 2-3; 9-10; 16-17; 5-6; 12-13 and 19-20). In fact, IC_{G^*} is lower with virgin bitumen 50/70 than bitumen 100/150, indicating that the difference between G_{fine}^* and G_{design}^* in the case of mixtures with bitumen 50/70 is lower than with bitumen 100/150. However, this does not necessarily mean that there are fewer clusters when 50/70 virgin bitumen is used, but is more likely related to the theoretical bitumen thickness and the influence of the fabrication temperature (160°C). Indeed, it is well known that the thickness of the virgin bitumen around the grains is affected by the viscosity of the bitumen and, consequently, by the fabrication temperature as well as the amount of bitumen added and the mixing energy (Duriez 1950). Consequently, in the case of bitumen 50/70, the quantity of virgin bitumen in the fine part is higher, G_{fine}^* is lower and the difference from G_{design}^* is less than for bitumen 100/150.

Moreover, another conclusion can be drawn from Table 4.5 regarding the variability of the results at different testing temperatures. The average of the Coefficient Of Variation (COV) of all the measurements at the same temperature decreases with increasing temperature. This value is equal to 13.9% at 40°C, 11.1% at 60°C and 6.6% at 80°C, which means that the dispersion of the results is lower at higher temperatures.

4.4.2. Modelling results

After having calculated IC_{G^*} for all the combinations, the Response Surface Models (RSMs) at every testing temperature can be developed. The coefficients of the model (Equation 4.4) are summarised in Table 4.6.

Table 4.6 Coefficients of model (Equation 4) for every testing temperature.

Coefficients	40°C	60°C	80°C
β_0	1.524	1.927	1.863
β_1	-0.056	-0.189	-0.092
β_2	0.206	0.220	0.206
β_{12}	0.193	0.152	0.308
β_{11}	-0.328	-0.769	-0.638
β_{22}	-0.166	-0.333	-0.215

The goodness of fit is represented by the ANOVA in Table 4.7.

Table 4.7 ANOVA table and R^2 for second-degree model at every testing temperature.

40°C	SS ¹	df ¹	MS ¹	F ¹	p-value ¹
2° degree	12.28	6	2.05	8.62E+02	1.51E-05
Residual	2.38E-03	1	2.38E-03		
Total	12.28	7			
60°C	SS ¹	df ¹	MS ¹	F ¹	p-value ¹
2° degree	15.47	6	2.58	1.09E+04	3.35E-07
Residual	0.00	1	0.00		
Total	15.47	7			
80°C	SS ¹	df ¹	MS ¹	F ¹	p-value ¹
2° degree	16.20	6	2.70	1560.89	6.20E-06
Residual	0.00	1	0.00		
Total	16.20	7			

¹SS: Sum of the Squares; df: degree of freedom; MS: Mean Squares; F-statistic; p-value, R^2 = coefficient of determination.

From Table 4.7 it can be seen that the phenomenon is correctly represented ($p\text{-value} \ll 0.05$) by a second-degree model with interaction. The values of IC_{G^*} increase up to a maximum, which corresponds to a specific percentage of RAP in the mixture. This behaviour was confirmed for all the types of virgin bitumen (50/70, 70/100, 100/150) at every testing temperature for the investigated type of RAP (Figure 4.8).

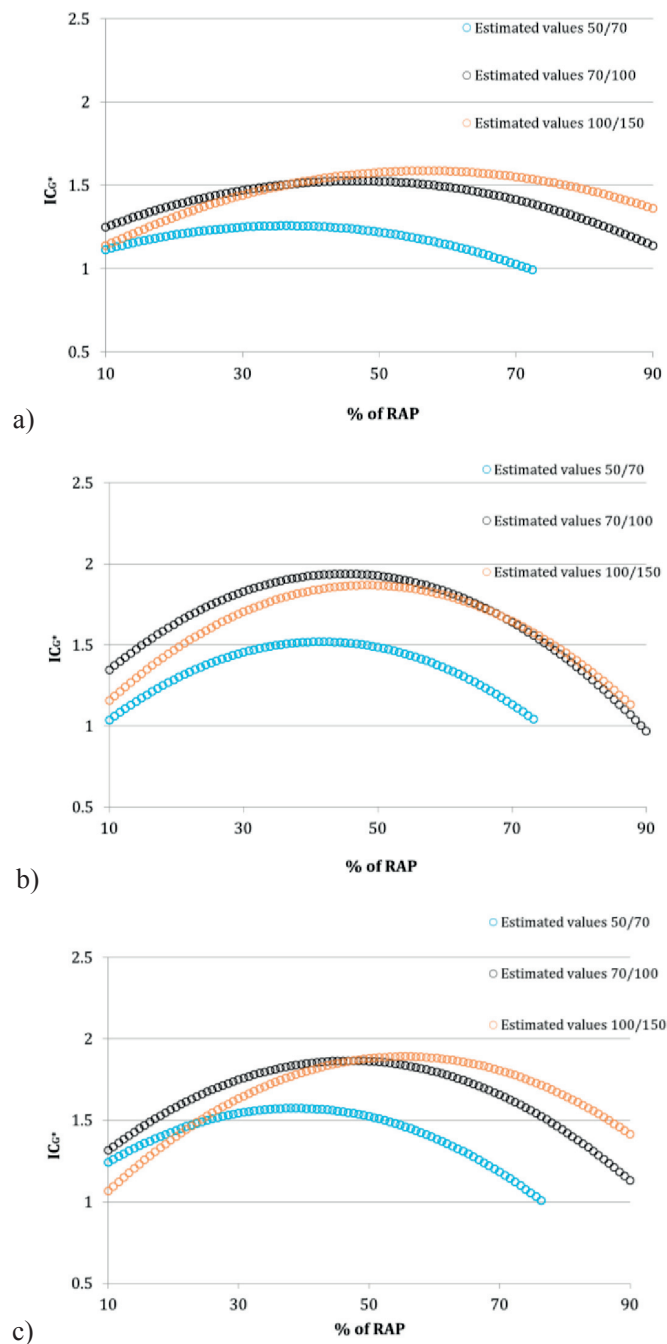


Figure 4.8 Estimated values of IC_{G^*} varying percentage of RAP and keeping constant virgin bitumen (50/70; 70/100 and 100/150) at a) 40°C, b) 60°C and c) 80°C.

The RSM obtained represents the trend of the dependent variable (IC_{G^*}) with respect to two independent variables: the percentage of RAP (x_1) and the penetration of the virgin bitumen (x_2). The result is a 3D curve that was cut in parallel to the x_1 (Figure 4.8) and x_2 (Figure 4.10) axes, to visualise and analyse in detail the effect of the two variables on IC_{G^*} .

In Figure 4.8 it can be observed that the values of IC_G^* for 10% RAP are almost the same for every virgin binder used and very close to 1. This result was expected because with the methodology applied, the IC_G^* values should converge to 1 for 0% of RAP. This is because in that case $G_{design}^* = G_{fine}^*$ since there is no presence of RAP binder. The IC_G^* convergence to 1 appears in almost all cases. The lack of convergence in a few cases could be due to the higher inaccuracy that characterises the extreme points of the domain.

Two phenomena play a role in decreasing IC_G^* after the maximum: only small-size RAP particles (<4 mm) can form new clusters and the abrasion effect of the virgin crushed aggregates that is correlated to the quantity and quality of virgin aggregates in the mixture.

As far as the first phenomenon is concerned, increasing the RAP percentage in the mixture means increasing the threshold sieve size. Thus, RAP particles with a diameter larger than 4 mm are also involved in the process without contributing to the cluster formation.

The second phenomenon detected in the present study that can explain the IC_G^* decrease is associated with the quantity and quality of the virgin aggregates in the mixture.

Indeed, the external crust of over-aged RAP bitumen is removed by the action of the sharp virgin aggregates exposing the softer bitumen under the crust that acts as glue, facilitating the clustering. When the amount of virgin aggregates decreases in the mixture, this abrasion effect is reduced, thus fewer potential contact points with softer bitumen are available for binding the particles. In Figure 4.8 this trend is clearly represented for the mixtures with virgin bitumens 50/70; 70/100 and 100/150.

A confirmation of this is shown in Figure 4.9 that highlights the different visual aspects of the bitumen: matt on the surface and shiny under the upper crust.



Figure 4.9 Part of RAP where crust was broken by abrasion effect of virgin aggregates.

Although further investigation is required to confirm this hypothesis, some results concerning the different layers of aged binder can be found in recent studies that have analysed the binder using Atomic Force Microscopy (AFM) (Das et al. 2015). The authors analyse the surface of the binder after 30 days of air and UV exposure (aged), and the same sample after being washed with distilled water for five minutes. As reported in the study, after washing the sample, the observed microstructures increased from 0 to 2.1%, revealing a different surface when a first thin layer is removed. The percentages of RAP that correspond to the maximum values of IC_{G^*} for every virgin bitumen at every testing temperature are summarised in Table 4.8.

Table 4.8 Percentages of RAP corresponding to maximum value of IC_{G^*} at every testing temperature and for different types of bitumen.

Type of virgin bitumen (pen. grade)	Testing temperature		
	40°C	60°C	80°C
50/70	34.9	41.1	37.5
70/100	46.6	45.1	47.1
100/150	58.4	49.0	56.7

Within the range of testing temperatures the maximum value of clustering occurs between 34.9 and 41.1 % of RAP for mixtures with virgin bitumen 50/70, between 46.6 and 47.1 % of RAP for mixtures with virgin bitumen 70/100 and between 49.0 and 58.4 % of RAP for mixtures with virgin bitumen 100/150. This should be taken into account in the production phase. As expected, the percentage of RAP that corresponds to maximum clustering also slightly increases when a softer virgin bitumen is used from among the investigated types.

The dependence of the cluster phenomenon on the penetration grade of virgin bitumen is shown in Figure 4.10 in the case of 30, 50 and 70% of RAP.

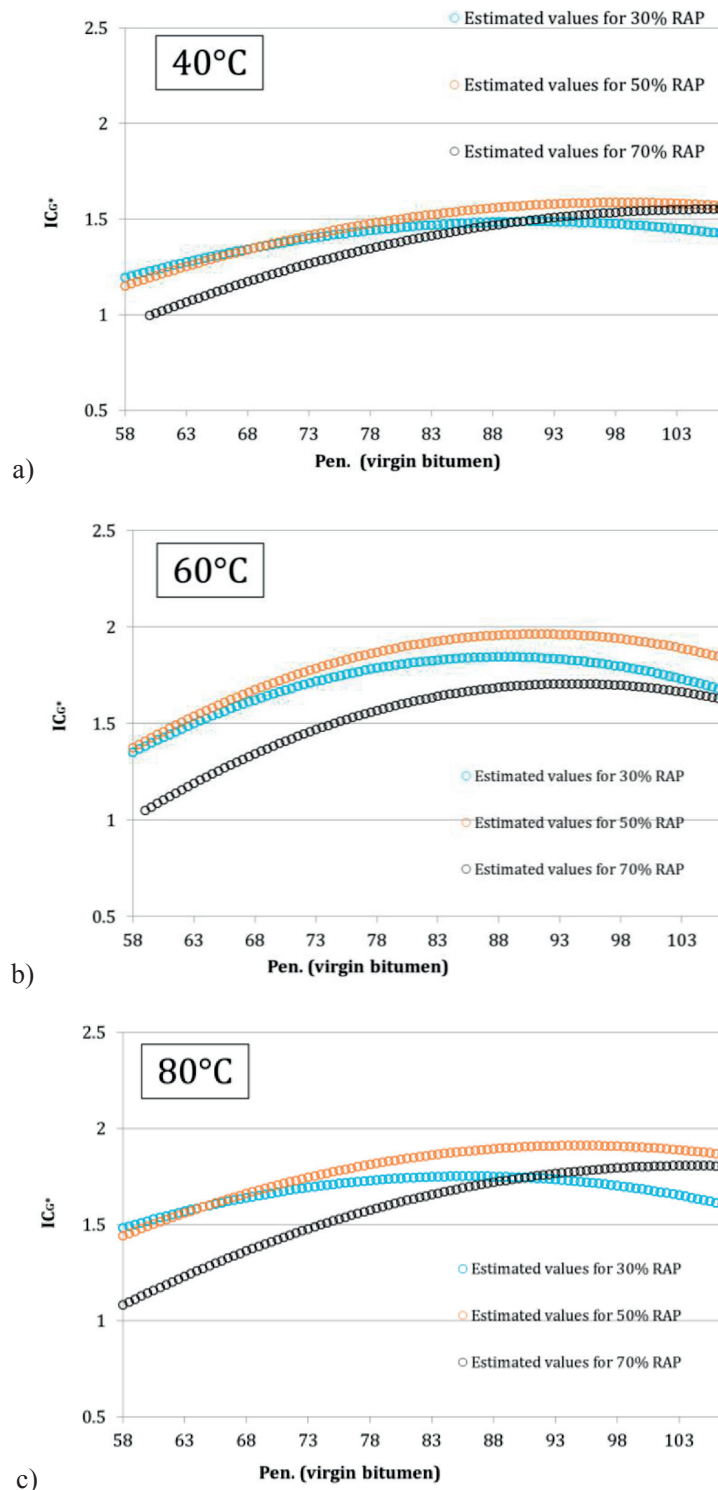


Figure 4.10 Estimated values of IC_{G^+} varying penetration of virgin bitumen and keeping constant percentage of RAP (30, 50 and 70%) at a) 40°C, b) 60°C and c) 80°C.

With the exception of the results obtained at 60°C where the behaviour shows higher nonlinearities, IC_{G^+} increases as the penetration of the virgin bitumen increases until it becomes stable when

penetration exceeds approximately $83 \cdot 10^{-1}$ mm. The same behaviour was observed for all other RAP percentages. In some cases IC_{G^*} decreases after having reached a maximum. This could be due to the distortions in the boundary of the investigated range of penetration and percentage of RAP that lead to a less precise description of the phenomenon at the extremes points.

Assuming that these decreases are artefacts, the curves in Figure 4.10 could be considered as horizontally stabilised after having exceeded a certain value of penetration and the reason could again be related to the virgin bitumen thickness around the RAP aggregates. The calculation of the theoretical thickness used to design the proportions of the virgin bitumen around the RAP aggregates is fundamental to the correct definition of G^*_{design} . Consequently, it also has a strong influence on the IC_{G^*} results. It is well known that the bitumen thickness depends on the viscosity of the binders and consequently on the heating. Nevertheless, all the bitumen thickness calculations proposed in the literature consider as main parameters only the specific surface and the effective volume of bitumen (Attia et al. 2009). Thus, the formula (Equation 4.2) used in this paper also does not take into account the viscosity of the virgin bitumen and the fabrication temperature. The latter was kept constant for every mixture (160°C), despite the use of different virgin bitumens, in order to keep the RAP bitumen thickness constant since it may be affected by different heating temperatures. However, keeping the fabrication temperature constant generates a different effect on the virgin bitumen thickness depending on the bitumen viscosity that is not considered in the methodology and would require a revision of the formula currently used.

For instance, in the present study, for penetrations of between $58 \cdot 10^{-1}$ mm and $83 \cdot 10^{-1}$ mm the bitumen is more viscous at the chosen fabrication temperature than the bitumen with penetrations of between $83 \cdot 10^{-1}$ mm and $107 \cdot 10^{-1}$ mm and the film around the aggregates changes until it attains a constant coating (exceeding $83 \cdot 10^{-1}$ mm). Consequently IC_{G^*} becomes stable between $83 \cdot 10^{-1}$ mm and $107 \cdot 10^{-1}$ mm, showing that the cluster formation is independent of the penetration grade of the virgin binder used in the mix. The variation of IC_{G^*} between $58 \cdot 10^{-1}$ mm and $83 \cdot 10^{-1}$ mm is mainly due to a limitation in the calculation of the theoretical thickness of virgin bitumen around the the RAP aggregates and implicitly suggests that the specific surface of the aggregates alone is not sufficient for an accurate calculation of the bitumen film thickness (Equation 4.2). In addition, the fabrication temperature and the penetration grade of the bitumen should be considered.

4.4.3. Mobilisation of RAP binder: the coarse part analysis

Another aspect of the study dealt with the analysis of the bitumen extracted and recovered from the coarse part of the mixtures (above the threshold sieve). This coarse part had been mixed with virgin bitumen and consisted of coarse virgin aggregates and new RAP particle clusters that did not pass through the threshold sieve (Figure 4.2). From this part only the coarse virgin aggregates were selected.

The complex modulus of the binder (G_{coarse}^*) was analysed with the DSR at three testing temperatures (40, 60 and 80°C) at 1 Hz.

A *reference mixture* was prepared using only virgin aggregates and virgin bitumen, following the same fabrication procedure as explained above. The complex modulus of the bitumen extracted from this reference mixture (G_{ref}^*) was compared with G_{coarse}^* . This comparison showed whether a mobilisation of the RAP binder occurs. Indeed, in this case G_{coarse}^* should be higher than G_{ref}^* , revealing the presence of RAP binder in the blend extracted from the coarse part.

Examples of the results of G_{coarse}^* and G_{ref}^* for different percentages of RAP are shown in Figures 4.11 and 4.12. The temperature 60°C was chosen as representative.

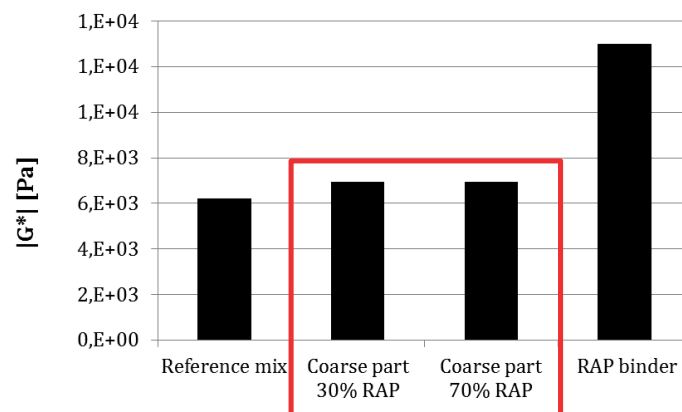


Figure 4.11 Comparison between norm of complex modulus at 1 Hz and 60°C of binder extracted from reference mixture with virgin bitumen 50/70, from coarse part of mix with 30 and 70% of RAP and virgin bitumen 50/70 and RAP binder.

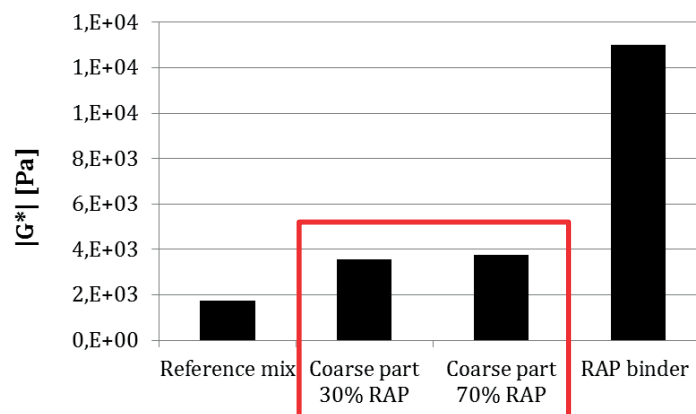


Figure 4.12 Comparison between norm of complex modulus at 1 Hz and 60°C of binder extracted from reference mixture with virgin bitumen 100/150, from coarse part of mix with 30 and 70% of RAP and virgin bitumen 100/150 and RAP binder.

From Figures 4.11 and 4.12 it follows that the bitumen extracted from the coarse part of a mixture with RAP is stiffer than the bitumen extracted from the reference mixture for two possible reasons:

RAP binder mobilisation and/or adherence of RAP particles to the virgin aggregates. Looking at the complex modulus of the binder from the coarse part of the mixtures with different percentages of RAP, it can be observed that the value does not change significantly. As the RAP quantity in the mixture increases from 30 to 70%, the characteristics of the bitumen on the virgin stones do not change. This leads the author to the hypothesis of adherence of RAP particles to the virgin aggregates rather than an actual mobilisation of RAP binder. Indeed, if more RAP is in the mixture, a higher quantity of RAP bitumen should migrate to the virgin aggregates. The higher amount of RAP binder should result in an increase of the complex modulus of the blend recovered in the case of 70% of RAP. Since this did not occur, it is assumed that the difference in complex modulus between the bitumen extracted from the reference mixture and from the coarse part is due to the adherence of RAP particles to the virgin stones and only to a minor extent the result of reactivation and mobilization of the RAP binder.

4.5. Conclusions

This chapter aimed to detect the binder blending or the mobilisation of the RAP binder. Nevertheless, other phenomena emerged: the cluster phenomenon, adherence of RAP particles to the virgin aggregates and the presence of reactivated and non-activated old binder.

The following conclusions regarding the above-mentioned phenomena can be drawn:

- With an increasing quantity of RAP in the mixture, the clustering phenomenon detected with the proposed methodology becomes less evident. This is because increasing the RAP percentage also means involving large-size RAP particles in the clustering process (higher threshold sieve) without contributing to the cluster formation. Moreover the abrasion effect of the virgin crushed aggregates and the existence of activated and non-activated RAP binder in the RAP bitumen thickness have an effect and this should be taken into account when the RAP content increases in the mixture. Thus, the type and quantity of virgin aggregates in the mixture as well as the type of RAP binder have an influence on the cluster formation. Taking their influence on the RAP cluster formation into account is fundamental to understanding how the total specific particle surface changes and to achieving a dosage of the virgin bitumen close to optimal. Further studies are required to confirm this mechanism.
- A significant mobilisation of RAP binder (coarse part analysis) was not observed.
- The variability of the IC_{G^*} measurements at high temperatures decreases, which leads to the hypothesis that the binder blends are more homogenous in the high temperature domain.
- The formula used in the present study (NCAT 1996) for determining the theoretical bitumen thickness around the aggregates needs to be revised. Indeed, the calculation should take into account the combined effect of the fabrication temperature and the viscosity of the bitumen.

The proposed methodology represents a first approach for investigating the clustering phenomenon of hot RAP in asphalt concrete, and it is not devoid of limitations. In order to extend the validity domain of the method, future work should include an extensive laboratory analysis with a wider set of types of RAP and virgin aggregates. Moreover, the separation of the mixture into two parts, a fine part composed of RAP and a coarse part composed of virgin aggregates, does not allow the case of the addition of new filler to be considered. A possible solution could be to carry out the same analysis, inverting the parts (fine part composed of virgin aggregates and coarse part composed of RAP). Note that only the complex modulus was considered as rheological tool to investigate the cluster formation. Future work could also include the analysis of other characteristics, such as the phase angle, in an attempt to achieve an even more comprehensive description of the phenomenon. The potential consequences of the cluster phenomenon are evident for defining the approach to the recycling and mix design of RAP mixtures:

- The clusters could prevent the uniform distribution of the virgin binder, increasing the heterogeneity of the mixture.
- The formation of clusters leads to a reduction of the amount of small-size grains in the mixture, causing variations in the design grading curve and in the quantity of bitumen required for an adequate coating of the grains.
- The clusters may be the source of trapped interstitial voids that cannot be reached by the virgin bitumen. This may result in a low compactability of the asphalt mixture.

Therefore in the next chapter these consequences will be evaluated and analysed to achieve a new mix design method for high RAP mixtures taking into account the physical phenomena occurring during a new mix phase.

Chapter 5

Advanced methodology for optimising the mix design of asphalt mixtures

The physical phenomena detected in the previous chapter led to the rethinking of the approach to recycling based on the potential consequences of these phenomena. Indeed, the formation of clusters leads to a reduction of the amount of small-size grains in the mixture, causing variations in the design grading curve and in the quantity of bitumen required for an adequate coating of the grains. Moreover, the clusters may be the source of trapped interstitial voids that cannot be reached by the virgin bitumen. Therefore, the objective of this chapter is to propose a new analytical method for estimating the dosage of virgin bitumen required in HMA with or without RAP, investigating the contributions of all the components of the mixtures and taking into account the RAP cluster phenomenon and its consequences during the mix.

5.1. Background

The estimation of the optimal bitumen quantity in HMA has always been a challenge since it is based on the thickness of the bitumen film, coating the mineral aggregate surface, as well as on other volumetric characteristics (VMA) (Attia et al. 2009; Kandhal and Foo 1996). The complexity of the determination of these properties is related to the fact that they have to be estimated and are not measured (Heitzman 2005). For instance, all the equations for the bitumen film calculation (Roque et al. 2002, Kandhal and Chakraborty 1996, Roberts et al. 1996, Coree and Hislop 2000, MDT 2006) assume the use of the Specific Surface Area (SSA) that in turn depends on the surface area factors. The origin and subsequent development of the calculation of the surface area factors currently used are vague in the literature. Hveem (1974) first proposed surface area factors that were subsequently adopted by the Asphalt Institute. This first method assumes that the particles are spheres with smooth surfaces (Zaniewski and Reyes 2003). Duriez and Arrambide (1962) proposed the following equation to define the SSA (m^2/kg):

$$SSA = 0.25 g + 2.30 c + 12 s + 135 f \quad (5.1)$$

where:

g = percentage of gravel (grains above 5-mm sieve) [%]

c = percentage of coarse sand (grains between 0.315 and 5-mm sieves) [%]

s = percentage of fine sand (grains between 0.080 and 0.315-mm sieves) [%]

f = percentage of filler (grains below 80 microns) [%]

Nevertheless, these coefficients were defined based on the approximation of considering the aggregates as cubes and without any distinction regarding the mineral aggregates and filler mineralogy and properties. Moreover, the same density is always assumed. Craus and Ishai (1977) later introduced other surface area factors but still considering the aggregates as spheres or cubes. Indeed, recent studies have indicated the necessity of revising the specific surface of the aggregate (Stimilli et al. 2015). Moreover, Chapuis and Legare (1992) extended the grading investigation to fine particles smaller than 80 microns to distinguish the contributions of different types of fillers in terms of shapes and sizes. However, this filler distinction was not integrated into mix design calculations. Indeed, there is a missing link between the measurements of the surface of the filler and their use in the mix design calculation. This step will be thoroughly discussed later in the paper.

The need for further studies regarding the SSA of aggregates and fillers and the contribution of the latter two to bitumen content calculations should be combined with efforts to define the optimal bitumen film thickness required to achieve high performance levels of asphalt mixtures. In fact, in this case too the literature is controversial, involving approximations, such as assuming all aggregates (small and large particles) as being uniformly and equally coated. Hence, it is possible to find several optimal values of thicknesses between 6 to 10.5 microns (Sengoz and Agar 2007; Campen et al. 1959, Kandhal and Chakraborty 1996). The definition of the optimal thickness should be carefully considered as poor coverage can cause lack of bonding between aggregate particles in the mixture, allowing water to penetrate more easily and cause moisture damage (Sengoz and Agar 2007). On the other hand too thick film may result in rutting distress.

5.1.1. Mix design of asphalt mixtures containing RAP

When using RAP, additional aspects to the general mix design of Hot Mixture Asphalt (HMA) should be taken into account. The Asphalt Institute (1993) proposed a formula for the quantity of virgin binder to be added for recycled mixtures, expressed as a percentage by weight of the total mixture:

$$p_{vb} = \frac{(100^2 - p_{na} \cdot p_{rb})p_{mb}}{100(100 - p_{rb})} - \frac{(100 - p_{na})p_{rb}}{100 - p_{rb}} \quad (5.2)$$

where:

p_{vb} = percentage by weight of total mixture of virgin binder to be added [%]

p_{mb} = percentage by weight of total mixture of binder required for type of mixture [%]

p_{na} = percentage of new aggregates in mixture [%]

p_{rb} = percentage by weight of binder contributed by RAP material [%].

The formula suggested by the Asphalt Institute does not consider other parameters related to the chemical and physical phenomena occurring during the fabrication of a new mixture with RAP. In

fact, several additional elements should be considered such as the aggregate and binder blend (Mc Daniel et al. 2001, Mangiafico et al. 2014, Shirodkar et al. 2010, Nguyen 2009, Kriz et al. 2014, Booshehrian et al. 2013, Nahar et al. 2012, Drut et al. 2009, Yousefi 2013.), the effect of the rejuvenator (Del Barco Carrion et al. 2015) and the variability of RAP materials (Bressi et al. 2015c).

One of the main issues is certainly the interaction between virgin and aged binder and how the latter functions in a new mixture in terms of workability, compactability and with regard to service performance. The investigations conducted in the previous Chapter led to the hypothesis that the blending between old and virgin binders is marginal. No actual migration of aged binder was found whereas when the latter is heated it becomes softer (reactivated binder) acting as glue and causing RAP-cluster formation. Two types of RAP clusters can be identified: “old clusters” that refer to RAP particle agglomeration already present before the mixing phase of the new mixture; “new clusters” that refer to the clusters of particles created during the new mixing phase. Clusters, old or new, may have important consequences concerning the RAP mixture behaviour that should be taken into account for the mix design procedure. They could prevent a uniform distribution of the virgin binder and uniform coating of the aggregates, increasing the heterogeneity of the mixture. In addition, the new RAP clusters lead to a reduction of small-size particles in the mixture, causing changes in the design grading curve. This may affect the voids and quantity of virgin bitumen required for adequate coating of the grains. Moreover, RAP has an impact on the compaction and workability of asphalt mixtures (Lo Presti et al. 2014) and therefore the volumetric properties of RAP mixtures have to be considered in order to achieve a correct mix design.

5.2.Objectives and research approach

In the first step, new surface area factors were calculated based on 3D images of virgin aggregates captured with laser scanner technology. In the second step, the filler’s properties and contribution to the specific surface area (SSA) calculation were investigated. The filler was considered separately because its behaviour and role in the mixtures are different from those of the coarse aggregates. Indeed, whereas the aggregates represent the “lytic skeleton” to be covered, the filler/bitumen mastic is in a diluted phase and has to fill the interstitial voids (Tunnicliff D.G. 1967). Therefore, the mastic could be considered as a suspension and the amount of bitumen coating the filler is higher than the bitumen coating the aggregates. In the third step, a cluster prediction model was introduced in the calculation that defines the final bitumen content. Indeed, the surface of RAP to be covered by bitumen was calculated separately from the virgin aggregates in order to take the reduction of small-size particles caused by clustering into account. These three steps allow the separate investigation of the contribution of virgin aggregates, filler and RAP, as well as the determination of the quantity of virgin bitumen required by each single component.

Once the overall equation for the mix design calculation was defined (fourth step), a laboratory verification was conducted. Marshall tests, gyratory compactor and the Indirect Tensile Strength Test (ITST) were performed to verify that the optimal binder content calculated with the proposed methodology represents a valid estimation of the measured one.

Finally, in the fifth step, the compaction and workability for mixtures with high RAP content were analysed, since it was essential to confirm whether the estimated bitumen content provided by the methodology met the volumetric requirements (compactability and air voids). A specific analysis was conducted to understand the impact of the aged reactivated binder and clusters in the compaction of RAP mixtures. The research stages are schematically shown in Figure 5.1.

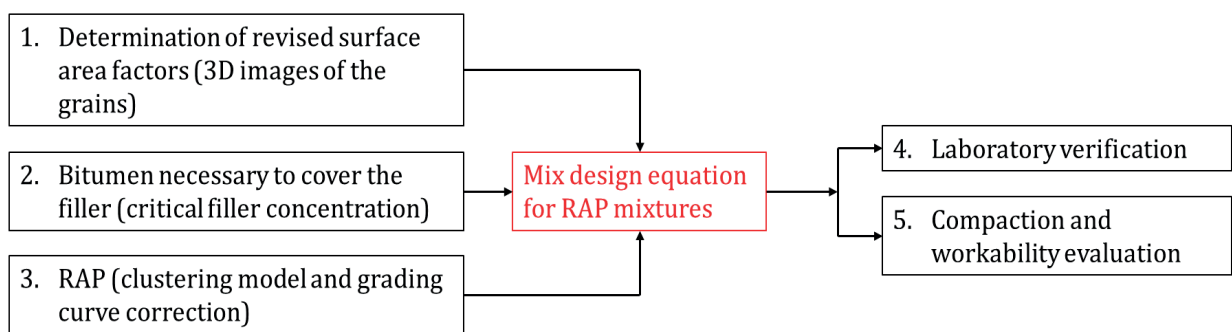


Figure 5.1 Research plan.

Mineral aggregates and limestone filler from a Swiss quarry in Choëx/Massongex (Switzerland), RAP 0/16 from Granges-de-Vesin (Switzerland) and unmodified virgin bitumen 70/100 were used. The main characteristics of the materials are summarised in Tables 1.1, 1.2 and 1.3 in Chapter 1.

5.3. Methodology

5.3.1. Revision of the surface area factors

Spheres or cubes were always used as approximation for estimating the surface area of mineral aggregates (Kandhal et al. 1996 and Stimilli et al. 2015). In order to overcome this simplification the real shapes of the aggregates were determined using the FARO ARM PLATINIUM laser scanner with a scanning head LINE PROBE III (accuracy 0.03 mm). This technology allows 3D images to be obtained that provide information regarding the number of faces and vertices of the aggregates, as well as their volume and surface.

At least twenty quarry stones of different grading classes (22.4/31.5, 31.5/40, 40/50 and 50/60 mm) were randomly selected and scanned. Since the stones from the same quarry were assumed to have the same petrography and therefore the same characteristics, it was decided to determine the surface and the volume of smaller aggregates by scaling the stones chosen as reference grains (22.4/31.5 mm) into different grading classes to compose a typical grading curve. According to the Swiss standards (SN

640431-1b-NA) several grading curves can be chosen depending on the type of layer (wearing, binder or base course). The most common curves include aggregates up to 31.5 mm and are composed of several fractions: 0.063/0.5; 0.5/1; 1/2; 2/4; 4/8; 8/16; 16/22.4; 22.4/31.5 mm. Therefore, all the reference stones were scaled according to all the grading classes to obtain aggregates representative of the other grading classes as shown schematically in Figure 5.2.

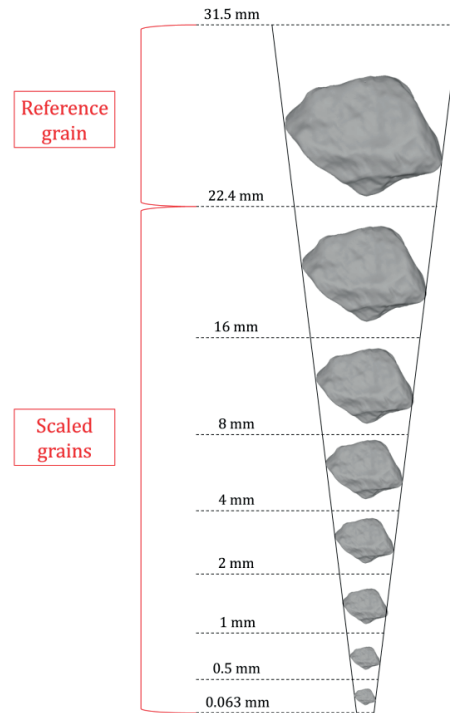


Figure 5.2 Schematic representation of fractions of aggregate scaling.

After all the stones had been scanned, the images were analysed and the averages of the surface and volume of those aggregates were calculated.

5.3.2. Scale factors

The images were analysed and scaled using Meshlab 1.3.3. This software allows the application of 50.000 meshes to the surface of the grain. It calculates the total area of an aggregate by summing up all mesh areas. The same procedure was carried out for all the stones. Subsequently, all the stones were scaled into the different grading classes mentioned above (see Figure 5.3).

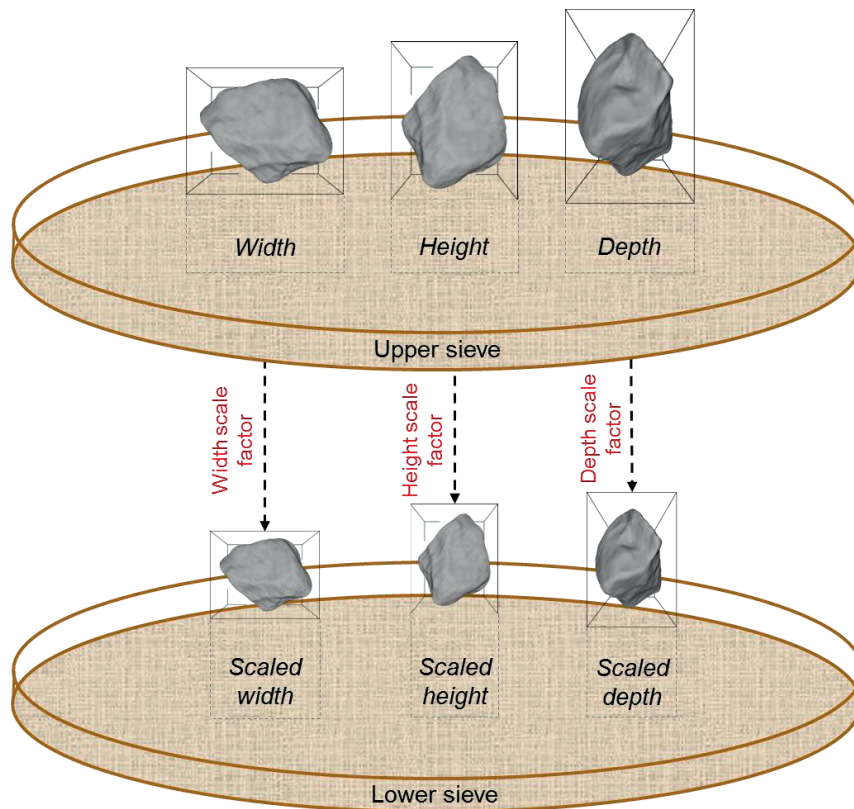


Figure 5.3 Schematic representation of procedure adopted to scale one aggregate.

Meshlab automatically creates the minimum bounding box that inscribes the stone. The minimum bounding box is the box characterised by the minimum volume containing the grain. In order to ensure that the aggregates were correctly scaled for each fraction it was necessary to establish a criterion for the virtual sieving taking into account the bidimensionality of the mesh sieve. Therefore, the stone passes through the sieve if at least two dimensions of the minimum bounding box containing the grain are smaller than the mesh sieve. On the other hand, the stone is retained in the sieve if at least two dimensions of the virtual box are bigger than the mesh sieve. The minimum bounding box is not necessarily the box that has the minimum or maximum sizes containing the aggregate. There could be a box (among the infinite boxes containing the grain) that has a smaller or a bigger size with respect to the minimum bounding box. Nevertheless, the shape of the grains allows another hypothesis to be made. Indeed, the stones according to the shape index requirements for bituminous mixtures are not elongated, which means that the length of the aggregate cannot be greater than three times the thickness. This leads to the idea of having regular and “almost” elliptical grains. This reduces the probability of having other boxes that behave differently in the virtual sieving with respect to the minimum bounding box. Indeed, for an ellipse the minimum bounding box corresponds to the box characterised by the minimum and maximum sizes. Thus in this phase the assumption was made of considering the stones to be almost elliptical, and the minimum bounding box as being representative

of the stone for the virtual sieving. More sophisticated statistical models are needed to estimate the probability as to whether the aggregates will pass or be retained by the sieves and to verify that the minimum bounding boxes are representative of the aggregates for a reliable virtual sieving.

This criterion for the virtual sieving was necessary to verify that each aggregate after being scaled could pass through the upper sieve and be retained by the lower sieve of the considered fraction as illustrated in Figure 5.3.

To obtain the scaled images specific scale factors have been applied to each dimension (height, width and depth) of the virtual minimum volume box, inscribing the stone according to the following procedure:

- Several large-size grains (31.5/40, 40/50 and 50/60 mm) were scanned. Large-size grains were chosen (>22.4 mm) to take into account the accuracy of the instrument (0.03 mm) that would not be sufficient for small grains. It was supposed that aggregates belonging to the same geological classification and crushed in the same plant have on average the same characteristics. Therefore, it is possible to assume that scaling the large-size aggregates into smaller grains leads to a reasonable representation of small aggregates of the same type. From the analysis of all the scaled images it was possible to calculate the characteristics (surface area and volume) of all the aggregates for every grading class.
- The averages of the area, volume and virtual box dimensions were calculated for the grains belonging to each fraction (22.4/31.5, 31.5/40, 40/50 and 50/60 mm). In this way an “average” grain was created for each fraction. An “average” grain is an aggregate characterised by the surface and the volume calculated as the average of all the samples in the same grading class.
- By plotting the average measured values of the dimensions of the virtual boxes bounding the stones for each fraction (22.4/31.5, 31.5/40, 40/50 and 50/60 mm) a regression for calculating the scale factors was obtained. The regression shows the average of each dimension of the minimum bounding box as function of the aggregates’ fraction size.
- Finally, the average of volume and surface area of the scaled grains belonging to the same grading class were calculated in order to obtain the “average” grain volume and surface for each fraction.

The idea is to calculate how many grains of a certain size are present in 1 kg of those aggregates and multiply the number of grains by the area of the “average” grain to obtain the surface area factors (α_i). Thus, once the “average” grain surface area and volume for each grading class were defined, α_i were calculated as follows:

$$V_{i1kg} = \frac{1}{\rho_a} \quad (5.3)$$

$$N_{i1kg} = \frac{V_{i1kg}}{v_i} \quad (5.4)$$

$$\alpha_i = N_{i1kg} \cdot s_i \quad (5.5)$$

where:

ρ_a = density of aggregates (same for all) [kg/m³]

V_{i1kg} = volume of 1 kg of aggregates of i-fraction [m³/kg]

v_i = volume of “average” grain of i-fraction [m³]

N_{i1kg} = number of “average” grains in every kg of aggregates [kg⁻¹]

s_i = surface area of “average” grain of i-fraction [m²]

α_i = surface area factor of aggregates for i-fraction [m²/kg].

Subsequently, multiplying α_i by the percentage in mass of each aggregate fraction belonging to the grading curve and summing up all the contributions allows the calculation of the total surface of mineral aggregates covered by the virgin bitumen (Equation 5.6).

$$SSA_{agg} = \sum \alpha_i \cdot (p_{i+1} - p_i) \quad (5.6)$$

where $(p_{i+1} - p_i)$ is the percentage by weight of aggregates smaller than size $i+1$ and larger than next size i and α_i are the revised surface area factors as compared to SF_i . Thus, the volume of bitumen required to cover all the aggregates is defined as:

$$V_{bit-agg} = \bar{t}_{opt-agg} \cdot \left\{ \sum \alpha_i \cdot (p_{i+1} - p_i) \right\} \quad (5.7)$$

where $\bar{t}_{opt-agg}$ is the optimal average thickness of virgin bitumen around the aggregates selected from literature as being equal to 10 microns to minimize the effect of ageing (Kandhal and Chakraborty 1996).

5.3.3. Filler

Two types of fillers commonly used for asphalt mixtures were analysed: limestone and hydrated lime. The positive effects of hydrated lime are well known even if the difference between the two fillers is bitumen- dependent (Little et al. 2005). Hydrated lime normally has a higher surface area than limestone; if the bitumen content remains constant, asphalt mixtures containing this filler will therefore have a much thinner bitumen film thickness. This may result in a more rut-resistant, but also a more fatigue-susceptible mixture (Zaniewski et al. 2003). The specific surface of fillers available to be covered by virgin bitumen is not easily measurable. The shape and agglomeration of the filler’s elementary (individual) particles affect the final available surface as well as the particle size distribution (Chapuis and Legare 1992). Thus, multiple tests were conducted to investigate the contribution of filler for optimizing the binder content in asphalt mixtures.

5.3.3.1. Particle size distribution (PSD) based on laser diffraction

PSD measurement provides information about the size of a set of particles representative of a certain material. In this study laser diffraction was used. It is based on the principle that particles passing through a laser beam will scatter light at an angle that is directly related to their size: large particles scatter at low angles, whereas small particles scatter at high angles. The scattering intensity data is analysed to calculate the size of the particles in terms of a volume-equivalent sphere diameter (d_v). The particle size distribution is determined by several measurements such as $d_{[v,0.1]}$, $d_{[v,0.5]}$, $d_{[v,0.9]}$. These are the equivalent circular diameters at which 10, 50 and 90% of the filler sample passes through the sieve. Moreover $d_{[4,3]}$ is the average equivalent circular diameter of the filler particles.

The PSD technique also provides an SSA measurement that is the result of two approximations and therefore is limited:

- The equivalent spherical diameter (d_v) is essentially based on the physical measured value (i.e. scattered light, settling rate) and approximated as the size of the sphere that corresponds to the data recorded (Figure 5.4a). This approximation can create problems if the individual particles have a very large aspect ratio and their shape differs significantly from spheres.
- The particles are not completely dispersed in the fluid during the test, thus some agglomerations of elementary particles may form and count as a singular particle Figure 5.4b. Additional distortions in the SSA measurements can be caused by the intragranular and intergranular porosity.

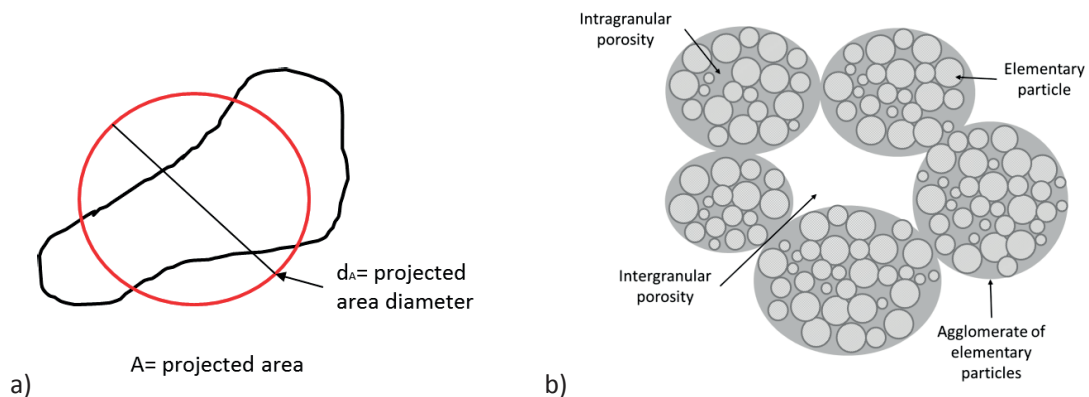


Figure 5.4 Schematic representation of some limitations of PSD method: a) non-spherical particles and b) elementary particles not completely dispersed in the medium causing inter and intragranular porosity.

The limitations of this method apply for small sizes ($<1 \mu\text{m}$), for non-spherical particles, and for materials with a low refractive index in relation to the dispersive medium. Hence, the PSD measurements alone were not sufficient to define a reliable value for the specific surface of the two

fillers. Therefore the results had to be coupled with other techniques such as surface area measurements (BET method) and microscopy techniques (ESEM).

5.3.3.2. Brunauer, Emmett and Teller (BET) method and agglomeration factor

The specific surface area of a powder can be determined by the physical adsorption of a gas on the surface of the solid and calculating the amount of adsorbed gas corresponding to a monomolecular layer on the surface. Physical adsorption results from relatively weak Van der Waals forces between the adsorbed gas molecules and the adsorbing surface area of the powder. The measurements were made using Micromeritics Gemini 2360 Surface Area Analyzer.

The BET method provides the real surface area because it is based on the gas adsorption of the real surface and on the complete dispersion of all the particles. This is why the SSA resulting from BET is generally significantly higher than from PSD with laser diffraction measurements. Furthermore, during asphalt production the bitumen added to the mixtures does not cover every singular particle and the filler is not completely dispersed in the bitumen. It becomes essential to quantify the degree of agglomeration of the particles, since the effective surface is not available to be covered.

The agglomeration factor (F_{ag}) is a very good indication of the degree of agglomeration and allows the comparison of powders and treatments. F_{ag} is calculated with the following Equations:

$$d_{BET} = \frac{6}{SSA_{BET} \cdot \rho_f} \quad (5.8)$$

$$F_{ag} = \frac{d_{[v,0.5]}}{d_{BET}} \quad (5.9)$$

where:

SSA_{BET} = specific surface area measured by nitrogen adsorption (BET method) [m^2/g]

ρ_f = filler density [g/cm^3]

d_{BET} = average diameter calculated with BET [μm]

$d_{[v,0.5]}$ = median diameter found with PSD [μm]

5.3.3.3. Environmental Scanning Electron Microscope (ESEM)

The ESEM allows the imaging of the specimen on the micro and nano-scale under different boundary conditions, temperature and environmental gas concentration. The ESEM experiments were performed with a Phillips ESEM-FEG XL30 microscope. In this study, the low vacuum mode was used with upper Inert Gas Purge (IGP), equal to 1.4×10^{-9} mbar and lower IGP 1.7×10^{-7} with a sample chamber pressure of 5.4×10^{-9} mbar and emission of current equal to 308 mA was used. The filler

samples were not coated and were imaged in their natural state. ESEM allowed the detection of the different shapes between the fillers and in comparison with spheres. Moreover, it allowed the agglomerations of the particles to be visualised.

5.3.3.4. Critical filler concentration

The measured surfaces of filler do not correspond to those available in the asphalt mixtures because the filler is not completely dispersed in the bitumen and its agglomeration level depends on the type of filler.

Since the level of agglomeration depends on the type of filler, the mechanism by which the latter interacts with bitumen had to be taken into account for defining the necessary amount of bitumen to cover it. As shown by Faheem and Bahia 2009 the stiffness of mastics increases as the filler concentration increases and two regions can be recognised: diluted and concentrated. In the diluted region the filler particles are separated by the volume of free bitumen volume. The bridge of bitumen between the particles is thick enough to ensure an almost constant stiffness. When the filler concentration increases, exceeding a certain threshold, the mastic enters the concentrated region, where the sudden increase of stiffness is due to the consumption of the free bitumen.

The *critical filler concentration* represents the transition between the diluted and the concentrated region and the maximum allowable limit of filler in the mastic. Indeed, any addition of filler beyond the critical concentration leads the mastic towards the concentrated region, where the mastic is poor in bitumen and its cohesion starts to weaken. The *critical filler concentration* is given by the following equation resulting from a regression analysis (Faheem and Bahia 2010):

$$\emptyset_c = 83.2 RV(\%) + 4.79 MBV \quad (5.10)$$

where:

$RV(\%)$ =Ridgen voids [%]

MBV = Methylene Blue Value (clay content) [-]

\emptyset_c =Critical filler concentration [% by volume]

The critical filler concentration was used to calculate the minimum bitumen quantity necessary to maintain the mastic in a diluted phase once the asphalt mixture is produced. This allows the mastic to maintain the required stiffness and suitable consistency to fill the voids in the bituminous mixtures. Therefore, the bitumen volume was calculated as follows:

$$V_{filler} = \frac{W_{filler}}{\rho_f} \quad (5.11)$$

$$\frac{\emptyset_c}{100} : 1 = V_{filler} : (V_{filler} + V_{bit-filler}) \quad (5.12)$$

$$V_{bit-filler} = \frac{V_{filler}}{\frac{\emptyset c}{100}} - V_{filler} \quad (5.13)$$

$$V_{bit-filler} = \frac{V_{filler} \cdot (1 - \frac{\emptyset c}{100})}{\frac{\emptyset c}{100}} \quad (5.14)$$

where:

V_{filler} = Filler volume [m^3/kg of mixture]

W_{filler} = Filler weight [kg/kg of mixtures]

ρ_f = Filler density [kg/m^3]

$\emptyset c$ = Critical filler concentration [% by volume]

$V_{bit-filler}$ = Minimum volume of bitumen required to maintain mastic in diluted phase [m^3/kg]

5.3.4. Modelling of RAP clustering

As mentioned above, the old reactivated binder trapped in the RAP material becomes softer during the re-heating, acting as glue and facilitating cluster formation between the small-size RAP particles. In order to readjust the target grading curve, taking into account the formation of new RAP clusters during a new mix phase, a clustering prediction model was developed considering only the new clusters and involving two variables: the RAP fraction size and RAP percentage.

A particular procedure was carried out to determine the amount of new clusters forming during a new mixing phase, considering different fractions and percentages of RAP. The virgin aggregates and RAP material were sieved separately for the following fractions: 0.063/0.5, 0.5/1, 1/2, 2/4, 4/8, 8/16 mm.

The amount of clusters was estimated using two fractions at a time, for each couple of fractions the same steps were applied. An example of the procedure is reported below (50% of 0.063/0.5-mm RAP and 50% of 0.5/1-mm virgin aggregates).

- 200 g of 0.5/1-mm virgin aggregate fraction was heated at 200°C for one hour
- 200 g of 0.063/0.5-mm RAP fraction was heated at 135°C for one hour. It is important to heat the RAP as little as possible as the heating further ages the already aged binder (Poulikakos et al. 2013).
- The two fractions were mixed together for two minutes by hand and left in the oven for one hour at 160°C to bring the mixture to the selected fabrication temperature. Note that the cluster phenomenon could be affected by the fabrication temperature, and the mixing energy and time. The fabrication temperature was kept constant for every mixture preparation. In this way, the probable effect of different types of heating on the thickness and state of the RAP bitumen was avoided.

- Once the mix was removed from the oven and cooled, it was sieved again with the 0.5-mm sieve. Part of the RAP was retained by the sieve (0.5 mm) because the RAP activated binder within the RAP was adhering to other RAP particles or virgin aggregates, creating new clusters that could not pass through the sieve. This is also why the virgin aggregate fraction just above that of the RAP was chosen. Indeed as soon as the RAP particles started to stick together they did not pass through the sieve and were retained in the upper fraction.
- The RAP material passing through the sieve (0.5 mm) was weighed after the procedure and the difference in mass between the initial passing RAP material was reported as a value of the percentage of new clusters for the fraction.

The procedure was carried out using several RAP percentages (x_1) and RAP fractions (x_2). Once the values of cluster percentages in mass for every combination had been obtained a multiple regression analysis was conducted. A second-degree model with interaction terms was applied (Equation 5.15). The variables were standardised to bring them onto a common scale.

$$C'_i = \beta_0 + \sum_{i=1}^k \beta_i x_i + \sum_{i=1}^k \beta_{ii} x_i^2 + \sum_{i < j} \sum \beta_{ij} x_i x_j + \varepsilon \quad (5.15)$$

where:

C'_i = percentage in mass of RAP new clusters of weight of RAP-i-fraction [%]

k = number of variables

β_0 = constant term

β_i and β_{ii} = coefficients of first- and second-degree terms respectively

x_i and x_i^2 = first- and second-degree terms respectively

β_{ij} = coefficients of interaction terms

$x_i x_j$ = interaction terms

ε = unknown error

The clustering model was introduced in the mix design calculation to readjust the proportions of every fraction of virgin aggregate in order to maintain the same target grading curve after the mixing process.

5.4.Verification in the laboratory

Once all the contributions (virgin aggregates, filler and RAP) had been investigated, a formula was developed for estimating the optimal bitumen amount to be added to the RAP mixtures.

Subsequently a verification was undertaken, on a laboratory mixtures without RAP and with 50% RAP with 4.5, 5, 5.5 and 6 % of 70/100 unmodified virgin bitumen by weight of the total mixture. The mix design method was applied to a Swiss standard binder course AC B 16 (i.e. asphalt concrete with maximum nominal size 16 mm). The target grading curve is reported in Table 5.1.

Table 5.1 Target grading curve of Swiss binder course AC B 16.

Sieve [mm]	Grading envelope AC-16 (passing material) [%]		Target grading curve (passing material)
	Low	High	
22.4	100	100	100
16	90	100	96
8	58	81	76
4	38	61	51
2	25	46	33
1	17	34	23
0.5	11	25	16
0.063	4	10	7

The following tests were performed to verify that the optimal bitumen amount calculated with the proposed formula really represents a valid estimation of the measured one:

- Marshall tests
- Giratory compaction test
- Indirect Tensile Strength Test (ITST)

Marshall tests were conducted on cylindrical samples with a diameter of 102 mm and a height of 64 mm. In order to compact the samples fifty blows were given on each side of the specimen. The testing load applied increases until it reaches a maximum, and then begins to decrease. The maximum load is recorded just before it starts to decrease. The optimum asphalt binder content is finally selected based on the combined results of the Marshall stability and flow as well as air void content. The minimum values required by the Swiss standard S 640 431-1b-Na for the Marshall stability and the flow and air voids are respectively 7.5 kN, 2-4 mm and 3-6%.

The gyratory compactor has in many cases replaced the Marshall hammer compaction. Producing asphalt specimens with the gyratory compactor is claimed to produce uniform values of density and air voids to be obtained, nevertheless the vertical distribution of the air-void content is rather different between the core and exterior (Partl et al. 2006). Despite, the limitations of both compaction techniques, these are the devices currently most used for specimen compactions. The following conditions were selected for the gyratory compactors:

- Sample size: 150-mm-diameter cylinder approximately 115 mm in target height
- Compaction pressure: 600 kPa
- Speed of rotation: 30 gyrations/min
- Inclination from the vertical axes: 1.25°

- Compaction temperature: 135°C

The Superpave gyratory compactor establishes three different gyration numbers: $N_{initial}$, N_{design} and N_{max} . N_{design} is the parameter considered in this study. It is the design number of gyrations required to produce a sample with the same density as that expected in the field in accordance with the indicated amount of traffic. Typically $N_{design}=100$ for 20-year traffic loading higher than 3 million Equivalent Single Axle Loads (ESALs) equal to 8.16 kN.

For the ITST, specimens with the same dimensions as for the Marshall tests were used. The deformation rate during loading was 0.85 mm/s. From this test it was possible to determine the tensile strength σ_t (Equation 5.16).

$$\sigma_t = \frac{2P}{\pi Dh} \quad (5.16)$$

where:

σ_t = Tensile strength [MPa]

P = Load [kN]

D = Specimen diameter [mm]

h = Specimen height [mm]

5.5. Results and specific applications

5.5.1. Aggregates

Scanned images were obtained from twenty aggregates of size 22.4-31.5 mm (an example is shown in Figure 5.5). The area and volume of each grain were calculated applying the meshes and a minimum bounding box was drawn for each grain to calculate the scale factors for every dimension (width, height and depth).

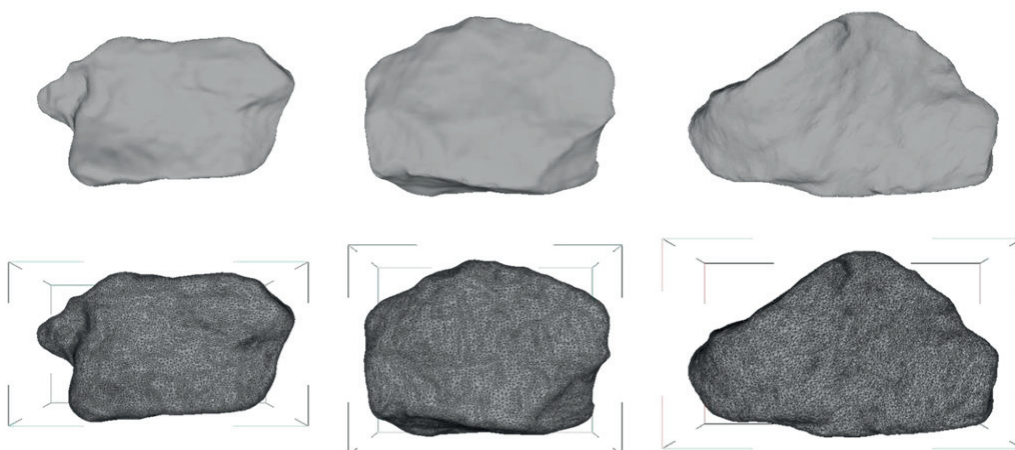
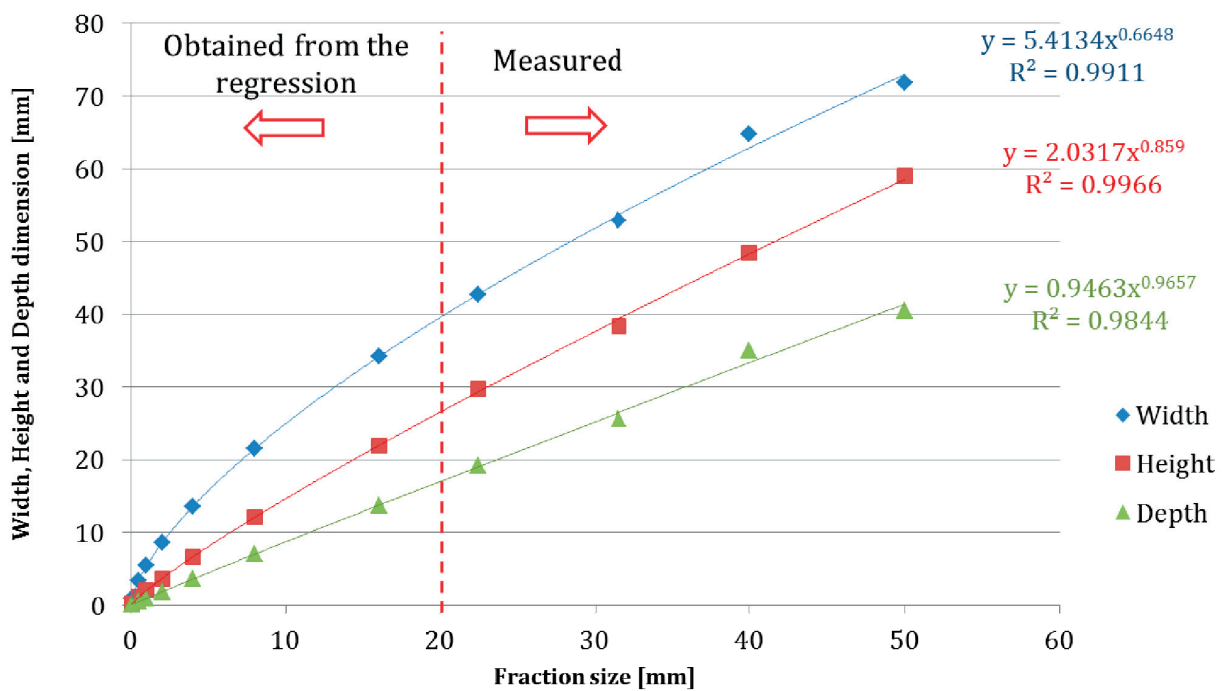


Figure 5.5 Example of aggregate images obtained from laser scan technology, meshes and box application with Meshlab software.

The scale factors applied to the width, depth and height of each box are reported in Table 5.2 as a result of the interpolation obtained from the procedure described in Section 5.3.2. The corresponding interpolation curves and equations are shown in Figure 5.6.

Table 5.2 Width, height and depth scale factors applied to aggregates.

Fraction	Width scale factor	Height scale factor	Depth scale factor
16	0,800	0,739	0,719
8	0,631	0,551	0,512
4	0,631	0,551	0,512
2	0,631	0,551	0,512
1	0,631	0,551	0,512
0.5	0,631	0,551	0,512
0.063	0,252	0,169	0,135



*The R^2 was calculated using the four points measured.

Figure 5.6 Interpolation curve and regression equations used to obtain scale factors.

Based on the scale factors, the images of the aggregates were scaled and the area and volume calculated. The average of the area and the volume for the aggregates of the same grading class are computed and used in Equation 5.5 to calculate the surface area factors (α_i). The results are reported in Table 5.3.

Table 5.3 Calculated values of new surface area factors (α_i).

Fractions [mm]	V_{i1kg} [m ³]	a_i [m ²]	v_i [m ³]	N_{i1kg} [kg ⁻¹]	α_i [kg/m ²]
22.4/31.5	3.65E-04	3,56E-03	1.30E-05	28.03	0.0999
16/22.4	3.65E-04	1,98E-03	5.00E-06	72.96	0.1444
8/16	3.65E-04	6,73E-04	9.44E-07	386.24	0.2599
4/8	3.65E-04	2,43E-04	1.64E-07	2223.06	0.5395
2/4	3.65E-04	7.73E-05	2.86E-08	12 735.20	0.9842
1/2	3.65E-04	2.63E-05	5.00E-09	72 955.72	1.9171
0.5/1	3.65E-04	9.28E-06	8.73E-10	417 939.18	3.8776
0.25/0.5	3.65E-04	3,42E-06	1,52E-10	2 394 235.23	8.1934
0.125/0.25	3.65E-04	1,16E-06	2,66E-11	13 715 781	15.8527
0.063/0.5	3.65E-04	3.95E-07	4.74E-12	77 012 279	30.4403

A comparison between α_i and the surface area factors proposed by Hveem (adapted to European sieves) and Craus&Ishai is reported in Figure 5.7.

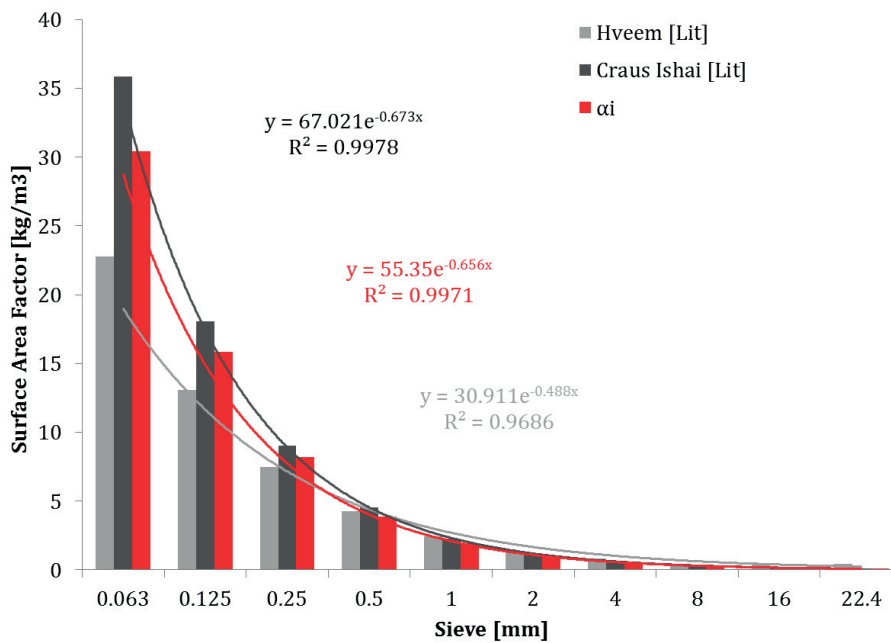


Figure 5.7 Comparison between Hveem ,Craus & Ishai and revised surface area factors (α_i).

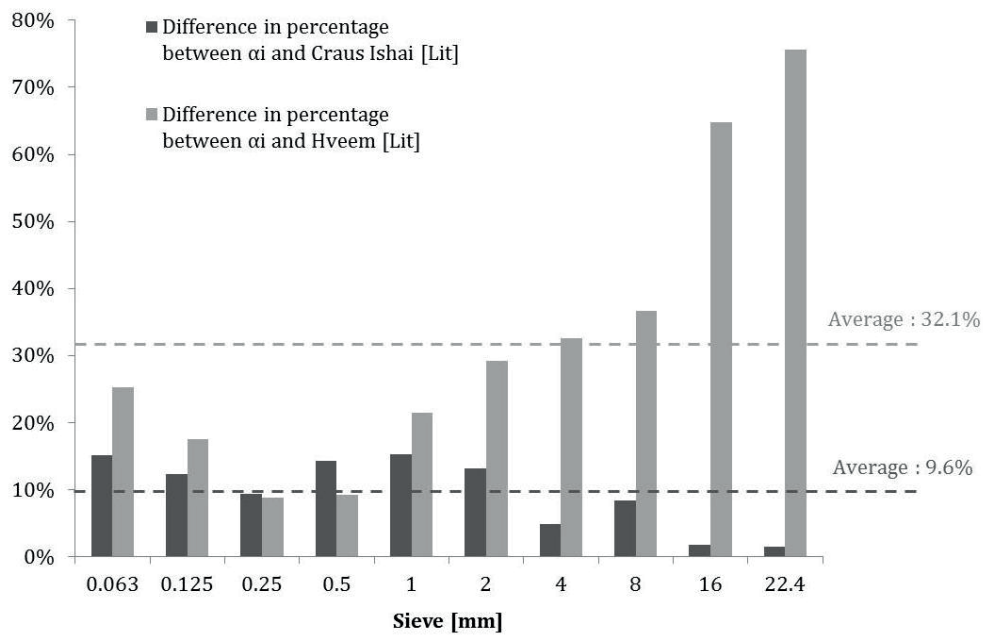


Figure 5.8 Differences in percentage between α_i , Hveem and Craus & Ishai for every sieve size sieve.

From the comparison in Figure 5.7 it can be seen that the Hveem surface area factors for particles retained by the 0.5-mm sieve are higher than the α_i . They become lower for particles passing through the 0.5-mm sieve. The Craus & Ishai surface area factors however are higher for particles passing through the 0.5-mm sieve and they become almost the same as α_i for the bigger grains ($d > 0.5$ mm). Thus, according to the results obtained for these specific aggregates, it emerges that Hveem underestimated the contributions of small particles ($d < 4$), while the Craus & Ishai area factors overestimate them. Neither considered the real shapes and surface of the aggregates. The differences between the factors reported in Figure 5.8 highlight that the Craus & Ishai factors are closer to α_i , while the discrepancy between the α_i and the Hveem factors is higher especially for the big particles. This difference is mitigated by the fact that the contribution of big particles to the total SSA is significantly lower than the contribution provided by the small particles.

Knowing the total SSA of aggregates, it is possible to calculate the bitumen required for coating the aggregates with a selected optimal bitumen film thickness of 10 microns according to the AC B 16 grading curve (Table 5.4). This first step excludes the filler contribution included in the next section.

Table 5.4 Calculated values of new surface area factors (α_i).

Fractions [mm]	α_i [m ²]	v_i [m ³]	N_{i1kg} [kg ⁻¹]	α_i [m ² /kg]	$(p_{i+1} - p_i)$ [%]	SSA_{agg} [m ² /kg]
		Eq.(3)	Eq.(4)	Eq.(5)	Eq.(6)	Eq. (6)
22.4/31.5	3,56E-03	1.30E-05	28.03	0.0999	-	-
16/22.4	1,98E-03	5.00E-06	72.96	0.1444	4	0.00577
8/16	6,73E-04	9.44E-07	386.24	0.2599	20	0.05199
4/8	2,43E-04	1.64E-07	2223.06	0.5395	25	0.13487
2/4	7.73E-05	2.86E-08	12 735.20	0.9842	18	0.17715
1/2	2.63E-05	5.00E-09	72 955.72	1.9171	10	0.19171
0.5/1	9.28E-06	8.73E-10	417 939.18	3.8776	7	0.27143
0.25/0.5	3,42E-06	1,52E-10	2 394 235.23	8.1934	2	0.16389
0.125/0.25	1,16E-06	2,66E-11	13 715 781	15.8527	4	0.63420
0.063/0.5	3.95E-07	4.74E-12	77 012 279	30.4403	3	0.91321
Total aggregate surface						2,54422
$\bar{t}_{opt-agg}$ [micron] (selected from literature)						10
$V_{bit-agg}$ [m ³ /kg]						2,5442E-05

5.5.2. Filler

The two laser diffraction PSD measurements carried out on the fillers shows significantly different results (Figure 5.9). The average PSD results obtained from a minimum of five repetitions and the BET results are reported in Table 5.5.

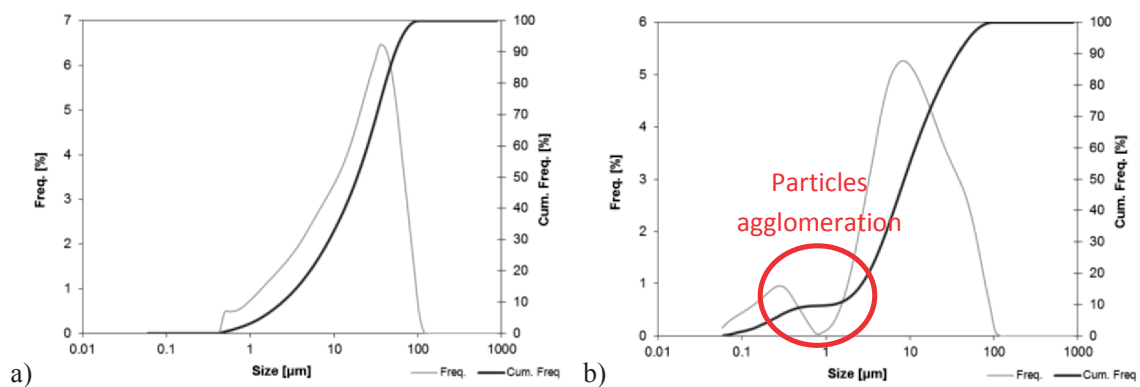


Figure 5.9 PSD for a) limestone and b) hydrated lime.

Table 5.5 Summary of PSD and BET results.

Type of filler	Mean diameter $d_{[4,3]}$ [μm]	$d_{[v,0.1]}$ [μm]	$d_{[v,0.5]}$ [μm]	$d_{[v,0.9]}$ [μm]	SSA_{PSD} [m^2/g]	SSA_{BET} [m^2/g]
Limestone	25.42	2.44	18.93	52.81	0.3526	6.0676
Hydrated lime	16.15	1,21	8.45	40.62	1.9065	12.8071

As can be seen from Figure 5.9 and Table 5.5 the two fillers exhibit different particle size distributions and hydrated lime is generally composed of smaller particles. Focusing on the SSA measurements it can be observed that the PSD and BET tests give significantly different results. This is because the filler particles are not completely dispersed in the fluid in the PSD tests and they tend to agglomerate as shown in Figure 5.9. Hydrated lime has almost double the specific surface of that of limestone. The degree of agglomeration (F_{ag}) was calculated (Equation 5.9) and the results of the calculation and F_{ag} are summarised in Table 5.6.

Table 5.6 Characteristic values for calculating F_{ag} .

Type of filler	SSA_{BET} [m^2/g]	ρ [g/cm^3]	d_{BET} [μm]	$d_{[v,0.5]}$ [μm]	F_{ag}
Limestone	6.0676	2.705	0.365	18.93	51.79
Hydrated lime	12.8071	2.249	0.212	8.45	40.57

The agglomeration of both fillers is high and the limestone has a greater tendency to agglomerate than hydrated lime. The clustering is also confirmed by the ESEM images (Figure 5.10), where the particles are agglomerated and overlapped; indeed they are not clearly recognisable.

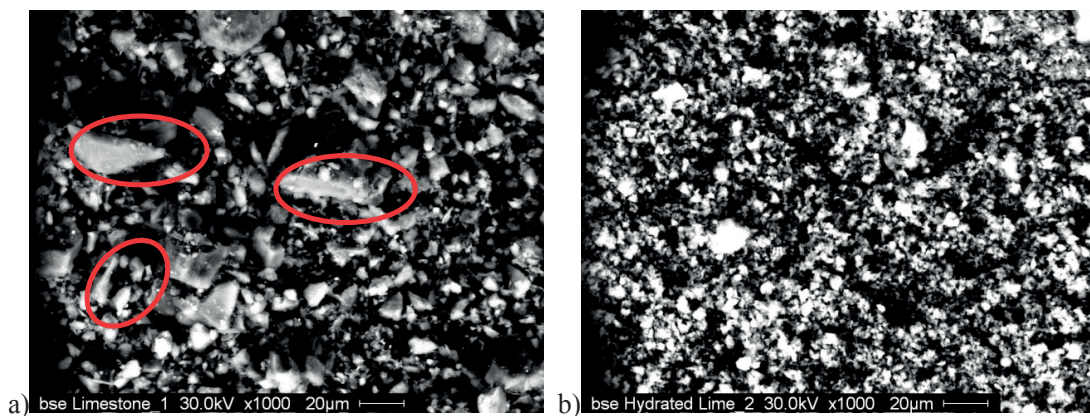


Figure 5.10 Electronmicrograph of a) limestone and b) hydrated lime particles.

Moreover, some limestone particles are elongated and not similar to spheres, thus once again the PSD measurements only cannot be reliable in this case for the calculation of the specific surface.

On the one hand, the SSA_{BET} measure is the more reliable because it takes into account the actual shapes of the particles that are completely dispersed. On the other hand, this value cannot be used in the calculation because it does not correspond to the effective SSA of the filler in the mixture due to its tendency to agglomerate.

To overcome this problem the *critical filler concentration* ($\emptyset c$) was used for defining the amount of bitumen required for coating the filler. Indeed, the results highlight the difficulties of applying the same principle of SSA calculation for the virgin aggregates to the fillers. Therefore, in this study the method of defining the correct quantity of bitumen for a suitable coverage of filler was based on the performance (stiffness) evaluation of the mastic (filler and bitumen) by varying the filler concentration as proposed by Faheem and Bahia. This represents the maximum allowable limit of filler in the mastic before the cohesive strength state is reached. The critical filler concentration and volume of bitumen necessary for maintaining the mastic in a diluted phase in the case of AC B 16 are summarised in Table 5.7. The method was applied only to the limestone because the Rigden voids of the hydrated lime (58%) exceeded the experimental validity domain used by Faheem and Bahia.

Table 5.7 Calculated value of bitumen volume necessary to maintain mastic in diluted phase.

Percentage of passing material in target grading curve [%]	$\emptyset c$ [% by volume]	Filler density ρ [kg/m ³]	V_{filler} [m ³ /kg]	Eq. (5.14) $V_{bit-filler} = \frac{V_{filler} \cdot (1 - \frac{\emptyset c}{100})}{\frac{\emptyset c}{100}}$ [m ³ /kg]
7	46	2705	2.5878E-05	3.064E-05

5.5.3. RAP clustering prediction model

The mass of new RAP clusters for different fractions and several percentages of RAP are summarised in Table 5.8.

Table 5.8 Summary of results of percentage of new clusters in mass for different RAP fractions and percentages of RAP.

Fraction [mm]	Percentage of RAP [%]	Percentage of new clusters in mass of weight of RAP fraction [%]
0.063/0.5	10	24.55
	30	55.05
	50	64.34
	70	45.35
	90	13.40
0.5/1	10	30.00
	30	58.80
	50	70.20
	70	59.25
	90	32.80
1/2	10	-
	30	39.25
	50	46.00
	70	24.80
	90	31.35
2/4	10	8.05
	30	11.75
	50	12.95
	70	9.14
	90	8.55

All the combinations in Table 5.8 tested according to the procedure explained in Section 5.3.4 allowed the quantification of the new RAP clusters for every RAP fraction and percentage of RAP. Therefore, a second-degree multiple regression analysis and the determination of the coefficients of the model (Equation 5.17) were carried out:

$$C'_i = 49.96 - 16.94x_1 - 1.47x_2 + 2x_1x_2 - 11.59x_1^2 - 24.08x_2^2 \quad (5.17)$$

where:

C'_i = percentage in mass of RAP new clusters of weight of RAP-i-fraction [%]

x_1 = standardised size of RAP fraction (0.063/0.5, 0.5/1, 1/2, 2/4 mm)

x_2 = standardised percentage of RAP [%]

The above model provides the percentage of RAP new clusters in mass for every RAP fraction once the standardised input parameters (type of fraction and percentage of RAP) are established.

The ANOVA in Table 5.9 reports the goodness of fit of the model presented in Equation 5.17.

Table 5.9 ANOVA table for second-degree model presented in Equation 5.16.

Clustering model	SS ¹	df ¹	MS ¹	F ¹	p-value ¹
2° degree	28012.24	6	4668.707	36.777	2.02E-07
Residual	1650.299	13	126.9461		
Total	29662.54	19			

¹SS: Sum of the Squares; df: degree of freedom; MS: Mean Squares; F-statistic; p-value

In order to include the clustering model in the mix design calculation it is necessary to weight the clustering according to the percentage of RAP material for every fraction:

$$C_i = C'_i \cdot RAP_{i_fraction} \quad (5.18)$$

where C_i is the percentage of the total mass of new RAP clusters for the i-fraction, $RAP_{i_fraction}$ is the mass of the i-fraction in the RAP grading curve. The RAP grading curve was then readjusted, taking into account the clustering according to the following equation:

$$\% RAP_{i_fraction\ readjusted} = (p_{i+1} - p_i - C_{i+1} + C_i) \quad (5.19)$$

where:

$\% RAP_{i_fraction\ readjusted}$ = percentage of RAP material between i and i+1 sieve readjusted after formation of new RAP clusters

p_{i+1} = percentage by weight passing through (i+1)-sieve [%]

p_i = percentage by weight passing through i-sieve [%]

C_{i+1} = percentage of mass of particles clustered and retained in (i+1)-sieve calculated in Equation 5.18 [%]

C_i = percentage of mass of particles clustered and retained in i-sieve calculated in Equation 5.18 [%]

Applying the same surface area factors as those calculated for the virgin aggregates, it is possible to determine the surface of RAP (SSA_{RAP}) after the new clustering occurred during the mixing process:

$$SSA_{RAP} = \sum_i^n \alpha_i (p_{i+1} - p_i - C_{i+1} + C_i) \quad (5.20)$$

where n is the number of fractions.

The main concept underlying the adjustment (see Figure 5.11) of the RAP grading curve (Equation 5.19) after the new clustering occurred during the mixing process is the subtraction of the clustered particles that move from the $RAP_{i_fraction}$ to the upper fraction and the addition of the clusters that move into the $RAP_{i_fraction}$ from the lower one. With the readjusted grading curve it is possible to calculate the surface of RAP (Equation 5.19). To clarify the conceptual model, a schematic representation is shown in Figure 5.11. Note that the cluster phenomenon occurs only among small-size RAP particles (Bressi et al. 2015d). Thus the phenomenon is considered only up to a particle size of 4 mm.

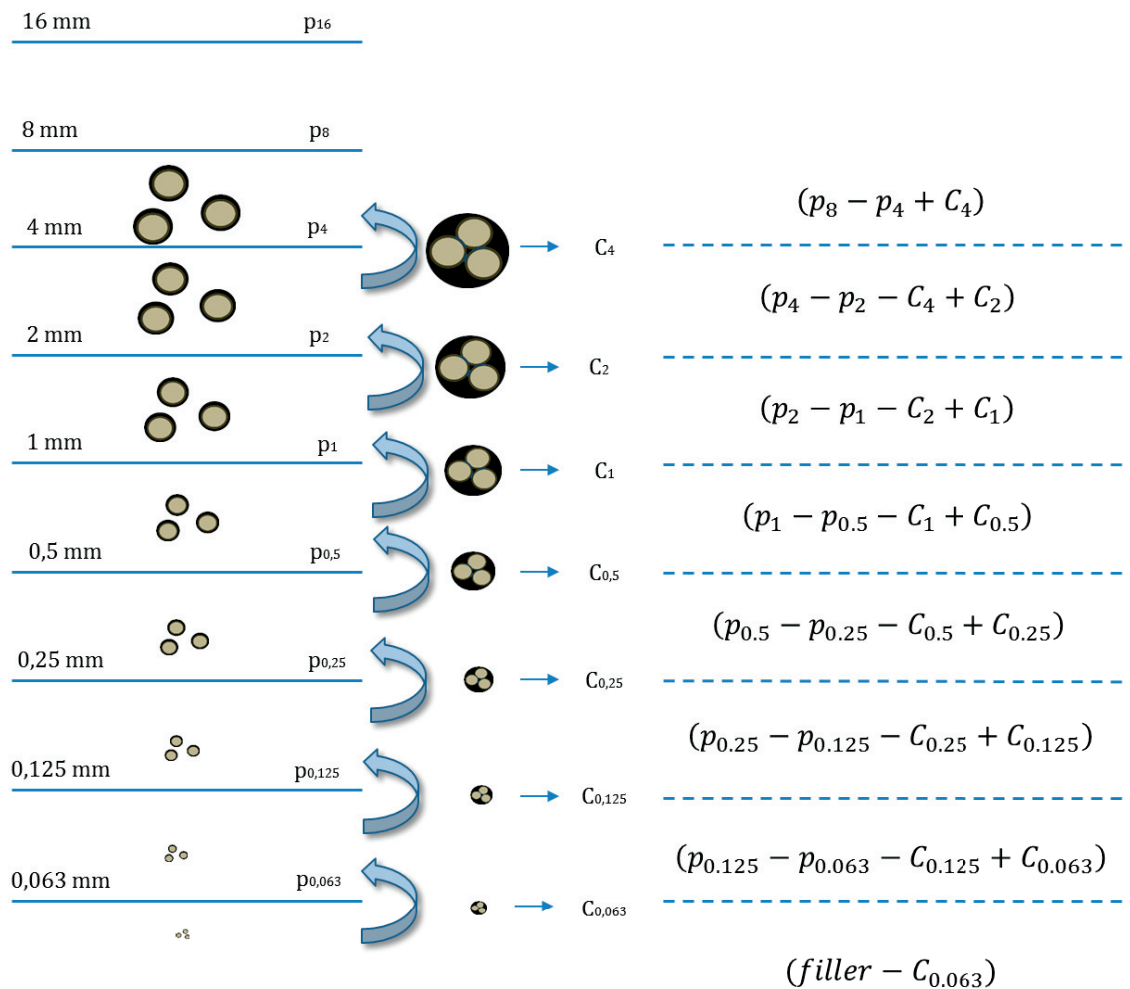


Figure 5.11 Schematic representation of readjustment of RAP grading curve based on cluster phenomenon.

5.6.Final theoretical formulation and laboratory verification

After defining the contributions of all the components (aggregates, filler and RAP) by Equations 5.6, 5.14 and 5.20 the amount of bitumen to be added to the RAP mixtures can be calculated as follows:

$$V_{bit} = \bar{t}_{opt-agg} \cdot \left\{ \left[(1 - \%RAP) \sum_i^n \alpha_i [(pt_{i+1} - pt_i) - (pr_{i+1} - pr_i - C_{i+1} + C_i)] \right] + \left[\%RAP \sum_i^n \alpha_i (pr_{i+1} - pr_i - C_{i+1} + C_i) \right] \right\} + \frac{V_{filler} \cdot (1 - \frac{\emptyset c}{100})}{\frac{\emptyset c}{100}} \quad (5.21)$$

where:

V_{bit} = estimation of optimal bitumen to add to mixture [m³/kg]

$\bar{t}_{opt-agg}$ = optimal average thickness of virgin bitumen around aggregates chosen equal to 10 microns [m]

$\%RAP$ = RAP percentage in asphalt mixture [-]

α_i = surface area factor of aggregates passing through i+1 sieve and retained in i-sieve [m²/kg]

pt_{i+1} = percentage of material passing through (i+1)-sieve in target grading curve of AC B 16 [%]

pr_{i+1} = percentage of material passing through (i+1)-sieve in RAP curve [%]

pt_i = percentage of material passing through i-sieve in target grading curve [%]

pr_i = percentage of material passing through i-sieve in RAP curve [%]

C_{i+1} = percentage of mass of particles clustered and retained in (i+1)-sieve [%]

C_i = percentage of mass of particles clustered and retained in i-sieve [%]

V_{filler} = volume of filler [m³/kg]

$\emptyset c$ = critical filler concentration [% by volume]

$(pt_{i+1} - pt_i) - (pr_{i+1} - pr_i - C_{i+1} + C_i)$ represents the amount of virgin aggregates to add to the mixtures for every fraction in order to readjust the target grading curve after the RAP clustering occurring during a new mix. Thus, Equation 5.22 can be written as:

$$V_{bit} = \bar{t}_{opt-agg} \cdot \left\{ \left[(1 - \%RAP) \sum_i^n \alpha_i (pa_{i+1} - pa_i) \right] + \left[\%RAP \sum_i^n \alpha_i (pr_{i+1} - pr_i - C_{i+1} + C_i) \right] \right\} + \frac{V_{filler} \cdot (1 - \frac{\emptyset c}{100})}{\frac{\emptyset c}{100}} \quad (5.22)$$

where:

pa_{i+1} = percentage of virgin aggregates passing through (i+1)-sieve to add to mixture [%]

pa_i = percentage of virgin aggregates passing through i-sieve to add to mixture [%]

To verify that the calculations developed in this research lead to a valid estimation of the bitumen dosage added to the mixture, the methodology was applied to a Swiss standard asphalt concrete binder course AC B 16. The steps and the results of the calculation for defining the optimal bitumen quantity in the case of 0% of RAP (Equation 5.21) are shown in Table 5.10.

Table 5.10 Calculated value of optimal quantity of bitumen to add to AC B 16 without RAP according to procedure developed.

Aggregates (>0.063 mm)				
Sieve size [mm]	Percentage of passing material in target grading curve [%]	$(p_{i+1} - p_i)$ [%]	α_i [kg/m ²]	Surface area per mass of aggregate [m ² /kg]
22.4	100	-	0.09985	-
16	96	4	0.14444	0.005777
8	76	20	0.25996	0.051992
4	51	25	0.53946	0.134866
2	33	18	0.98415	0.177147
1	23	10	1.91711	0.191711
0.5	16	7	3.87755	0.271428
0.25	14	2	8.19452	0.16389
0.125	10	4	15.85269	0.634197
0.063	7	3	30.44027	0.913208
$SSA_{agg} = \sum \alpha_i \cdot (p_{i+1} - p_i)$ [m ² /kg]				2.544217
$\bar{t}_{opt-agg}$ [micron]				10
Volume of bitumen covering the aggregates [m ³ /kg]				2.544E-05
Filler (<0.063 mm)				
Percentage of passing material in target grading curve [%]	$\emptyset c$ [% by volume]	Filler density [kg/m ³]	V_{filler} [m ³ /kg]	$V_{bit-filler} = \frac{V_{filler} \cdot (1 - \frac{\emptyset c}{100})}{\frac{\emptyset c}{100}}$ [m ³ /kg]
7	46	2705	2.5878E-05	3.064E-05
Optimal quantity of bitumen				
	Total volume of bitumen [m ³ /kg of aggregates]	Bitumen density [kg/m ³]	Mass of bitumen [%]	Optimal percentage of bitumen in mixture [%]
	5.609E-5	1030	0.0578	5.46

Thus, if 50% of RAP is used in AC B 16, the theoretical calculation leads to the results in Table 5.11.

Table 5.11 Calculated value of optimal quantity of bitumen to add to AC B 16 with 50% of RAP according to procedure developed.

Sieve [mm]	RAP grading curve percentage passing [%]	50% RAP percentage passing [%]	$\%RAP(pr_{i+1} - pr_i)$ [%]	$\%RAP(pr_{i+1} - pr_i - C_{i+1} + C_i)$ [%]	α_i [m ² /kg]	RAP surface for every fraction [m ² /kg]
22.4	100.0	50.0	-	-	-	-
16.0	100.0	50.0	-	-	-	-
8.0	72.8	36.4	13.6	13.6	0.260	0.035
4.0	37.6	18.8	17.6	21.4	0.540	0.115
2.0	16.6	8.3	10.5	12.03	0.984	0.118
1.0	6.7	3.4	5.0	2.4	1.917	0.046
0.500	2.4	1.2	2.2	0.6	3.878	0.023
0.250	0.9	0.5	0.8	0.0	8.195	0.000
0.125	0.3	0.2	0.3	0.04	15.855	0.008
0.063	0.1	0.1	0.1	0.00	30.440	0.000
RAP total surface [m²/kg]						0.3461
Sieve [mm]	Target grading curve percentage passing [% by weight]	RAP percentage passing readjusted after cluster [% by weight]	Grading curve of virgin aggregates required to maintain target curve [% by weight]	$(1 - \%RAP)(pa_{i+1} - pa_i)$ [% by weight]	α_i [m ² /kg]	Surface of virgin aggregates for every fraction [m ² /kg]
22.4	100.0		50.0	-	-	
16.0	96.0	50.00	45.9	4.1	0.1444	0.00585
8.0	76.0	36.45	39.5	6.4	0.2600	0.01664
4.0	51.0	15.09	35.9	3.6	0.5395	0.01961
2.0	33.0	3.05	29.9	6.0	0.9841	0.05872
1.0	23.0	0.64	22.4	7.6	1.9171	0.14551
0.500	16.0	0.05	16.0	6.4	3.8775	0.24831
0.250	14.0	0.05	14.0	2.0	8.1945	0.16389
0.125	10.0	0.00	10.0	4.0	15.8549	0.62649
0.063	7.0	0.00	7.0	3.0	30.4403	0.91321
Virgin aggregate surface [m²/kg]						2.19822
Total surface (RAP+virgin aggregates) [m²/kg]						2.5443
Volume of bitumen to cover virgin aggregates and RAP [m³/kg] (with $\bar{t}_{opt}=10$ micron)						2.544E-05
Volume of bitumen to cover filler [m³/kg]						3.043E-05
Total bitumen volume [m³/kg]						5.587E-05
Bitumen density [kg/m³]						1030
Percentage of virgin bitumen to add to mixture [% by weight of total mixture]						5.44

The percentage of bitumen calculated in Table 5.11 represents the estimation of the optimal binder quantity to add to the mixture after readjusting the grading curve due to the RAP cluster phenomenon occurring during a new mix phase. Indeed, Equation 5.22 allows manipulating the size and amount of virgin aggregates to adjust the curve, knowing the change caused by the RAP clustering. Moreover, it would potentially be possible to use different bitumen film thicknesses for different particle sizes. The

density is assumed to be constant for all the aggregates. To verify the theoretical results obtained, laboratory tests were conducted. When RAP is not used, Equations 5.22 is still valid because all the terms related to RAP are equal to zero since the RAP percentage is zero. Thus, the percentage of bitumen that represents the estimation the optimal binder quantity to add to the asphalt mixture without RAP was calculated in Table 5.10. Four mixtures were fabricated with 4.5, 5.0, 5.5 and 6% of bitumen in the mixtures. The characteristics of the virgin bitumen chosen for the mixture fabrication are summarised in Table 1.3 Chapter 1. The Marshall stability, Marshall quotient stability/flow, air voids, VMA, VFB and density (SN EN 12697-6-8-30-34), gyratory compactability and ITST (SN EN 12697-6-8-23) at different temperatures (-10; 15 and 40°C) were measured. The results for AC B 16 without RAP are summarised in Figures 5.12, 5.13, 5.14 and in Table 5.12.

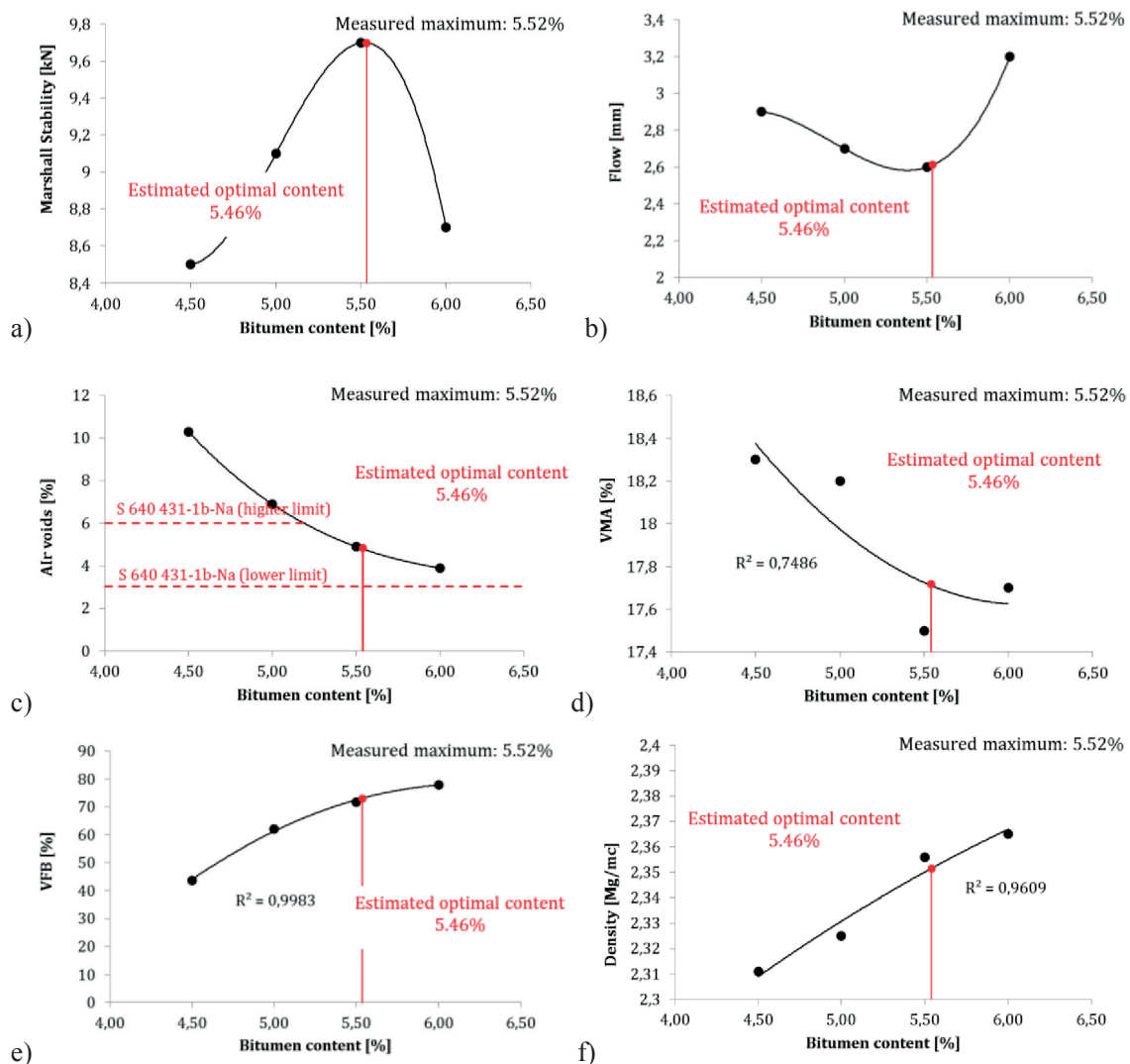


Figure 5.12 Results obtained with Marshall tests and compaction for AC B 16 without RAP (average of four samples for every combination).

In the case of AC B 16 without RAP, the optimal binder quantity measured maximising the Marshall Stability is equal to 5.52% of bitumen content in the mixture, as shown in Figure 5.12a. This value meets the Swiss standard specifications (S 640 431-1b-Na) that are: 7.5 kN for the Marshall stability, 2-4 mm of flow and 3-6% of air void range. The optimal bitumen content value estimated by the proposed methodology is equal to 5.46%, which differs from the measured one (5.52%) by only 1.06% and also meets all the requirements.

Additional combinations were tested with the gyratory compactor. The results are summarised in Table 5.12 and Figure 5.13.

Table 5.12. Summary of results of gyratory compactability for AC B 16 without RAP (average of three samples).

Binder content [%]	Number of gyrations*	Compactability [%]	Air voids N_{design} [%]	Slope of compactability regression curve
4.5	$N_{initial}$	81.3	9.4	3.67
	N_{design}	90.6		
	N_{max}	92.2		
4.9	$N_{initial}$	82.5	7.8	3.82
	N_{design}	92.2		
	N_{max}	93.9		
5.0	$N_{initial}$	82.0	8.2	3.81
	N_{design}	91.8		
	N_{max}	93.4		
5.3	$N_{initial}$	83.1	6.8	3.96
	N_{design}	93.2		
	N_{max}	95.0		
5.5	$N_{initial}$	84.1	5.8	3.97
	N_{design}	94.2		
	N_{max}	96.0		
5.7	$N_{initial}$	84.7	5.1	3.99
	N_{design}	94.9		
	N_{max}	96.7		
6.0	$N_{initial}$	84.9	4.9	3.98
	N_{design}	95.1		
	N_{max}	96.9		

* $N_{initial}$ =8 gyrations; N_{design} =100 and N_{max} =160

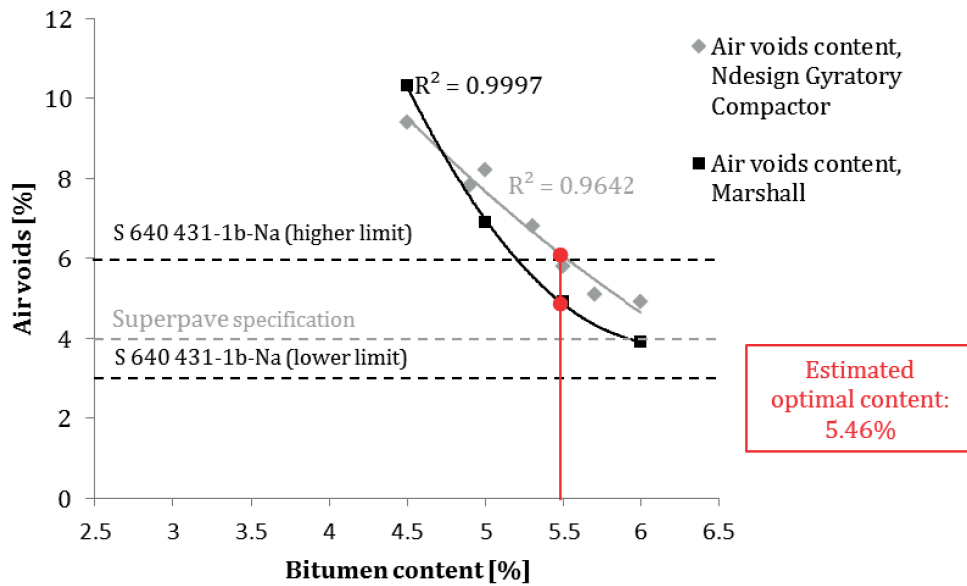
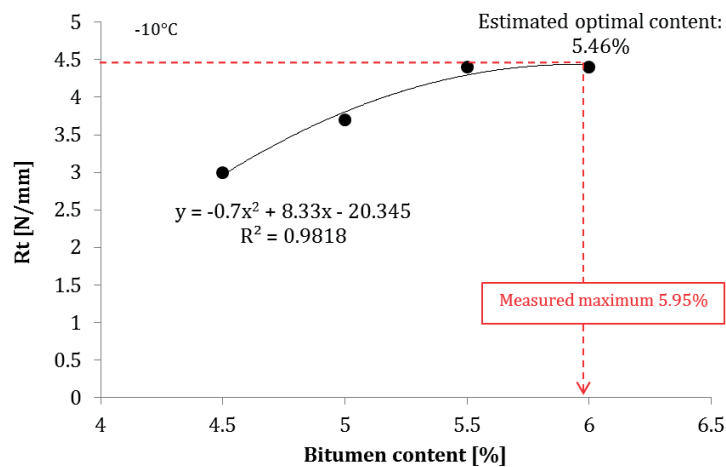


Figure 5.13 Comparison between air void content measured with Marshall test and gyratory compactor in AC B 16 without RAP.

The gyratory compactor and Marshall tests gave slightly different results in the air void plot. This was to be expected considering the two different ways of compacting the samples. The 4% of voids for N_{design} that corresponds to the Superpave specification is not reached for the bitumen contents used. Using the gyratory compactor, the value of air voids extrapolated for the estimated optimal bitumen content is 6.16%. The allowable range indicated by the Swiss standard is from 3 to 6% and the value is therefore just above the limit. Nevertheless, this could be due to non-optimal aggregate packing.

The ITST results at three temperatures (-10, 15 and 40°C) for AC B 16 without RAP are shown in Figure 5.14.



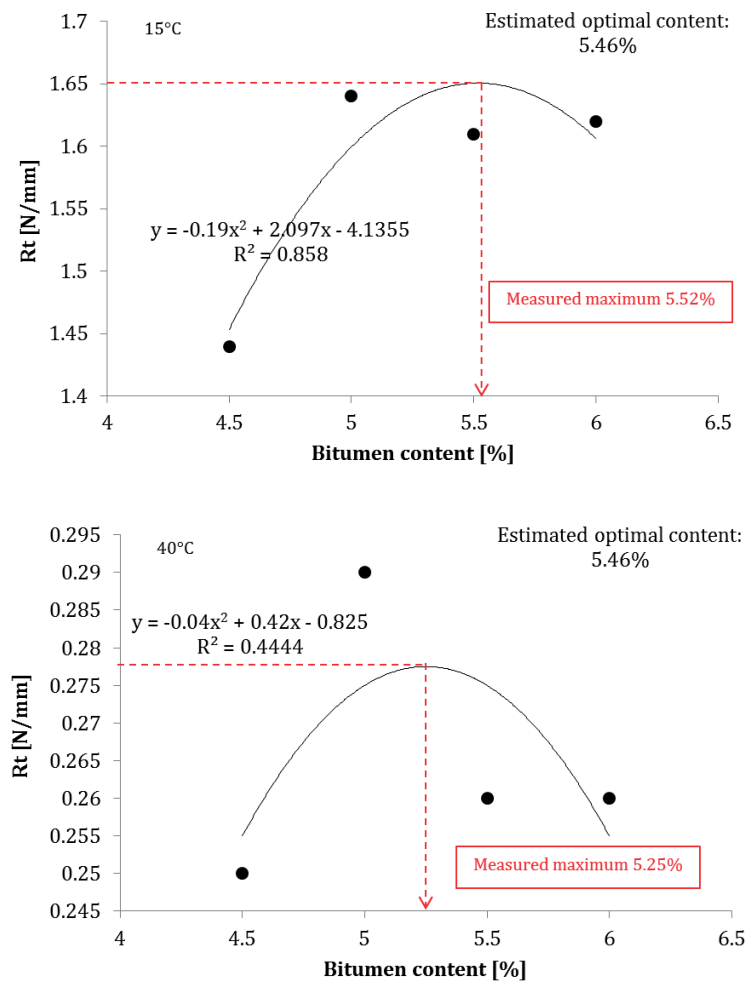


Figure 5.14 ITST results for AC B 16 without RAP at three temperatures: a) -10°C, b) 15°C and c) 40°C.

The ITS tests (Figure 5.14), as expected, show different results for different temperatures. When the temperature increases the tensile resistance decreases and the maximum is reached for lower amount of bitumen: 5.95, 5.52 and 5.25% for -10; 15 and 40°C respectively. Note that the curve at 40°C shows a low R^2 . At 15°C the bitumen content that maximises the tensile resistance is 5.52%, exactly the same quantity that maximises the Marshall stability.

Considering all the tests conducted, it is possible to assert that for AC B 16 without RAP the optimal bitumen quantity measured is 5.52% of the mixture. The optimal bitumen content value estimated by the proposed methodology is equal to 5.46%, which differs from the measured one by only 1.06%. The estimated bitumen quantity meets all the Swiss standard requirements.

The results of the Marshall and ITS tests for AC B 16 with 50% of RAP are reported in Figures 5.15 and 5.16.

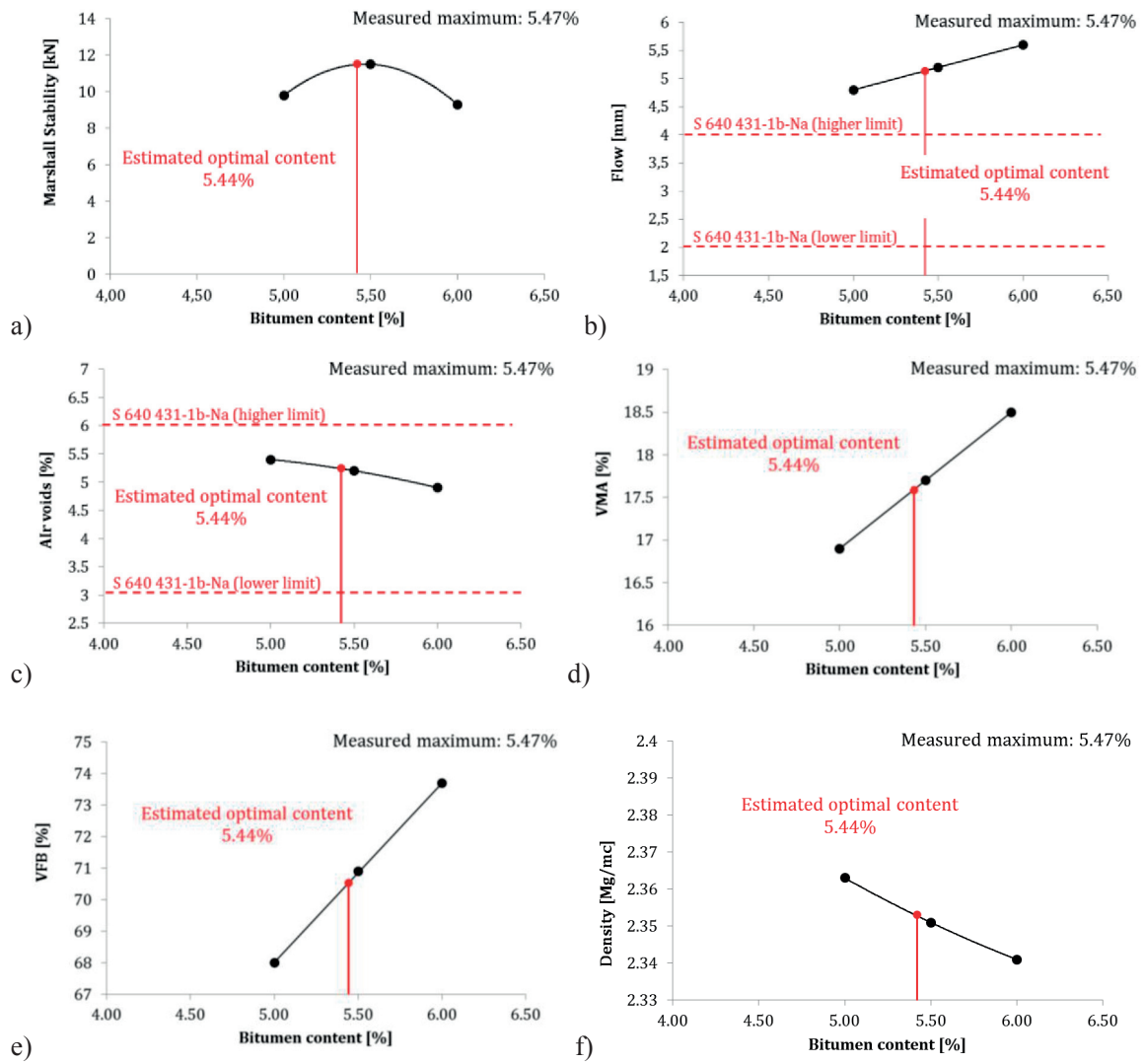


Figure 5.15 Marshall test results for AC B 16 with 50% of RAP. The bitumen content refers to virgin bitumen to be added to mixture.

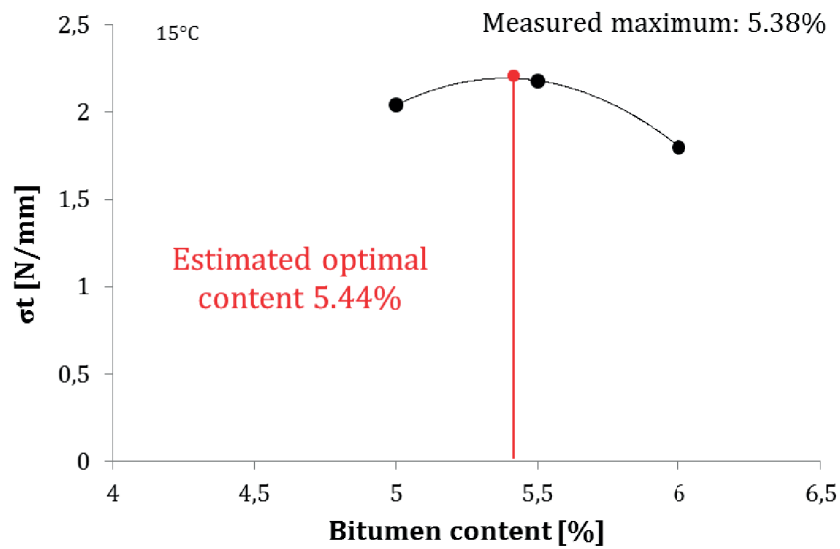


Figure 5.16 ITST results (σ_t) at 15°C for AC B 16 with 50% of RAP. The bitumen content refers to virgin bitumen to be added to mixture.

The Marshall tests conducted (Figure 5.15) show that the bitumen quantity calculated with the proposed methodology (5.44%) represents a reliable estimation of the measured optimal value (5.47% of the asphalt mixture). The requirements for Marshall stability and air voids are met, although the flow exceeds the admissible range of between 2 and 4 mm. This is because the old binder in the RAP becomes softer during heating and acts as a lubricant, increasing the flow during load application. The optimal bitumen quantity according to the ITST (Figure 5.16) at 15°C is 5.38% of the mixture. The theoretical calculation provides also in this case a reliable estimation of the optimal bitumen quantity measured; indeed the values differ by only 1.1%.

Figure 5.17 shows a comparison of the compactability trend as a function of the bitumen quantity for AC B 16 mixtures without RAP; with 50% of RAP without changing virgin aggregate proportions after RAP particle agglomeration, and mixture with 50% of RAP where proportions of virgin aggregates have been changed considering RAP clustering by readjusted grading curve.

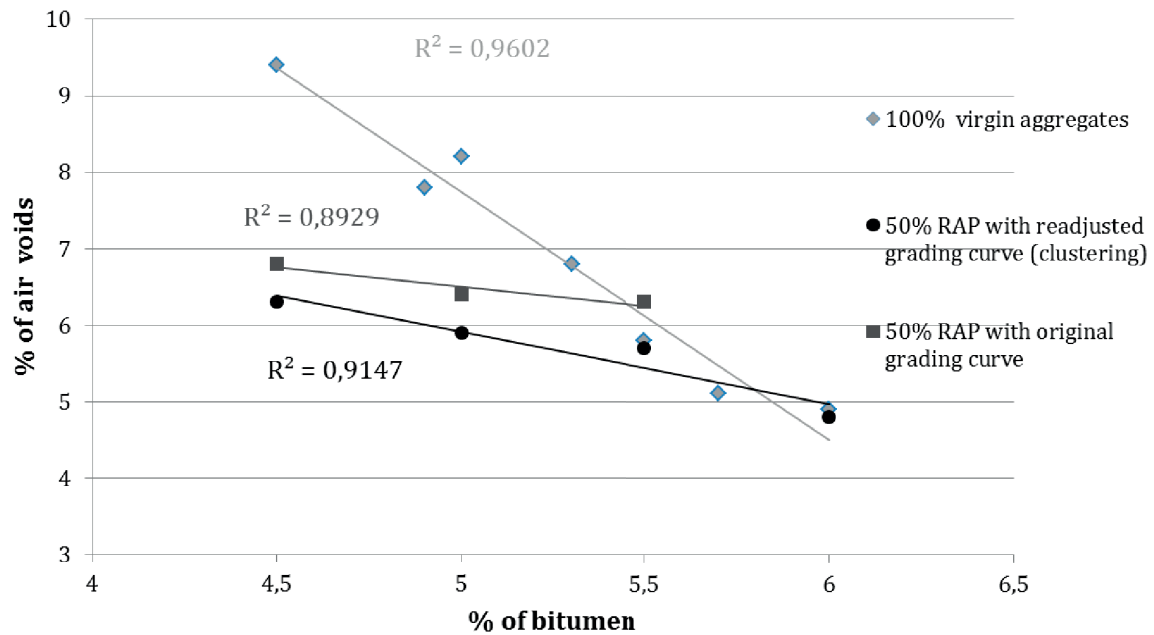


Figure 5.17 Gyratory air void content for AC B 16 asphalt mixtures with 100% of virgin aggregates, with 50% of RAP without considering clustering and 50% of RAP considering clustering for readjustment of grading curve.

From Figure 5.17 it is clear that the compactability of virgin and RAP mixtures is significantly different. For low bitumen content (4.5 and 5 %) the effect of the aged binder in both RAP mixtures is significant because it acts as lubricant increasing the compactability. As the amount of virgin binder increases the air voids decrease more rapidly in the case of a virgin mixture. The effect of the aged binder in RAP mixtures becomes less evident and is probably masked by the presence of intergranular voids trapped in the RAP clusters. The air voids trapped in the old RAP clusters, before the new RAP mixing, are not attainable by the bitumen. Thus, even if virgin bitumen is added, the air voids cannot be filled. Moreover with the formation of new RAP clusters during the mixing a reduction in the small-size particles occurs. This causes a change in the final grading curve and an increase in the amount of air voids. Thus, for mixtures with 50% of RAP without the proposed readjustment of the grading curve, it appears difficult to achieve an acceptable air void content (<6%). However, if clustering is taken into account and specific amounts of virgin aggregates are added to replace the agglomerated small-size RAP particles, the compactability of the mixture improves and an acceptable range of air voids is obtained. A consequence of these conclusions is that it is essential to break the old RAP clusters and avoid the presence of intergranular voids in order to reach the acceptable void range. One possible solution could be to select an appropriate mixing energy during the asphalt mixture fabrication.

Finally, the results of Marshall stability for the AC B 16 with and without RAP summarized in Tables 5.13 and 5.14 allow other conclusions to be drawn.

Table 5.13 Marshall Stability results, mean, STD and COV for AC B 16 without RAP.

Virgin bitumen added to the mixture [% by weight]	Marshall Stability [kN]	Mean	STD	COV	\overline{COV}
5.0	9.8	9.4	0.716	0.076	0.050
	10.2				
	8.7				
	8.9				
5.5	9.8	9.8	0.058	0.006	
	9.8				
	9.7				
	9.7				
6.0	9.5	8.7	0.591	0.068	
	8.5				
	8.1				
	8.8				

Table 5.14 Marshall Stability results, mean, STD and COV for AC B 16 with 50% of RAP.

Virgin bitumen added to the mixture [% by weight]	Marshall Stability [kN]	Mean	STD	COV	\overline{COV}
5.0	10.2	9.7	0.550	0.057	0.044
	9.8				
	9.8				
	8.9				
5.5	11.9	11.5	0.386	0.034	
	11.8				
	11.1				
	11.3				
6.0	9.4	9.4	0.386	0.041	
	9.2				
	9.0				
	9.9				

The statistical study conducted on the aged binder and on the binder blends (Chapters 2 and 3) highlighted the higher variability in the response when the RAP binder blends with the virgin bitumen. Nevertheless, from the comparison between the results in Tables 5.13 and 5.14 it is possible to observe that the average of the coefficient of variation does not change significantly if 0% or 50% of RAP is used. This led once again to the hypothesis that, in the case investigated, the RAP binder does not blend with the virgin bitumen, since the higher variability detected in the behaviour of the binder blend is not confirmed on the mixture scale. Further studies are needed to confirm that.

5.7. Summary of findings and conclusions

This study proposes a new mix design approach for hot-recycled HMA with and without RAP based on the optimisation of bitumen quantity in the mixtures. The methodology focuses on the separation of three main contributions that reflect different roles and behaviours in the mixture: virgin aggregates ($d > 0.063$ mm), filler ($d < 0.063$ mm) and RAP. The aggregate part (virgin or RAP) is related to the surface calculation, and the filler contribution related to the mastic performance. Thus, the optimal quantity of bitumen required to coat both is based on two different criteria: for the aggregates it is the specific surface, for the filler it is the *critical filler concentration* for maintaining the mastic (filler and bitumen) in a diluted phase. Moreover, in the case of RAP a clustering prediction model was introduced in the calculation to readjust the grading curve, taking into account the phenomenon of the RAP particle agglomeration.

The analysis of each component led to the following findings:

- The calculations of the revised surface area factors (α_i) for the aggregates analysed are based on the real shape and surface of the grains and do not require the approximation of spheres or cubes. These surface area factors differ from the previous ones calculated in the literature (Hveem and Craus&Ishai) by an average of 32.1% (Hveem) and 9.6% (Craus&Ishai).
- Hydrated lime has almost double the specific surface of limestone because hydrated lime is composed of smaller particles. Both fillers show a tendency to agglomerate, especially the limestone.
- The determination of the specific surface of the filler that can be coated by bitumen is not easily measurable because of its agglomeration and composition. It is thus necessary to further investigate how the particle agglomeration reduces the SSA of the filler.
- The *critical filler concentration* enables this problem to be solved by defining the minimum quantity of bitumen required to maintain the mastic (bitumen+filler) in a diluted state. By introducing the *critical filler concentration* another criterion different from SSA has been proposed for determining the bitumen required for the filler coating.

The above-mentioned findings led to the development of the theoretical formula for the optimal bitumen quantity in the mixture:

$$V_{bit} = \bar{t}_{opt-agg} \cdot \{SSA_{agg} + SSA_{RAP}\} + V_{bit-filler}$$

$$V_{bit} = \bar{t}_{opt-agg} \cdot \left\{ \left[(1 - \%RAP) \sum_i^n \alpha_i (pa_{i+1} - pa_i) \right] + \left[\%RAP \sum_i^n \alpha_i (pr_{i+1} - pr_i - C_{i+1} + C_i) \right] \right\} + \frac{V_{filler} \cdot (1 - \frac{\emptyset c}{100})}{\frac{\emptyset c}{100}}$$

where:

V_{bit} = estimation of the volume of optimal bitumen to add to mixture [m³/kg]

$\bar{t}_{opt-agg}$ = optimal average thickness of virgin bitumen around aggregates chosen equal to 10 microns

$\%RAP$ = RAP percentage in asphalt mixture [-]

α_i = surface area factor of aggregates passing through i+1 sieve and retained in i-sieve [m²/kg]

pa_{i+1} = percentage of virgin aggregates passing through (i+1)-sieve to be added to mixture [%]

pa_i = percentage of virgin aggregates passing through i-sieve to be added to mixture [%]

pr_{i+1} = percentage of material passing through (i+1)-sieve in RAP curve [%]

pr_i = percentage of material passing through i-sieve in RAP curve [%]

C_{i+1} = percentage of mass of particles clustered and retained in (i+1)-sieve [%]

C_i = percentage of mass of particles clustered and retained in i-sieve [%]

V_{filler} = volume of filler [m³/kg]

$\emptyset c$ = critical filler concentration [% by volume]

With the methodology proposed it is possible to manipulate the virgin aggregates in order to readjust the grading curve, knowing the change caused by the RAP clustering. Moreover, potentially it would be possible to use different bitumen film thicknesses for different sizes of particles.

The first verification carried out in the laboratory on the AC B 16 without RAP (Marshall stability and quotient flow/stability, gyratory compactor and ITST) gave positive and promising results. Indeed, the optimal quantity of bitumen estimated (5.46% of the mixture) is similar to that measured with the Marshall stability and ITST equal to 5.52%. The difference is 1.06%. The voids percentage that corresponds to the estimated bitumen quantity lies within the limits if the Marshall compaction is considered. It is just above the allowable range if the gyratory compactor ($N_{des}=100$) is used (6.16%). The bitumen quantity estimated allows the production of asphalt mixtures that meet all the Swiss standard requirements.

The second verification in the laboratory was carried out on the AC B 16 with 50% of RAP. The theoretical formula also in this case estimates a reliable value of optimal bitumen content (5.44%) that is comparable to the measured values obtained with Marshall (5.47%) and ITST (5.38%). All the requirements are met except for the flow in the Marshall test. This is because the aged binder becomes softer during heating and acts as a lubricant, increasing the flow during load application. The compactability, measured with the gyratory compactor for RAP mixtures is different from that of virgin mixtures. The reduction of the amount of small-size particles due to the clustering and

intergranular voids trapped in the old RAP clusters prevents the achievement of an acceptable air void content. The RAP particle agglomeration causes a change in the final grading curve and an increase in the amount of air voids. The mixtures designed with the readjustment of the grading curve and a calculation of the specific amounts of virgin aggregates for every fraction to replace the agglomerated small-size RAP particles exhibit improved compactability (acceptable void content). Nevertheless, these results show that it is essential to select an appropriate mixing energy during asphalt mixture fabrication in order to break the old RAP clusters and prevent the presence of intergranular voids in the old clusters.

The variability on the mixtures test results does not increase when RAP is used, contrary to what has happened in the case of the singular use of aged binder and binder blends artificially reproduced. This led to the hypothesis that the amount of RAP binder that blends with virgin bitumen during the fabrication process is negligible otherwise higher variability would have been reflected on the RAP mixture behaviour.

Chapter 6

General conclusions and future work

6.1. Conclusions

The present study aimed at providing a framework for optimising the bitumen quantity in HMA especially when using high quantities of RAP material. Several stages of investigation were carried out.

Firstly, an accurate analysis of the variability of virgin and artificially-aged binders was conducted. Knowing the impact of different ageing levels on binder rheology allows the variability and reliability of the results to be determined when aged binder is involved. Moreover, the analysis allows some conclusions to be drawn regarding the long-term behaviour of the bitumen. Indeed, this part of the study highlighted the fact that at medium and high temperatures the rheology and its variability change with different ageing levels. The inclusion of RAP material and consequently RAP binder in the mixture may result in an increase of the uncertainties regarding the process. Therefore, it is necessary to consider that the results of a mix design calculation for RAP mixtures could be affected by higher variability.

This was verified with the analysis of the binder blend that led to the hypothesis of non-homogenous material. Indeed, decomposing the variability of the test results into the measurement accuracy and the variability due to the physical phenomenon allows the assertion to be made that most of the variability detected is due to this phenomenon. Knowing that the variability of the aged binder is higher than that of the virgin binder has important consequences if the binders blend during a new mix phase. Thus, it became essential to understand how the aged and the virgin binders interact and to know whether the blend is homogeneous by providing a simulation of what happens in a new mix containing RAP assuming the hypothesis of 100% blending. From the development of nonlinear binder blending charts it was also possible to confirm that when the temperature decreases, every effect (amount and type of RAP binder and type of virgin binder) on the blend rheology is cushioned, becoming null when the threshold of -30°C is exceeded. The important result is that the stiffness or complex modulus of the blend is more influenced by the amount of aged binder than by the rheological characteristics of the aged binder. This is a positive result as far as production is concerned, since once the degree of blending is determined; it is easier to control the amount of RAP in the mix than the rheological characteristics of its binder. Moreover, the presence of a plateau region in the stiffness behaviour at low temperatures suggests the existence of a *latent stiffness*, i.e. the heavier molecules of the aged bitumen float in the blend, but their effect is absorbed and cushioned by a predominant matrix of new

bitumen. When the aged binder starts to create a dense network in the blend the stiffness increases rapidly. Further work is needed to confirm this behaviour.

The idea was to reproduce artificially and investigate the full blending phenomenon occurring in a new mix with RAP, nevertheless the behaviour observed on the bitumen scale was not confirmed on the mixture scale. Other phenomena emerged: the cluster phenomenon, adherence of RAP particles to the virgin aggregates and the presence of reactivated and non-activated old binder.

These phenomena and their possible effects on the recycling approach and mix design were analysed. Indeed, it was essential to investigate and understand the chemo-physical phenomena and mechanisms occurring during the mixing process that represent the source of the mixture characteristics in order to define a new approach for optimising the mix design of RAP mixtures.

A new methodology and a clustering index (IC_{G^*}) were defined to assess the presence of RAP clusters when new mixtures containing RAP are fabricated. With an increasing quantity of RAP in the mixture, the clustering phenomenon detected with the proposed methodology becomes less evident. This is because increasing the RAP percentage also means involving large-size RAP particles in the clustering process (higher threshold sieve) without contributing to the cluster formation. Moreover the abrasion effect of the crushed virgin aggregates and the existence of activated and non-activated RAP binder in the RAP bitumen thickness have an effect and this should be taken into account when the RAP content increases in the mixture. Thus, the type and quantity of virgin aggregates in the mixture as well as the type of RAP binder have an influence on the cluster formation. Taking their influence on the RAP cluster formation into account is fundamental to understanding how the total specific particle surface changes and to achieving a close to optimal dosage of virgin bitumen. The potential consequences of the cluster phenomenon must be taken into account for defining the approach to the recycling and mix design of RAP mixtures:

- The clusters could prevent the uniform distribution of the virgin binder, increasing the heterogeneity of the mixture.
- The formation of clusters leads to a reduction of the amount of small-size grains in the mixture, causing variations in the design grading curve and in the quantity of bitumen required for an adequate coating of the grains.
- The clusters may be the source of trapped interstitial voids that cannot be reached by the virgin bitumen. This may result in a low compactability of the asphalt mixture.

These aspects were then analysed in order to propose a new mix design approach for HMA with and without RAP based on the optimisation of the bitumen quantity in the mixtures. The key to the methodology is the separation of three main contributions that reflect different roles and behaviours in the mixture: virgin aggregates ($d > 0.063$ mm), filler ($d < 0.063$ mm) and RAP. All these components can be manipulated separately.

New revised surface area factors were calculated based on the real shape and surface of the grains and the latter do not require the approximation of spheres or cubes. This allowed the surface calculation related to the aggregate part (virgin or RAP) to be implemented. The filler contribution was based on the determination of the mastic performance since the specific surface of the filler to be coated by bitumen is not easily measurable due to its agglomeration and composition. Therefore, the *critical filler concentration* concept was used for maintaining the mastic (filler and bitumen) in a diluted phase. Moreover, in the case of RAP a clustering prediction model was introduced into the calculation to readjust the grading curve, taking into account the phenomenon of the RAP particle agglomeration. The above-mentioned findings led to the development of the theoretical formula for the optimal bitumen quantity in the mixture.

Two verifications carried out in the laboratory on the AC B 16 without RAP and with 50% of RAP gave positive and promising results. Indeed, the optimal quantities of bitumen estimated are similar to those measured and they allow the production of asphalt mixtures that meet all the Swiss standard requirements except for the flow in the Marshall test in the case of the RAP mixture. This is because the aged binder becomes softer during heating and acts as a lubricant, increasing the flow during load application. The compactability, measured with the gyratory compactor, for RAP mixtures is different from that of virgin mixtures. The reduction of the amount of small-size particles due to the clustering and intergranular voids trapped in the old RAP clusters prevents the achievement of an acceptable air void content. The RAP particle agglomeration causes a change in the final grading curve and an increase in the amount of air voids. The mixtures designed with the readjustment of the grading curve and a calculation of the specific amounts of virgin aggregates for every fraction to replace the agglomerated small-size RAP particles exhibit improved compactability (acceptable void content). Nevertheless, these results show that an appropriate mixing energy must be selected during asphalt mixture fabrication in order to break the old RAP clusters and prevent the presence of intergranular voids in the old clusters.

The higher variability detected in the behaviour of the binder blend was not confirmed on the mixture scale strengthening the hypothesis of the negligible migration of RAP binder in the case investigated.

The methodology represents a first step towards a new mix design approach for asphalt mixtures. Based on the results, it is considered successful in estimating the value of the optimal bitumen quantity for mixtures with and without RAP. The advantage of applying this methodology is the reduction of laboratory testing efforts since the estimated value of the optimal bitumen quantity represents a reliable prediction of the measured one. Moreover, the formula allows the control of the bitumen film thickness around the different components of the asphalt mixture (mineral aggregates, RAP and filler). Thus, the optimal bitumen film thickness around the aggregates can be changed depending on requirements and it would potentially be possible to use different bitumen film thicknesses for

different particle sizes. Moreover, by knowing the RAP grading curve and establishing the RAP percentage, it would be possible to calculate the agglomeration of RAP particles for every fraction and readjust the target grading curve, modifying the amount of virgin aggregates for every fraction. The methodology proposed gives the possibility to add or remove singular components separately. For instance, it is possible to add other elements to the mixture once their specific surface is calculated through the laser scanning technology and Meshlab. The surface area factors could be calculated with the methodology proposed and the elements could be added in the calculation readjusting the percentages of the others. An example could be represented by the addition of the fibres. These advantages confer to the methodology the necessary flexibility for an advanced mix design process that has to deal with several new materials developed in the recent years.

6.2. Future works

Even if the methodology is promising, additional work is needed to validate it, using other materials (RAP, virgin aggregates and filler), other types of mixtures and other fabrication temperatures. In particular RAP clustering should be investigated with RAP originating from other sources and for different fabrication temperatures. Indeed, the formation of RAP clusters might depend on the several factors as for instance the fabrication temperature, the mixing time and energy, the characteristics of the RAP binder. Additional studies are necessary to evaluate the effects of these parameters on the clustering phenomenon in order to implement the RAP clustering model for the readjustment of the grading curve. The methodology to detect the RAP clustering should be applied also to warm and cold mix asphalt.

The RAP clustering raises another problem to be solved: the distribution of the virgin bitumen in the asphalt mixtures. Indeed, the clustering can cause an increase of heterogeneity and significant differences in the bitumen film thickness coating the individual particles and/or clusters. A microscopic investigation could help to visualize the distribution of the binders and the effective bitumen film thickness around the aggregates (RAP and virgin).

Moreover, the asphalt mixtures resulting from the proposed mix design should be tested to evaluate their stiffness, permanent deformation and fatigue resistance. In fact, these tests could provide not only important information for the introduction of the properties of these materials in pavement design methods, but they could also help to define a more appropriate way to define the optimal recipe in case of asphalt mixtures containing RAP. Indeed, in those cases the Marshall stability or the gyratory compactor could not be sufficient to identify the optimal recipe and they could be used side by side or replaced by other tests that allow other criteria to be satisfied when high RAP content is used.

To conclude, new construction and/or rehabilitation of road pavements must be designed with the absolute objective of increasing environmental and economic sustainability. Since transport and

infrastructures have a significant impact on the quality of life, they must ensure a high-level performance in order to minimise maintenance interventions and costs and user discomfort. This can be achieved with the use of high quality materials and a different approach to recycling. Indeed, it is necessary to conceive a new way to design asphalt mixtures, maximising the use of recycled material and maintaining the same performance level as that of conventional asphalt mixtures.

The methodology proposed takes a step in this direction by considering the physical phenomena and mechanisms occurring during the mixing process as the source of the mixture characteristics. Therefore, the maximum durability of these materials depends on the maximum amount of knowledge being gathered at every stage of their fabrication.

References

- AASHTO standard practice R 30. Standard practice for mixture conditioning of hot mix asphalt.
- Al-Qadi I., Elseifi M., Carpenter S.H. (2007). Reclaimed Asphalt Pavement-A literature review. (Research Report FHWA-ICT-07-001). Illinois Center of transportation.
- Anderson, D.A. and L. (1994) Binder Characterization, Vol. 3: Physical Properties', SHRP-A-369, Strategic Highways Research Program, Nat. Research Council, Washington, D.C.
- Asphalt Institute. Mix design methods for asphalt concrete and other hot mix types. MS-2, 1993.
- ASTM D 2872. Standard Test Method for Effect of Heat and Air on a Moving Film of Asphalt (Rolling Thin-Film Oven Test).
- ASTM, ASTM D6521 (2008). Standard practice for accelerated aging of asphalt binder using a pressurized aging vessel (PAV). West Conshohocken. PA: American Society Testing & materials.
- ASTM C670. Standard practice for preparing precision and bias statements for test methods for construction materials.
- ASTM C802. Standard practice for conducting an interlaboratory test program to determine the precision of test methods for construction materials.
- Attia M.I., Abdelrahman M.A. Molakatalla U., Salem H.M. (2009). Field evaluation of Asphalt Film thickness as a design parameter superpave mix design. International journal of pavement research and technology.
- Bevington P.R. and Robinson D. K. (1969). Data reduction and error analysis for the physical sciences. Third edition, Mc Graw Hill.
- Bilal M. Ayyub and Mc Cuen R. (2011) Probability, Statistics and Reliability for engineers and scientists (Third edition). A Chapman & Hall book. Taylor and Francis Group.
- Booshehrian A., Mogawer W. S. and Bonaquist R. (2013). How to construct an asphalt binder master curve and assess the degree of blending between RAP and virgin binders. Journal of Materials in Civil Engineering, pp. 1813-1821.
- Bowers B. F., Moore J., Huang B., Shu X. (2014). Blending efficiency of Reclaimed Asphalt Pavement: An approach utilizing rheological properties and molecular weight distributions. Fuel 135 p. 63-68.
- Box E.P. George, Hunter J. Stuart, Hunter William G. (1978). Statistics for experiments. Design, innovation, and Discovery. Wiley series in Probability and statistics. John Wiley and Sons, inc. Publication.

- Bressi S., Dumont A.G., Carter A., Bueche N. (2015a). A multiple regression model for developing a RAP binder blending chart for stiffness prediction. 6th International Conference Bituminous Mixtures and Pavements, Thessaloniki (Greece).
- Bressi S., Dumont A.G., Pittet M. (2015b). Cluster phenomenon and partial differential aging in RAP mixtures. *Construction and Building materials*. Manuscript submitted for publication.
- Bressi S., Carter A., Bueche N., Dumont A. G. (2015c). Impact of different ageing levels on binder rheology. *International Journal of Pavement Engineering*, pages 1-11. DOI:10.1080/10298436.2014.993197
- Bressi S., Pittet M., Dumont A.G., Partl M.N. (2015d). A framework for characterizing RAP clustering in asphalt concrete mixtures. *Construction and Building Materials* (accepted).
- Campen, J.F., J.R. Smith, L.G. Erickson, and L.R. Mertz (1959). The Relationships between Voids, Surface Area, film thickness and stability in bituminous paving mixtures. In *Proceedings, AAPT*, Vol. 28.
- Chapuis R.P., Légaré P.P. (1992). A simple method for determining the surface area of fine aggregates and fillers in bituminous mixtures. Book *Asphalt mixture performance*. Meininger editor. ASTM STP 1147.
- Coree B.J. and Hislop W.P. (2000) A laboratory investigation into the effects of aggregate related factors of critical VMA in asphalt paving mixtures. Iowa DOT project TR-415, CTRE management project 98-20. Center for transportation research and Education, Iowa state university.
- Craus J., and Ishai I. (1977). A method for the determination of the surface area of fine aggregate in bituminous mixtures. *Journal of testing and evaluation*. Vol. 5.
- Das P.K., Baaj H., Kringos N. and Tighe S. (2015). Coupling of oxidative ageing and moisture damage in asphalt mixtures. *Road materials and Pavement Design*.
- De la Roche C. et al. (2013). Hot recycling of bituminous mixes. *Advances in interlaboratory testing and evaluation of bituminous mixes (Chapter 7)*. State of the art Report of the RILEM Technical Committee 206-ATB.
- Del Barco Carrion A.J., Lo Presti D., Airey G. (2015). Binder design of high RAP content hot and warm asphalt mixture wearing courses. *Road materials and pavement design*.
- Doehlert D. H. (1970). Uniform shell design. *Journal of the Royal Statistical Society. Series C (Applied Statistics)*, Vol. 19, No. 3 pp. 231-239. Published by Wiley for the Royal statistical society.
- Drut C., Wang L. and Zhu T. (2009) Laboratory investigation of reclaimed asphalt pavement mixed with pure binder using X-ray CT scanner. *Critical Issues in Transportation Systems Planning, Development, and Management*© ASCE.
- Duriez M. (1950) *Traité de matériaux de construction*. Dunod.

- Duriez M. and Arrambide J. (1962) Nouveau traité de matériaux de construction Tomes 1-2-3 Dunod, Paris.
- El Beze Laëtitia (2008). RECYCLAGE À CHAUD DES AGREGATS D'ENROBES BITUMINEUX : Identification de traceurs d'homogénéité du mélange entre bitume vieilli et bitume neuf d'apport. Thesis University of Cezanne.
- EN 12697-1 (2012) Bituminous mixtures – test methods for hot mix asphalt – Part 1: soluble binder content.
- EN 12697-3 (2013) Bituminous mixtures – test methods for hot mix asphalt – Part 3: bitumen recovery: rotary evaporator.
- EN 1426: 2007 Bitumen and bituminous binders - Determination of needle penetration.
- EN 1427: 2007 Determination of the softening point – Ring and ball method.
- EN 12591: 2009 Bitumen and bituminous binders. Specifications for paving grade bitumens
- EN 13108-8: 2005. Bituminous Mixtures. Materials Specifications. Part 8: Reclaimed Asphalt.
- Epps, J.A., Little, D.N., Holmgreen, R.J., and Terrel, R.L. (1980). Guidelines for Recycling Pavement Materials, NCHRP Report No. 224, Transportation Research Board, Washington, DC.
- Faheem A.F., Bahia H. (2009) “Conceptual Phenomenological Model for Interaction of Asphalt Binders With Mineral Fillers”, Journal of the Association of Asphalt Paving Technologists, Vol. 78.
- Faheem A.F. and Bahia H. U. (2010) Modelling of Asphalt Mastic in terms of Filler Bitumen Interaction. Road Materials and Pavement Design.
- Federal Highway Administration. (1978–1983). Demonstration Project 39—Asphalt Recycling, Federal Highway Administration, Washington, DC.
- Federal Highway Administration. (2011). Reclaimed Asphalt Pavement in Asphalt Mixtures: State of the Practice. Report No. FHWA-HRT-11-021. Federal Highway Administration, Washington, DC.
- Ferry, J. D. (1980). Viscoelastic properties of polymers (3rd edition) New York, NY: John Wiley & Sons.
- Heitzman M.A., (2005) Development of new film thickness models for hot mix asphalt, dissertation. Iowa State University, Department of Civil Engineering, Ames, Iowa.
- Hussain A. and Q. Yanjun. (2013) Effect of Reclaimed Asphalt Pavement on the Properties of Asphalt Binders. International Conference on Rehabilitation and Maintenance in Civil Engineering.
- Hveem F. N. (1974). Mix design method for asphalt concrete MS-2 the Asphalt Institute college park, Md.
- Kalman B. et al. (2013). Re-Road- Summary Report. End of life strategies of asphalt pavements. Re-Road.
- Kandhal P.S. and Chakraborty S. Effect of asphalt thickness on short and long term aging of asphalt paving mixtures. National Center for Asphalt Technology, 1996.

- Kandhal P., Foo K.Y. (1997). Designing recycled hot mixture asphalt mixtures using superpave technology. NCAT Report no. 96-5 p.7-22.
- Kandhal P. S., Foo K.Y., (1996) Mallick R.B. A critical review of VMA requirements in Superpave NCAT Report n. 98-1.
- Kenis, W. and Wang, W., Pavement variability and reliability. (2004) Available from: <http://www.ksu.edu/pavements/trb/A2B09/CS13-12.pdf>, last visited: January.
- Kim, H.B and Buch, N, (2003). Reliability-based pavement design model accounting for inherent variability of design parameter.In: 82nd Transportation Research Board annual meeting, Washington, DC
- Kriz P., Grant D.L, Veloza B. A., Gale M.J., Blahey A. G., Brownie J. H. (2014) Blending and diffusion of reclaimed asphalt pavement and virgin asphalt binders. Road Materials and Pavement Design, 78-112. DOI: 10.1080/14680629.2014.927411.
- Little D.N. and Petersen C. (2005). Unique effects of hydrated lime filler on the performance-related properties of asphalt cements: physical and chemical interactions revisited. Journal of materials in civil engineering.
- Lo Presti D., Khan R., Airey G., Collop A. (2014). Laboratory mix design of Asphalt Mixture containing reclaimed material. Advances in materials science and engineering
- Mangiafico S., Di Benedetto H., Sauzéat C., Olard F, Pouget S., Planque L.. (2014). New method to obtain viscoelastic properties of bitumen blends from pure and reclaimed asphalt pavement binder constituents. Road materials and pavement design.
- Mickey R., Dunn O. J., Clark V. A. (2009). Applied statistics. Analysis of Variance and Regression (Third edition). Wiley series.
- Minnesota department of transportation (2006). Asphalt film thickness calculation spread sheet. Minnesota department of transportation.
- Montgomery Douglas C. (2000) Design and Analysis of Experiments-5th Edition. John Wiley & Sons.
- Nahar S.N. et al. (2012). First observation of the blending zone morphology at the interface of reclaimed asphalt binder and virgin bitumen. Transportation Research Board.
- Navaro J., Bruneau D., Drouadaine I., Colin J., Dony A, Cournet J. (2012) Observation and evaluation of the degree of blending of reclaimed asphalt concretes using microscopy image analysis. Construction and Building Materials 37 pag. 135-143. doi:10.1016/j.conbuildmat.2012.07.048.
- NCAT. Roberts F.L., Kandhal P.S., Brown E.R., Dah-Yinn L. and Kennedy T.W. (1996) Hot mix asphalt materials, mixture design and construction, Second edition, National Asphalt Pavement Association, Research and Education Foundation, Lahanam, Maryland, USA.
- NCHRP National Cooperative Highway Research Program. (1978). Program Synthesis of Highway Practice No. 54: Recycling Materials for Highways, Transportation Research Board, Washington, DC.

- NCHRP Report 452. McDaniel, R., and R. M. Anderson. (2001) Recommended Use of Reclaimed Asphalt Pavement in the Superpave Mixture Design Method: Technician Manual. TRB, National Research Council, Washington, D.C.
- Nguyen V. H. (2009) Effects of Laboratory Mixing Methods and RAP Materials on Performances of Hot Recycled Asphalt Mixtures. Thesis University of Nottingham.
- Ott, R. L., and M. Longnecker (2000). An Introduction to Statistical Methods and Data Analysis, 5th ed. Duxbury Press, Pacific Grove, Calif.
- Partl M., Flisch A., Jönsson M. (2006). Comparison of Laboratory Compaction Methods using X-ray Computer Tomography. Road Materials and Pavement Design. DOI:10.1080/14680629.2007.9690071
- Poulikakos L. D., Dos Santos S., Bueno M., Kuentzel, S. Hugener, M. Partl M.N. (2013). Influence of short and long term aging on chemical, microstructural and macro-mechanical properties of recycled asphalt mixtures. Construction and Building Materials.
- Rinaldini E., Schuetz P., Partl M.N., Tebaldi G., Poulikakos L.D . (2014) Investigating the blending of reclaimed asphalt with virgin materials using rheology, electron microscopy and computer tomography. Composites: Part B 67 (2014) 579-587; 2014. doi:10.1016/j.compositesb.2014.07.025.
- Roberts F.L., Kandhal P.S., Brown E.R., Dah-Yinn L. and Kennedy T.W. (1996). Hot mix asphalt materials, mixture design and construction, Second edition, National Asphalt Pavement Association, Research and Education Foundation, Lahanam, Maryland, USA.
- Roque R., Birgisson B., Tia M., and Nukunya B. (2002). Evaluation of Superpave criteria for VMA and fine aggregate angularity, volume 1 of 2. University of Florida, USA.
- Sengoz B., Agar E. (2007) Effect of asphalt film thickness on the moisture sensitivity characteristics of hot-mix asphalt. Building and environment 42
- Shirodkar, Mehta, Nolan, Sonpal, Norton, Tomlinson, Sauber, DuBois. (2010). A Study to Determine the Degree of Partial Blending of Reclaimed Asphalt Pavement (RAP) Binder for High RAP Hot Mix Asphalt. Transportation Research Board.
- Snedecor G.W. and Cochran W.G. (1983). Statistical methods 6th edn. The Iowa State University Press, Ames, Iowa. USA.
- Stimilli A., Virgili A., Canestrari F. (2015). New method to estimate the “re-activated” binder amount in recycled hot-mix asphalt. Road materials and pavement design.
- Strategic Highway Research Program (SHRP) (1994) National Research Council, Washington, DC;SHRP-A-370(4):39.
- Swiertz D., Mahmoud E, Bahia H.U. (2011) Estimating the effect of recycled asphalt pavements and asphalt shingles on fresh binder, low-temperature properties without extraction and recovery. Transportation Research Record: Journal of the Transportation Research Board, 2208, 48-55.
- Swiss Association of Roads and Transportation Experts. National annex SN 640 431-1b-NA, 2006.

- Tunnicliff D.G. (1967) Binding effects of mineral filler. Proceedings Association of Asphalt Paving Technologists, Vol. 36.
- Welch BL. (1938). The significance of the difference between two means when the population variances are unequal. *Biometrika* 29:350–62.
- Yousefi Rad F. (2013) Estimating blending level of fresh and RAP binders in recycled hot mix asphalt. Master of Science, University of Wisconsin Madison.
- Zaniewski J.P. and Reyes C.H. (2003). Evaluation of the effect of fines on asphalt concrete. Asphalt technology program. Department of civil and environmental engineering.

Annexes

Table A-1. Stiffness values obtained at different ageing levels and different temperatures.

Ageing level	Stiffness at -30°C [MPa]	Stiffness at -20°C [MPa]	Stiffness at -10°C [MPa]
Virgin	1 050	405	80.7
	884	408	94.8
	988	405	87.1
	787	455	128
	750	392	108
	964	454	127
	910	420	128
	922	406	113
	930	403	109
	922	405	113
	1 010	429	120
	881	390	102
RTFOT	1 150	459	145
	1 230	455	124
	1 010	393	156
	1 010	531	145
	-	478	144
	1 050	510	152
	1 030	520	166
	972	510	173
	984	499	154
	1 030	470	163
	896	510	153
	966	500	159
RTOFOT + PAV	1 080	515	201
	1 140	595	239
	1 080	531	213
	987	474	191
	1 040	504	202
	1 020	524	203
	928	464	206
	1 160	659	248
	999	531	187
	1 090	524	177
	983	487	208
	965	459	193

Table A-2. Complex modulus values obtained at different ageing levels and different frequencies (temperature=20°C).

Ageing level	Complex modulus at - 0.4 Hz [Pa]	Complex modulus at - 1 Hz [Pa]	Complex modulus at - 10.3 Hz [Pa]
Virgin	543 280	667 190	1 447 700
	543 360	1 043 800	3 220 600
	545 160	1 048 400	3 231 100
	545 370	1 050 400	3 239 700
	549 820	1 061 400	3 260 500
	553 740	1 064 600	3 262 900
	556 960	1 080 500	3 263 700
	557 350	1 086 200	3 273 600
	-	-	3 281 200
-	-	3 288 000	
RTFOT	1 323 000	2 011 400	2 981 500
	1 322 000	2 026 400	3 421 100
	1 271 300	2 045 400	3 799 300
	1 299 300	2 082 700	3 812 000
	1 334 200	2 093 900	3 816 000
	1 345 500	2 103 400	3 859 200
	1 362 200	2 110 900	3 860 800
	-	-	3 860 900
	-	-	4 906 300
RTOFOT + PAV	2 612 600	3 673 993	3 975 900
	2 640 900	3 674 093	4 368 600
	2 654 400	3 247 400	4 402 800
	3 289 900	3 284 300	4 427 100
	3 303 400	3 306 700	4 955 300
	3 323 100	3 948 800	4 972 700
	3 328 500	3 955 500	4 983 200
	3 334 000	3 962 200	4 984 100
	3 349 800	4 013 400	4 989 100
	3 360 200	-	4 993 800
	3 390 100	-	5 001 100
	3 393 100	-	5 002 300
	3 398 100	-	5 002 800
	3 404 500	-	-

Table A-3. Complex modulus values obtained at different ageing levels and different frequencies (temperature=50°C).

Ageing level	Complex modulus at - 0.4 Hz [Pa]	Complex modulus at - 1 Hz [Pa]	Complex modulus at - 10.3 Hz [Pa]
Virgin	1 492.2	3 497.6	20 444
	1 313.1	3 126.7	24 843
	1 318.5	3 040.4	22 885
	1 342.4	3 072.7	22 675
	1 261.8	3 395.3	23 323
	1 370.5	3 106.4	28 437
	1 259.2	2 740.8	18 752
	1 181.5	2 948.9	19 518
	1 073.1	2 465.1	20 030
	1 067.6	2 408.7	24 132
	1 157.3	2 506	16 427
	1 071.9	2 639.9	16 634
	1 090.5	2 211.3	15 340
	1 099.8	2 462.9	17 820
	1 170.5	2 718.9	21 689
1 142.4	2 466.7	22 101	
RTFOT	4 671.2	10 894	75 511
	4 492.4	11 171	72 912
	4 145.1	9 733.7	77 120
	4 091.9	8 956.6	55 532
	3 992.6	8 389.8	66 726
	3 803.7	8 481.6	61 036
	3 764	7 742.5	52 654
	3 485.9	7 701.2	51 215
	3 528.6	15 662	54 087
	3 537	7 365.3	55 242
	2 938	6 470	58 045
	3 555.5	6 177.6	46 158
	3 112.7	7 110.5	45 245
	3 228.9	6 307.5	93 981
	3 748.4	5 895.7	54 059
3 807.6	7 208.4	43 086	
RTOFOT + PAV	25 585	67 206	337 070
	29 601	72 371	344 360
	31 183	68 047	204 030
	33 485	63 855	127 830
	33 768	87 008	359 530
	33 883	54 170	202 460
	33 982	67 489	341 070
	34 149	66 647	1 128 400
	34 513	51 191	356 360
	34 726	93 674	5 594 700
	44 059	48 454	218 540
	-	53 056	199 730
	-	57 105	181 520
	-	39 341	359 100
	-	59 146	341 590
-	37 821	1 637 700	

Table A-4. Complex modulus obtained for all the blend combinations at 30°C.

	Combination	Percentage of RAP binder in the blend [%]						
		0	10	20	40	50	70	80
G* [Pa]	RAP 50/70 and virgin 50/70	6.27E+05	7.11E+05	8.47E+05	1.03E+06	1.23E+06	1.66E+06	1.61E+06
	RAP 70/100 and virgin 70/100	4.02E+05	3.68E+05	4.62E+05	6.44E+05	8.39E+05	1.04E+06	1.34E+06
	RAP 50/70 and virgin 70/100	6.27E+05	5.01E+05	-	-	4.11E+05	-	8.74E+05
	RAP 70/100 and virgin 50/70	4.02E+05	5.43E+05	-	-	1.12E+06	-	1.35E+06

Table A-5. Complex modulus obtained for all the blend combinations at 40°C.

	Combination	Percentage of RAP binder in the blend [%]						
		0	10	20	40	50	70	80
G* [Pa]	RAP 50/70 and virgin 50/70	1,22E+05	1,51E+05	1,87E+05	2,33E+05	3,20E+05	4,48E+05	4,50E+05
	RAP 70/100 and virgin 70/100	5,37E+04	-	6,50E+04	1,10E+05	1,39E+05	1,89E+05	2,93E+05
	RAP 50/70 and virgin 70/100	1,22E+05	8,74E+04	-	-	9,14E+04	-	8,83E+04
	RAP 70/100 and virgin 50/70	5,37E+04	1,04E+05	-	-	2,25E+05	-	3,09E+05

Table A-6. Complex modulus obtained for all the blend combinations at 60°C.

	Combination	Percentage of RAP binder in the blend [%]						
		0	10	20	40	50	70	80
G* [Pa]	RAP 50/70 and virgin 50/70	2,65E+03	4,70E+03	8,22E+03	1,15E+04	1,65E+04	2,50E+04	2,74E+04
	RAP 70/100 and virgin 70/100	1,39E+03	1,37E+03	-	3,69E+03	4,17E+03	5,24E+03	8,48E+03
	RAP 50/70 and virgin 70/100	2,65E+03	2,48E+03	-	-	6,29E+03	-	5,79E+03
	RAP 70/100 and virgin 50/70	1,39E+03	3,02E+03	-	-	8,99E+03	-	1,19E+04

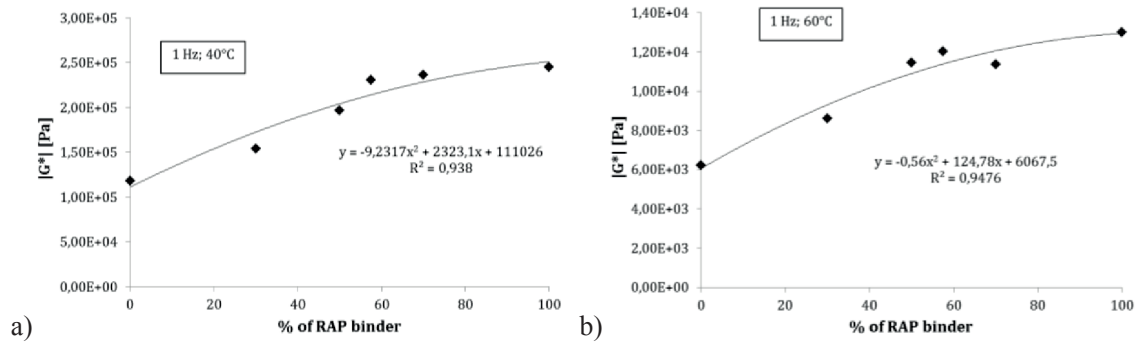


Figure A-1 Artificially-aged binder blending charts with virgin binder 50/70 at a) 40°C and b) 60°C.

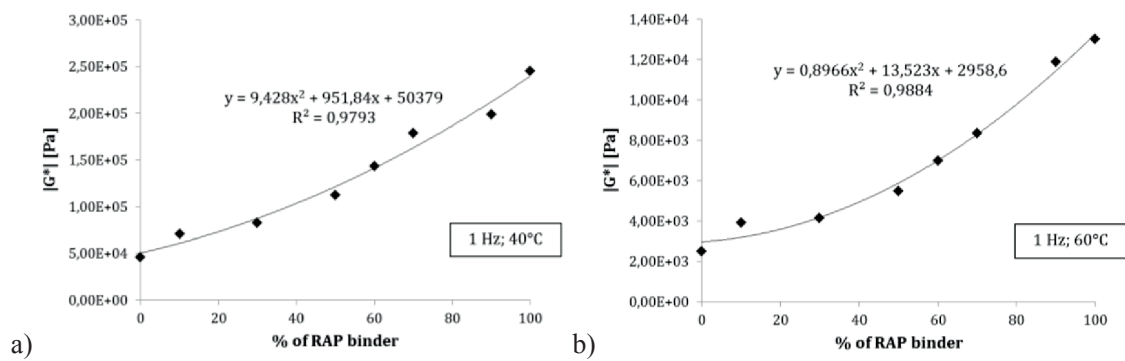


Figure A-2 Artificially-aged binder blending charts with virgin binder 70/100 at a) 40°C and b) 60°C.

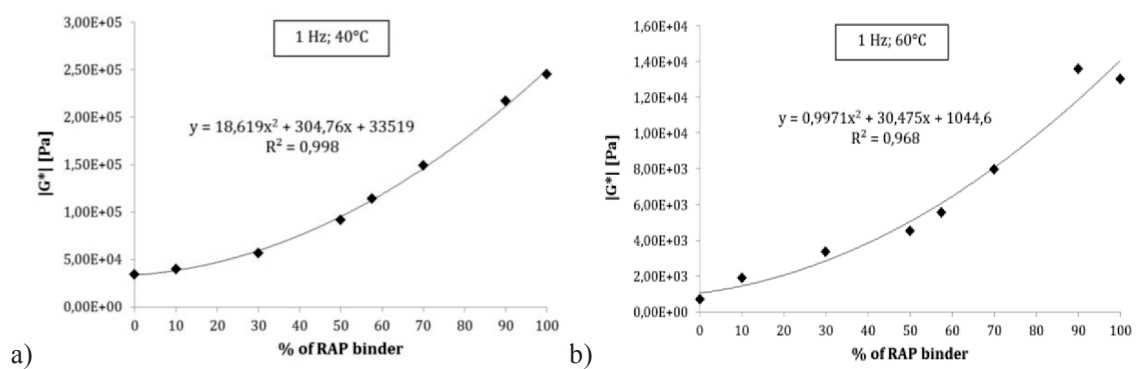


Figure A-3 Artificially-aged binder blending charts with virgin binder 100/150 at a) 40°C and b) 60°C.

Sara Bressi

Personal information

Address Rue du Simplon, 29
1006 Lausanne, Switzerland

Phone +41 (0)078 930 57 85

E-mail sara.bressi@gmail.com

Date of birth 26.07.1985

Birthplace Guastalla (RE) Italy

Gender Female

Citizenship Italian



Profile

I am a civil engineer that, after having worked for two years in a private company, has started a PhD in the Laboratory of Traffic Facilities (LAVOC), École Polytechnique Fédérale de Lausanne (EPFL), Switzerland. I am highly motivated to continue the experience of teaching and scientific research at the University.

From the beginning of my professional experience I have been involved in several research studies regarding road infrastructures. I am currently participating in a three-year project concerning the revision of pavement design and reinforcement methods used in Switzerland (REDIRE), in line with the current initiatives that are under way for their improvement. My current research focuses on projects aiming at studying the mechanical behaviour and performance of bituminous mixtures containing high quantities of Reclaimed Asphalt Pavement (RAP). Moreover, during recent years collaboration with experts on statistics has allowed me to acquire knowledge regarding sensitivity analysis, risk analysis and reliability applied to the pavement design domain for more reliable prediction of infrastructure durability. The work I have done in several laboratories such as at the University of Parma (Italy), ETS Montreal (Canada), EMPA Zurich (Switzerland) has allowed me to acquire a professional knowledge of road materials (bitumen and asphalt mixtures), resulting in my appointment as head of the materials laboratory at LAVOC (Laboratoire des voies de circulation - EPFL, Switzerland).

Research, Teaching and Professional experience

Research

June 2015-present

National project "Forschungspaket Recycling von Ausbauasphalt in Heissmischgut: VP6: In-situ Validierung (VSS 2005/457)" Project partners: EMPA (Zurich) and LAVOC-EPFL (Lausanne). The project aims at increasing the amount of recycled material in asphalt mixtures using specific additives (rejuvenators). I am currently the LAVOC representative for the project led by EMPA.

2013 - present

REDIRE project (Révision des méthodes de dimensionnement et renforcement des chaussées)- Establishment of an innovative methodology for Swiss pavement design. Project funded by the Swiss Federal Roads Office (OFROU). I am one of the main scientific contributors for the development of every task.

Sept. 2014- present

FundBitS (Functional Durability-related Bitumen Specification). Research project funded by CEDR Transnational Road Research Program. I review internationally available data in order to develop performance-based bitumen characteristics that may be introduced into bitumen specification standards.

June 2010- June 2012

« Cold and warm mixtures for fiber-reinforced asphalts »
Regional Program for Industrial Research, Innovation and Technology (Emilia Romagna).
Scientific contributor and main responsible of the project involving several partners: University

of Parma (Faculty of Civil Engineering), University of Modena and Reggio Emilia (Faculty of Civil Engineering and Faculty of Material Science) and Turchi Cesare S.r.l.

Teaching Assistency

Fall semester 2014

Assistant of Bachelor course « Statistics and Probability »
Master Thesis supervisor: "Determination of blending of RAP binder with virgin binder in recycled asphalt concrete". EMPA Zurich

Spring semester 2013

Assistant of MSc course « Voies de circulation »
Master Thesis supervisor: "Effects of double coating method on mechanical properties for cold-in-place recycling mix: foam bitumen and emulsion". ETS Montreal

Spring semester 2012

Assistant of MSc course « Voies de circulation »
Assistant of Bachelor course "Analysis I"

Professional

July 2015

Winning candidate of a Marie Curie scholarship for an experienced researcher that commences in December 2015 in the framework of a European project SUP&R ITN (Sustainable Pavement & Railway Initial Training Network). The SUP&R ITN, through a consortium of universities and research centres from five different European countries (UK, Italy, France, Ireland, Spain), aims at forming a new generation of multidisciplinary European researchers, capable of conceiving, planning and executing sustainable road and railway infrastructures.

June 2015 - present

Head of the laboratory of materials at LAVOC (Laboratories of Traffic Facilities). I am currently responsible of the laboratory leading and planning the work of the technicians. I am the responsible of all the experimental tests conducted.

2013-present

Member of the Swiss Association VSS (Research and standardization in the field of road and transportation)

June 2010- June 2012

Civil engineer and R&D responsible for Turchi Cesare S.r.l.:

- Responsible for research projects « Cold and warm mixtures for fiber-reinforced asphalts »
- CE certification of aggregates
- Call for public tenders
- Realization of different particular projects as a racetrack and sustainable urban surface asphalt layers

Education

July 2012 – present (Dec. 2015)

Doctoral student and research assistant of School of Architecture, Civil Engineering and Environmental Engineering (ENAC), Section of Environmental Sciences and Engineering (SSIE), Laboratory of Traffic Facilities (LaVOC), École Polytechnique Fédérale de Lausanne (EPFL), Switzerland.

Thesis subject: A new methodology for the mix design optimization of RAP mixtures

Director: Prof. A.-G. Dumont,

Co-Director: Prof. M. Partl

Aug. 2014– Oct. 2014

Short-Term Scientific Period at Empa - Swiss Federal Laboratories for Materials Science and Technology Zurich, Switzerland

Road engineering/Sealing components Department

Scientific collaborators: Prof. M. Partl and Senior Scientist Lily Poulikakos

Sept. 2013– Dec. 2013

Short-Term Scientific Period at Ecole Technologique Supérieure (ETS) of Montreal, Canada

Civil Engineering Department
Scientific collaborator: Prof. Alan Carter

Oct. 2010

Succeeded the professional practice examination for the engineering license

Sept. 2007 – Feb. 2010

Master of Science (MSc)
Curriculum: Road infrastructures
Thesis title: Reologia dei bitumi modificati con cere
Grade: 110/110 cum laude
Faculty of Civil Engineering University of Parma

Sept. 2004 – Sept. 2007

Bachelor degree
Thesis title: Valutazione della resistenza a fatica dei conglomerati bituminosi provenienti dal riciclaggio a freddo di seconda generazione
Grade 110/110
Faculty of Civil Engineering University of Parma

Awards and Honours

March 2014

Italian national scholarship “Homo Sapiens Sapiens” for the PhD year abroad 2012/2013

March 2010

Italian national scholarship “Homo Sapiens Sapiens” for excellent performance in study in the year 2008/2009

March 2009

Italian national scholarship “Homo Sapiens Sapiens” for excellent performance in study in the year 2007/2008

Projects and articles

In preparation

Bressi S., Dumont A-G. *Towards a new mix design method for asphalt mixtures containing RAP*. 8th International Conference on Maintenance and Rehabilitation of Pavements (MAIREPAV8), Singapore, 27–29 July 2016 (abstract accepted).

Journal articles

Bressi S., Dumont A-G., Partl M.N. *An advanced methodology for the mix design optimization of Hot Mix Asphalt*. Materials and design (under review)

Bressi S., Dumont A-G., Partl M.N. *Advanced methodology for optimization of mixture design of asphalt concrete containing reclaimed asphalt pavement material*. Materials and structures. (under review)

Cavalli, M.C., Griffa, M., Bressi, S., Partl, M.N., Tebaldi, G., Poulidakos, L. D. *Characterization of asphalt concrete with recycled components by multi-scale imaging*, Journal of Microscopy. (under review)

Bressi S., Pittet M., Dumont A.G., Partl M.N. (2015). *A framework for characterizing RAP clustering in asphalt concrete mixtures*. Construction and building material. (in press)

Bressi S., Carter A., Dumont A. G., Bueche N. (2015). *A nonlinear binder blending chart for the low temperature domain*. Road Materials and Pavement design (accepted with modifications).

Bressi S. Cavalli M. C., Partl M.N., Tebaldi G. Dumont A.G. Poulidakos L.D. (2015) *Particle Clustering Phenomena in Hot Asphalt Mixtures with High Content of Reclaimed Asphalt Pavements*.

Construction and Building Materials. doi:10.1016/j.conbuildmat.2015.09.052

Bressi S., Dumont A.G., Pittet M. (2015). *Cluster phenomenon and partial differential aging in RAP mixtures*. Construction and Building Materials (in press). DOI: 10.1016/j.conbuildmat.2015.09.024

Bressi S., Carter A., Bueche N., Dumont A. G.. 2015. *Impact of different ageing levels on binder rheology*. International Journal of Pavement Engineering, pages 1-11. DOI:10.1080/10298436.2014.993197.

Bressi S., Dumont A. - G. (2014). *Dimensionnement des chaussées: état actuel et évolution*. Route et trafic, num. 3 p.12 - 21.

Conference papers and presentations

Gandi A., Ben-Salem F., Bressi S., Carter A., & Bueche N., (2016), Double Coating of Full Depth Reclamation Materials, 6th Eurasphalt & Eurobitume Congress. Prague. Czech.

Bressi S. *Teneur en liant optimale des enrobés avec recyclé*. Journée d'étude de la route et des Infrastructures. SwissTech Convention Center EPFL Lausanne, 26 November 2015.

Bueche N., Dumont A.G., Pittet M., Bressi S. *Asphalt mixture with RAP: Mix design optimization*. 8th International RILEM Symposium SIB2015 – 7-9 October 2015, Ancona, Italy.

Bressi S., Pittet M., Dumont A.G., Partl M.N. *A framework for characterizing RAP clustering in asphalt concrete mixtures*. Workshop contribution. 8th International RILEM Symposium SIB2015 – 7-9 October 2015, Ancona, Italy.

Bressi S., Carter A., Dumont A. G., Bueche N. A Multiple regression model for developing a RAP binder blending chart for stiffness prediction. 6th International Conference: Bituminous Mixtures & Pavements Thessaloniki, Greece, 10-12 June 2015.

Bressi S., Furbringer J.M., Féart M.A., Dumont A.G. *Global Sensitivity Analysis and Monte Carlo Analysis of Swiss design method applied to flexible pavements*. EATA Conference Stockholm 2015.

Bressi S., Dumont A.G., Bueche N. *Warm Mix Asphalt key parameters: a statistical analysis methodology*. ENAC-EDCE Research day, Lausanne.

Bressi S. *Paramètres de performance dans les méthodes de dimensionnement*. Journée technique. Performances des chaussées: attentes et exigences. EPFL Lausanne 2012.

Other conference and seminars

- Instructional Skills Workshop, 2014 EPFL, Lausanne
- 3rd International Conference on Transportation infrastructure ICTI-2014, Pisa
- End of life strategies of Asphalt Pavement, Re-Road 2012, Bruxelles
- International Congress SIIV "Sustainability of Road Infrastructure" 2012, Rome
- European Asphalt Technology Association (EATA) Conference, 2010, Parma

Skills and competences

- Deep knowledge of Design of experiments : statistical approach to treat laboratory data;
- Deep knowledge of statistical tools applied to pavement design;
- Experience in developing solutions with Matlab and R language;
- Deep knowledge of pavement design software: Bisar, MePADS, Pavement-ME, Alizé-LCPC;
- Knowledge of AutoCAD, EasyFit, MS office tools;
- Recent courses attended: Fourier Analysis and boundary value problems, Intelligent Transportation System (ITS);

- Deep knowledge in using laboratory equipment for bitumen tests;
- Deep knowledge in using laboratory equipment for asphalt mix tests.

Language Skills

Italian	Native		
	Comprehension	Speaking	Writing
English	C2	C1	C1
French	B2	B2	B1

Hobbies and interests

Diploma of flute achieved at the Conservatory of Parma "A. Boito" in 2004 with the grade: 9/10. I have participated/organized charity concerts for different occasions as for example the International Day for the Elimination of Violence against Women.

